






## REVIEW

View Article Online  
View Journal | View Issue



Cite this: *Nat. Prod. Rep.*, 2023, 40, 412

## Unusually cyclized triterpenoids: occurrence, biosynthesis and chemical synthesis

Hidayat Hussain, <sup>\*a</sup> Jianbo Xiao, <sup>bc</sup> Akbar Ali, <sup>d</sup> Ivan R. Green <sup>e</sup> and Bernhard Westermann <sup>\*a</sup>

Covering: 2009 to 2021

Biosynthetically, most of the syntheses of triterpenes follow the cascade cyclization and rearrangement of the acyclic precursors viz., squalene (S) and 2,3-oxidosqualene (OS), which lead to the very well known tetra- and pentacyclic triterpene skeletons. Aside from these, numerous other triterpenoid molecules are also reported from various natural sources and their structures are derived from "S" and "OS" via some unusual cyclization operations which are different from the usual tetra- and pentacyclic frameworks. Numerous compelling advances have been made and reported in the identification of these unusual cyclized mono-, di-, tri- and tetracyclic triterpenes between 2009 and 2021. Besides a dramatic increase in the newly isolated uncommon cyclized triterpenoids, substantial progress in the (bio)-synthesis of these triterpenes has been published along with significant progress in their biological effects. In this review, 180 new unusual cyclized triterpenoids together with their demonstrated biogenetic pathways, syntheses and biological effects will be categorized and discussed.

Received 3rd May 2022

DOI: 10.1039/d2np00033d

rsc.li/npr

1	Introduction	5	Biosynthesis of isomalabaricane and malabaricane triterpenoids
2	Iridal triterpenes	6	Tetanordammarane and polypodane triterpenoids
2.1	Monocyclic iridals	7	Biosynthesis of tetranordammaranes
2.2	Bicyclic iridals	8	Schiglautone and volvalerane type triterpenes
2.3	Tricyclic iridals	9	Biosynthesis of schiglautone and volvalerane type triterpenes
2.4	Tetracyclic iridals	10	Unusual tricyclic seco/nor-lanostane
2.5	Miscellaneous iridal triterpenoids	11	Biosynthesis of seco/nor-lanostane
3	Biosynthesis	12	Siphonanes and siphonellines
3.1	Biosynthesis of monocyclic iridals	13	Sodwanones and neviotines
3.2	Biosynthesis of bicyclic iridals	14	Biosynthesis of siphonanes, siphonellines, sodwanones, and neviotines
3.3	Biosynthesis of tri- and tetracyclic iridals	15	Onocerane and belamchinane-type triterpenoids
3.4	Biosynthesis of miscellaneous iridals	16	Biosynthesis of onocerane and belamchinane-type triterpenoids
4	Tricyclic 6-6-5 triterpenes	17	Chemical synthesis of unusual cyclized triterpenoids
4.1	Isomalabaricanes-type terpenes	17.1	Isomalabaricane-type triterpenoids
4.2	Isomalabaricane-derived nor-terpenoids	17.1.1	Synthesis of 21-desoxy-iridogermanal
4.3	Malabaricane type triterpenes	17.2	Isomalabaricane-type triterpenes
		17.2.1	Total syntheses of (±)-rhabdastrellic acid A and (±)-stelletins A and E
		17.2.2	Synthesis of BC-ring model of globostellatic acid X methyl esters
		17.3	Polypodanes
		17.3.1	Total synthesis of (+)-myrrhanol C

<sup>a</sup>Department of Bioorganic Chemistry, Leibniz Institute of Plant Biochemistry, Weinberg 3, Halle (Saale) D-06120, Germany. E-mail: Hidayat.Hussain@ipb-halle.de; Bernhard.Westermann@ipb-halle.de

<sup>b</sup>International Research Center for Food Nutrition and Safety, Jiangsu University, Zhenjiang 212013, China

<sup>c</sup>Department of Analytical Chemistry and Food Science, Faculty of Food Science and Technology, University of Vigo – Ourense Campus, Ourense, E-32004, Spain

<sup>d</sup>Department of Chemistry, Government College University Faisalabad, Faisalabad 38000, Pakistan

<sup>e</sup>Department of Chemistry and Polymer Science, University of Stellenbosch, Private Bag X1, Matieland, Stellenbosch 7600, South Africa

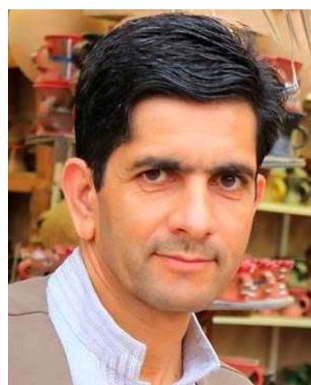


17.3.2	Total synthesis of (+)-myrrhanols A, B and (+)-myrrhanones A, B
17.4	Schiglaunanes
17.4.1	Total synthesis of an atropisomer of schiglaunone A
17.4.2	Synthesis of an advanced intermediate of schiglaunone A
17.5	Unusual tricyclic seco/nor-lanostane
17.5.1	Studies towards the total synthesis of kadcotrine B
17.6	Abudinols
17.6.1	Total synthesis <i>ent</i> -abudinol B
17.7	Muzitones
17.7.1	Total synthesis of muzitone and <i>ent</i> -muzitone
18	Conclusions
19	Author contributions
20	Conflicts of interest
21	Acknowledgments



*Dr. Akbar Ali is currently working as assistant professor at the department of chemistry, G. C. University Faisalabad. Before, he worked for 3 years as assistant professor at institute of Chemistry, University of Sargodha. Dr Akbar Ali has completed his PhD in the area of synthetic organic chemistry from Federal University of Sao Carlos, Brazil and Leibniz Institute of Plant Biochemistry (IPB), Germany. To*

*date he has more than 70 publications in reputed international journals with around 250 impact factor, 1102 citations, 20 h-index and 34 i10-index. His interests include organic synthesis, click chemistry, green and photo chemistry and asymmetric organocatalysis.*



*Hidayat Hussain was Post Doc (2004–2007), senior scientist (2009–2010) in University of Paderborn Germany, and Post Doc fellow (2007–2008) at University of Maine France. He worked at Uni. Nizwa Oman as Associate Professor (2011–2017) and AvH guest Professor (2018–2019) at Leibniz Institute of Plant Biochemistry (IPB), Germany. He was also a Visiting Professor at Scripps Institution*

*of Oceanography in 2017. Currently Dr Hidayat is associated with IPB, Germany and has 350 publications with impact factor over 1070. According to the Stanford University database, his name is included in the top 2% of the most-cited scientists for 2020, 2021 and 2022.*

## 22 Notes and references

# 1 Introduction

Triterpenes represent a versatile group of terpenes comprised of six isoprene subunits and to date over 30 000 triterpenes have been identified from various natural sources.<sup>1</sup> Moreover, around 200 different triterpene skeletons have been reported to be derived from cyclization products of squalene (S), oxidosqualene (OS), or bis-oxidosqualene (BOS) catalysed by triterpene synthases.<sup>2</sup> Apart from these, constantly new enzymes are identified which arrange precursors to these skeletons. Very recently, Tao *et al.*<sup>3</sup> described the non-squalene-dependent triterpene biosynthesis and discovered two chimeric fungal class I triterpene synthases (TrTSSs) for the conversion and production of hexaprenyl diphosphate into triterpenes.

Triterpenes are naturally present in fruit, vegetables and medicinal plants and are hence part of the daily human diet. A driving force behind triterpene research is the wide range of biological and pharmacological effects including cytotoxicity, inhibition of pathogenic microbes, anti-inflammatory, anti-protozoal, antitubercular, and antifeedant effects to name but a few. In addition, some triterpenes have illustrated enzymatic effects and have been shown to modulate specific receptor functions.<sup>4–7</sup>

The large majority of triterpenoids are 6-6-6-5 tetra-cycles, 6-6-6-6-5 pentacycles, or 6-6-6-6-6 pentacycles and these compounds are biosynthetically formed *via* cascade cyclizations and rearrangements of either squalene (S) or 2,3-oxidosqualene (OS). Although the majority of the triterpenes contain tetra- or pentacyclic skeletons, together with these triterpenes derived from cyclization processes there are a number that deviate from these mainstream polycyclization of S and OS to tetra- or pentacyclic compounds which have been reported from Nature. These triterpene structures, referred to as “unusually cyclized triterpenoids” are generated from unusual cyclizations of



*Dr. Jianbo Xiao is current a full professor of Jiangsu University (China) and a distinguished researcher of University of Vigo (Spain). He has worked as a Postdoc supported by AvH foundation at University of Würzburg, Germany (2013–2015) and then worked as an assistant professor in University of Macau (2015–2020). His research is focusing on chemistry and function of natural products. Dr Xiao*

*has been selected as Clarivate Analytics Highly Cited Researchers for 5 times since 2016. He has accepted and published more than 300 peer reviewed papers including Nature Reviews Drug Discovery, Seminars in Cancer Biology, and so on.*



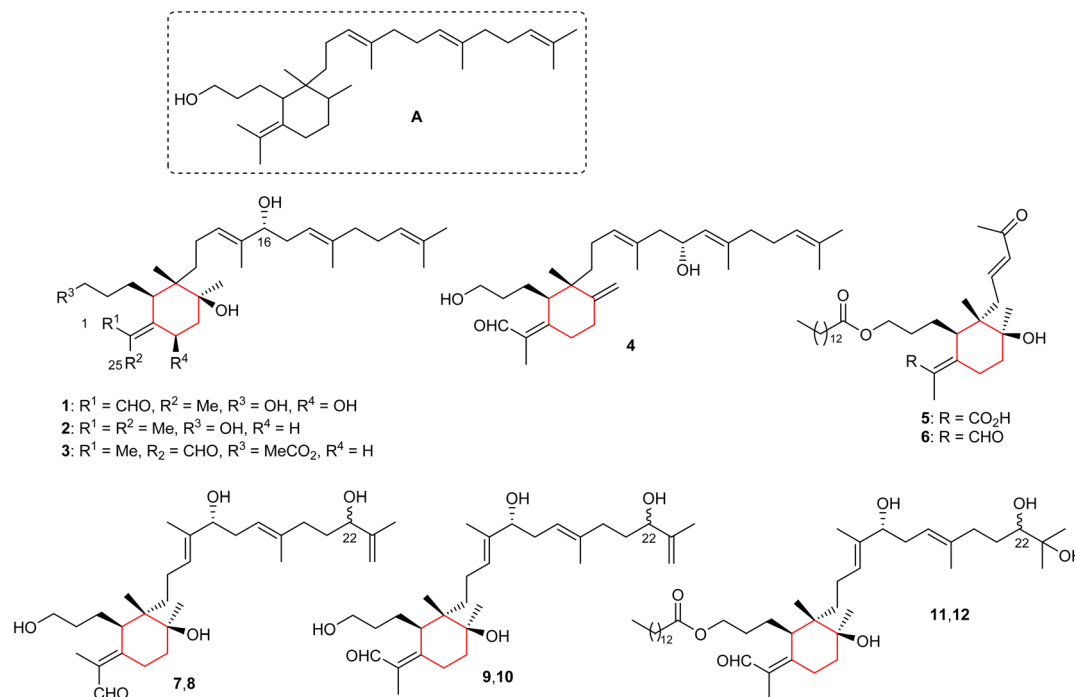
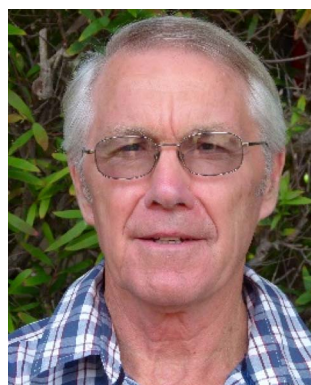


Fig. 1 Structures of monocyclic iridals 1–12.

squalene (S) and 2,3-oxidosqualene (OS).<sup>2,8</sup> These “unusually cyclized triterpenes” are biosynthesized *via*: (i) incomplete cyclization of the S-derived molecules whose cyclization processes start from the epoxide or terminal isopropylidene core and generate mono-, bi- and tricyclic triterpenoid skeletons. (ii) Cyclization of S or OS to generate polycyclic triterpenoid skeletons followed by cleavage of the already established ring systems. (iii) Two independent cyclizations of the S- or OS-derived molecule.<sup>8</sup>

This review provides a comprehensive and critical coverage of 180 new unusual cyclized triterpenoids reported from January

2009 through to December 2021, and serves to complement the previous review of unusual cyclized triterpenoids published in Natural Product Reports.<sup>8</sup> In addition, this review includes a few previously omitted articles published between 1998 and 2008. Notably, included are *nor*-iridal and *nor*-isomalabaricane terpenes which are biosynthetically derived from iridal and isomalabaricane-type triterpenoids. In much the same way as the previous review, the format focuses on the discovery of new unusual cyclized triterpenoids from natural sources along with their synthesis and biological effects. Additionally, recent studies of the fascinating biosynthesis of these unusual cyclized



Ivan Green graduated with a PhD in Synthetic Organic Chemistry in 1972 from the University of Cape Town. He started his career as Lecturer in 1973 and was made a full Professor in 1986 and later a Senior Professor in 1990 at the University of the Western Cape where he lectured for 39 years until his retirement in July of 2011. Upon retirement, he was invited to join the University of

Stellenbosch as a Research Associate where he is involved in doing research in various topics. He has over 200 publications, and has supervised 24 PhD students.



Prof. Dr Bernhard Westermann received his PhD in 1989, Profs. W. Sucrow and H.-J. Altenbach at the University of Paderborn, Germany. After a postdoctoral stay at the University of Toronto, Canada (Prof. J. B. Jones) from 1990 to 1991, he started his independent scientific career at the University of Paderborn. After his habilitation in 1998, he stayed as an associate professor. In 2004 he

moved to the Leibniz-Institute of Plant Biochemistry as head of Biofunctional Synthesis, where he continues to work on topics dealing with natural product synthesis, ligation strategies with multicomponent reactions, ligation strategies, and plant hormones.



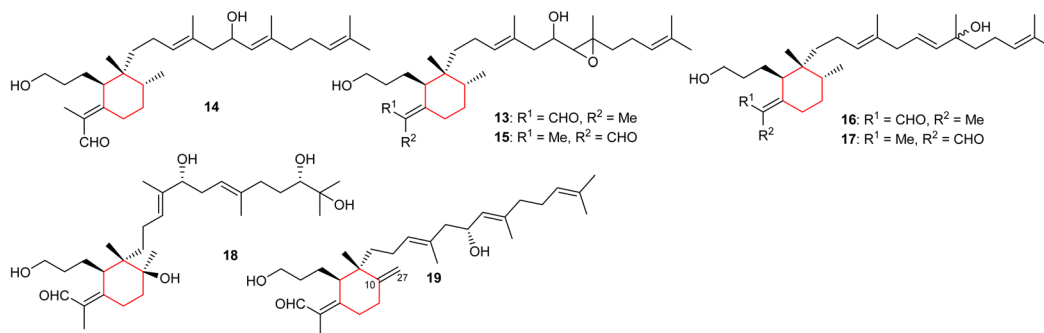


Fig. 2 Structures of monocyclic iridals 13–19.

triterpenoids are covered in this review. There have been numerous synthetic strategies towards forming these unusual cyclized triterpenoids as end products and these studies are also covered in this review. Notably, characteristic features of unusual cyclized triterpenoids with their high degree of skeletal and structural diversification are also discussed.

## 2 Iridal triterpenes

### 2.1 Monocyclic iridals

The basic iridal nucleus is depicted in Fig. 1 and this skeleton forms from squalene epoxide. In addition, the majority of the iridal natural products are typified by a C-1 carbonyl function (mostly aldehyde), and an ester, or alcohol at C-3. Four monocyclic iridal

triterpenes *viz.*, 8-hydroxylisoiridogermanal (1), belamcandane A (2), 3-*O*-acetyliridobelamal A (3), and belamcandal A (4) (Fig. 1) have been isolated from the rhizomes of *Belamcanda chinensis* collected from China. Iridals 1–3 feature a hydroxyl group at C-16 of the polyene side chain while triterpene 4 has a hydroxyl group at C-17.<sup>9</sup> In addition, compounds 1 and 4 have an aldehyde function at C-1 and C-25, respectively. On the other hand, compound 3 is a rare iridal terpenoid which is lacking a carbonyl function at C-1 or the C-25 position. Bioassays for compounds 1–4 revealed inactivities towards various human cancer cells.<sup>9</sup>

Iriwattins A (5) and B (6) (Fig. 1), two unusual sixteen carbon comprising *nor*-iridal triterpenes were isolated from the flower *Iris wattii*. Furthermore, compounds 5 and 6 illustrated notable protein-tyrosine phosphatase 1B (PTP1B) enzyme inhibition of

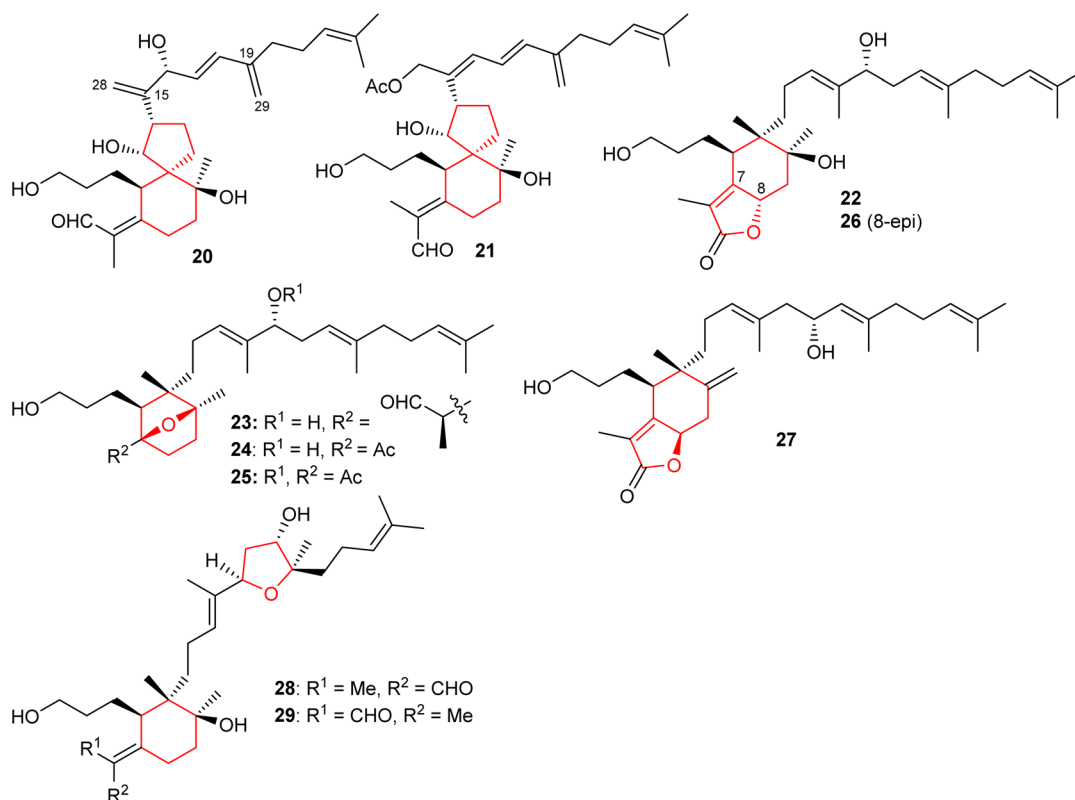


Fig. 3 Structures of bicyclic iridals 20–29.



52% and 14%, respectively.<sup>10</sup> Iritectol D (7), 22-epiiritectol D (8), iritectol E (9), 22-epiiritectol E (10), iritectol F (11), and 22-epiiritectol F (12) were produced by *Iris tectorum*. All of them were isolated as pairs of C-22 epimers and all possess a hydroxyl group at C-16 of the polyene side chain while metabolites 11/12 have a C-14-ester group at the C-3 hydroxyl group of the side chain of the ring along with an additional hydroxyl moiety at C-23.<sup>11</sup>

Three monocyclic iridal-type triterpenoids 13–15 (Fig. 2) were isolated from *Iris delavayi*. Iridal 13 is the geometrical isomer of 15, with respect to the aldehyde group at C-1. In addition, metabolites 13–15 are rare iridals missing the C-10 tertiary hydroxyl group.<sup>12</sup> A literature survey revealed that only a few iridals described earlier are missing the C-10 tertiary hydroxyl group, such as marneral,<sup>13</sup> marnerol,<sup>13</sup> and 22,23-epoxy-10-deoxy-21-hydroxyiridal.<sup>14</sup> Furthermore, compounds 13 and 15 contain an epoxide function at the C-18/C-19 position of the side chain.<sup>12</sup>

In another report, two iridal-type triterpenoids, named forrestins A (16) and B (17), were reported from *I. forrestii*. Both compounds are geometrical isomers of each other with respect to the aldehyde group. Moreover, compounds 16 and 17 have a tertiary hydroxyl group at C-19 of which the stereochemistry has not been established.<sup>15</sup> Shi *et al.*<sup>16</sup> reported iridojaponal C (18) from *I. japonica* and this compound illustrated moderate hepatoprotective effects. Moreover, iridal 18 has three hydroxyl groups in the polyene side chain. In 2018, Chen *et al.*<sup>17</sup> reported the isolation of 17-hydroxyl-27-ene-iridal (19) from *I. confusa*. It features an exocyclic double bond between C-10/C-27 which is interestingly, also present in belamcandal A (4). Compounds having an exocyclic double at C-10/C-27 are very rare and were not reported in the previous review.<sup>8</sup>

## 2.2 Bicyclic iridals

Spirioiridoconfal C (20) along with isobelamcandal (21) (Fig. 3) were reported from related *I. confusa*. Metabolites 20 and 21 are spirioiridoconfals bearing C-19 and C-29 based exocyclic double bonds while compound 20 has an additional exocyclic bond at C-15 and C-28. Metabolite 20 (IC<sub>50</sub>: 85 μM; SI = 2.1) illustrated anti-HBV pronounced effects towards HBV DNA replication.<sup>17</sup> A literature survey revealed that the earlier described iridotectoral B<sup>18</sup> and hoogianal<sup>19</sup> have a similar cyclopentane based spirocyclic core and were reported from the *Iris* species. *Belamcanda chinensis* rhizomes, collected from the Hebei province in China, produced two unusual iridal triterpenes named belamcanolide A (22), and belamcanoxide A (23). The latter compound demonstrated good cytotoxic effects towards colon (HCT-116), liver (HepG2), gastric (BGC-823), and lung (NCI-H1650) cancer cells with IC<sub>50</sub> ranging from 3.2 to 7.5 μM.<sup>20</sup>

Two *nor*-iridals named belamcanoxide B (24) and 16-*O*-acetylbelamcanoxide B (25) were isolated from *Belamcanda chinensis*. Furthermore, belamcanoxide B (24) illustrated good cytotoxic effects towards MCF-7 and HCT-116 cell lines with IC<sub>50</sub>: 3.4 and 5.6 μM respectively.<sup>9</sup> In addition, this plant produces two further iridal lactones *viz.*, belamcanolides B (26), and C (27).<sup>9</sup> Compounds 22, 26, and 27 are rare examples of a 5/6-fused bicyclic iridal lactone, in which these metabolites bear a furanone ring (lactone ring) attached between C-7 and C-8.

Interestingly, compounds 23–25 feature an ether linkage between C-7 and C-10 of the 6-membered ring. In addition, molecule 23 is a structurally unique iridal having an isolated aldehyde in place of the α,β-unsaturated aldehyde moiety which is common for iridal-type triterpenoids. It is interesting to note that compounds 22 and 26 are C-8 epimers while iridals 22, 23, and 26 feature a hydroxyl group at C-16.<sup>9</sup>

Both geometrical isomers *viz.*, iritectorols C (28)<sup>11</sup> and G (29)<sup>21</sup> (Fig. 3), include the tetrahydrofuran moiety between C-16/C-19 in the polyene side chain, and are produced by *Iris tectorum*. Iritectorol 28 illustrated good cytotoxic effects towards liver cancer (HePG2) with IC<sub>50</sub>: 4.1 μM. On the other hand, it also possessed moderate effects towards ovarian cancer (A2780: IC<sub>50</sub>: 6.5 μM), colon cancer (HCT-16: IC<sub>50</sub>: 9.7 μM), and lung cancer (NCI-H1650: IC<sub>50</sub>: 9.8 μM).<sup>21</sup> Additionally, iritectol G (29) illustrated anti-epileptic effects *via* inhibiting spontaneous (IC<sub>50</sub>: 8.2 μM) and 4-aminopyridine-evoked calcium oscillations (IC<sub>50</sub>: 12.5 μM).<sup>21</sup>

## 2.3 Tricyclic iridals

Li *et al.*<sup>22</sup> reported four iridal-type triterpenoids named polycycloiridals P-T (30–34) (Fig. 4) from *Belamcanda chinensis*, which is an ornamental plant of the Iridaceae family. These bicyclic metabolites have an additional cyclopentane core unit resulting from a C-18 and C-22 cyclization of the homofarnesyl chain. Furthermore, iridals 30/31 and the corresponding 32/33 are pairs of Δ<sup>2(7)</sup> olefinic geometric isomers. Moreover, compound 34 has an ethoxy group at C-12 and based on extraction protocols, the authors proposed that this compound might be an artifact, although as yet, not proven.

Investigations of *B. chinensis* extracts yielded two unusual tricyclic-iridal triterpenoids named belamcandanes A (35) and B (36) (Fig. 4). It was found that these metabolites carry a rare α-terpineol moiety in their polyene side chain. Both compounds

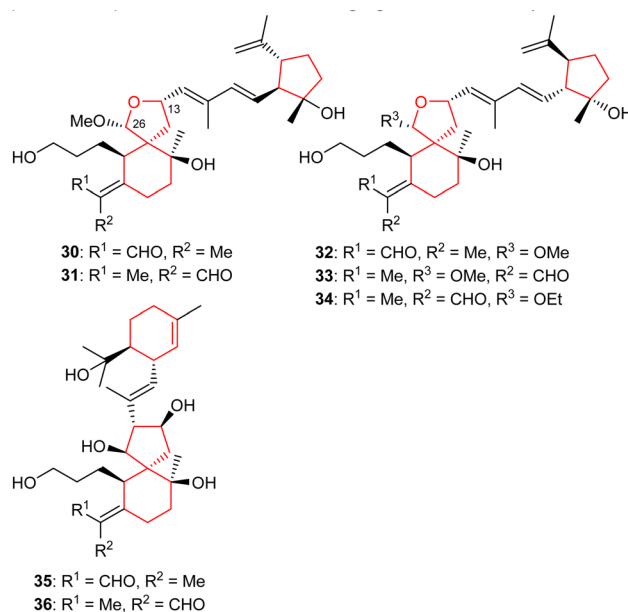


Fig. 4 Structures of tricyclic iridals 30–36.



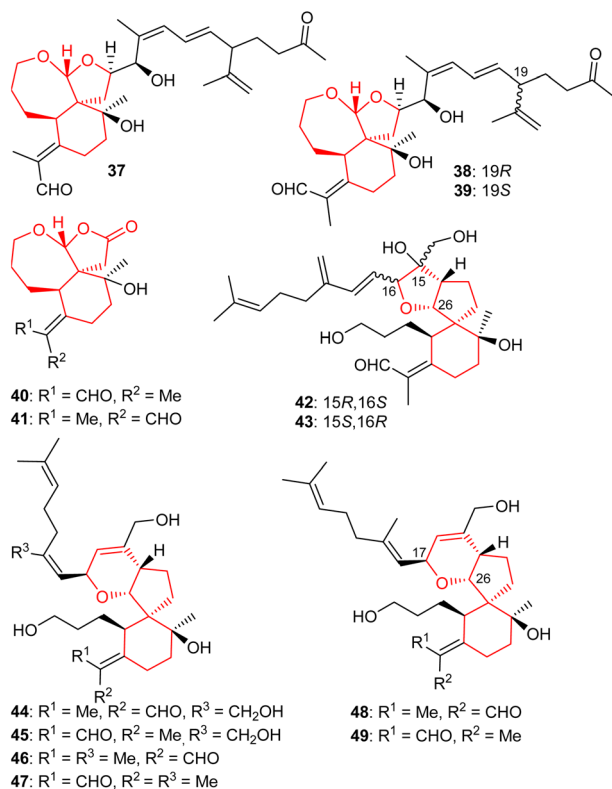


Fig. 5 Structures of tricyclic iridals 37–49.

possessed moderate hepatoprotective effects while they were not active towards NCI-H1650, HepG2, BGC 823, HCT-116, and A2780 cancer cells.<sup>23</sup> Iridals 30–34 feature a spiro furan ring formed *via* the C-13 hydroxyl group attack to a C-26 aldehyde group. A literature survey revealed that iridotectoral A,<sup>18</sup> (13*R*)-iridotectoral C,<sup>24</sup> and D,<sup>18</sup> have a similar furan based spiro cyclic core reported from other *Iris* species.

A further three iridal-type triterpenoids, iritector G (37), iritector H (38) and 19-*epi*-iritector H (39) (Fig. 5) bearing a rear-ranged homofarnesyl side chain and a 6/7/5 core system, were also reported from *I. tectorum*. Moreover, compound 37 is the second compound having been assigned the same name *viz.*, iritector G because compound 29 has already been reported with the same name. Iridals 38 and 39 are C-19 epimers and this diastereomeric mixture was shown to possess moderate neuroprotective effects.<sup>25</sup>

In another report, iridojaponal A (40) and B (41) were produced by *Iris japonica*. Notably, iridojaponal A (40) and B (41) are sixteen carbon comprising degraded iridals. Iridals 40 and 41 demonstrated moderate hepatoprotective effects.<sup>16</sup> Chen *et al.*<sup>17</sup> reported that the spiroiridoconfals A (42) B (43) were isolated from *I. confusa*. Metabolites 42 and 43 are spiro-iridals bearing a C-16 and C-26 based tetrahydrofuran ring.

Six iridal-type triterpenoids, named spiroiridotectals A–F

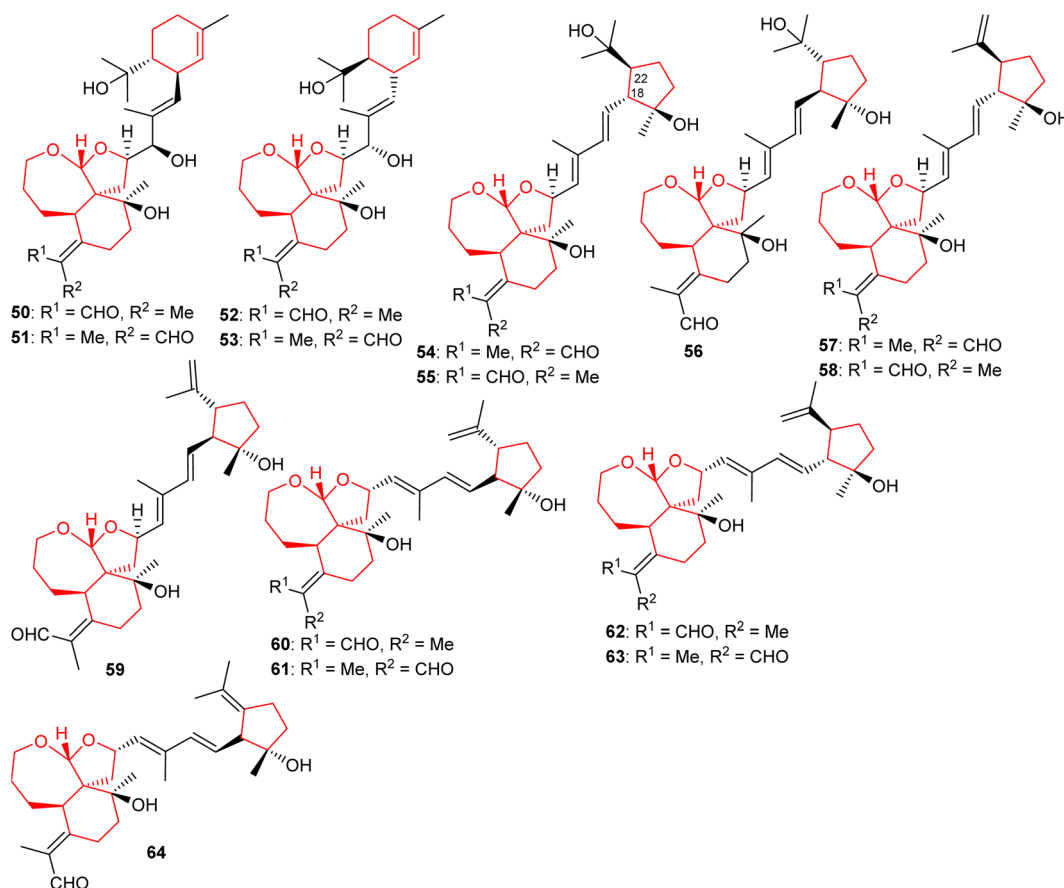
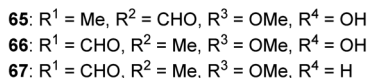


Fig. 6 Structures of tetracyclic iridals 50–64.





(44–49) representing three pairs of geometrical isomers (with respect to aldehyde group), were produced by *I. tectorum*. Interestingly, compounds 44–49 feature a 3,6-dihydro-2*H*-pyran core between C-17 and C-26. Moreover, iridals 44 and 45 are geometrical isomers of compounds 46 and 48 with respect to the *exo*-C-18/19-double bond only. Furthermore, metabolites 44, 45 and 49 possess moderate neuroprotective effects towards PC12 cell.<sup>26</sup> In addition, spirioiridotectal D (45) suppressed NO production with an IC<sub>50</sub>: 0.54 μM.<sup>27</sup>

Four new iridal polycycloiridals A–D (**50–53**) (Fig. 6), having an unusual  $\alpha$ -terpineol group were isolated from *I. tectorum*. Iridals **50** and **52** have a distinct absolute configuration at the  $\alpha$ -terpineol group. Moreover, compounds **50–53** illustrate hepatoprotective effects towards D-galactosamine-induced toxicity with activity ranging between 65 to 96%.<sup>28</sup> In another report, polycycloiridals

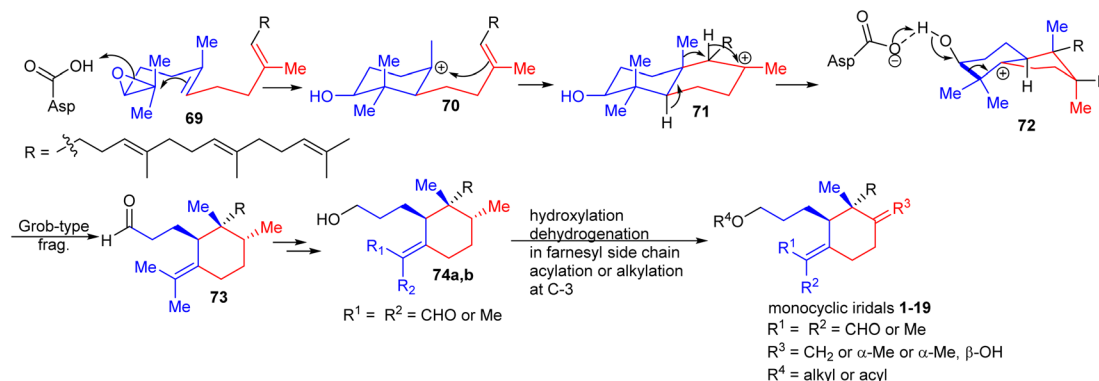
## 2.5 Miscellaneous iridal triterpenoids

Three spiroiridal-isoflavone hybrid compounds named belamcandans A–C (**65–67**) (Fig. 7), have been isolated from *B. chinensis*. Metabolites **65–67** represent rare iridal-flavone hybrid compounds. Biological investigation of these compounds demonstrated that they were not active towards lung cancer (NCI-H1650), hepatocellular cancer (HepG2), stomach cancer (BGC 823), colon cancer (HCT-116), and breast cancer (MCF-7).<sup>20</sup> An unusual dimeric iridal-type triterpenoid, named dibelamcandal A (**68**) having two iridal type triterpenoid units and linked *via* a cyclohexene ring (gives rise to dimerization *via* a [4 + 2]-cycloaddition), was reported from *B. chinensis*. Furthermore, this compound illustrates promising molluscicide effects towards *Pomacea canaliculate* with an LC<sub>50</sub>: 1.3 µg mL<sup>-1</sup>.<sup>29</sup>

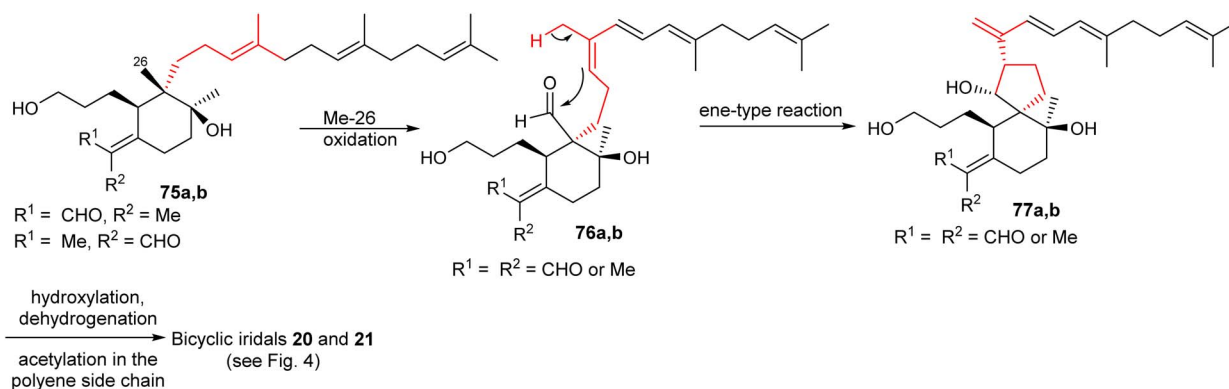
### 3 Biosynthesis

### 3.1 Biosynthesis of monocyclic iridals

Oxidosqualene cyclases are key enzymes which are responsible for the intriguing structural diversity of triterpenes derived from oxidosqualene (**69**)<sup>30,31</sup> (Scheme 1). Over 100 triterpene skeletons have been reported from oxidosqualene (**69**) *via* catalytic variability in cation- $\pi$  annulation, ring expansion, hydride or 1,2-methyl shifts, and deprotonation. In 2006, Xiong *et al.*<sup>30</sup> experimentally proved that oxidosqualene (**69**) is converted into bicyclic **72** *via* cyclization, hydride and 1,2-methyl shifts, which subsequently undergoes a Grob-type fragmentation to achieve monocyclic iridal skeleton **73**. The latter compound could be reduced or oxidized in order to achieve iridals **74a,b** (see also



**Scheme 1** Biosynthesis of monocyclic iridals **1–19**. Reproduced from ref. 30 and <sup>31</sup> with permission from the John Wiley and Sons.



Scheme 2 Hypothetical biosynthesis of bicyclic iridals **20** and **21**. Reproduced from ref. 23 with permission from the Elsevier.

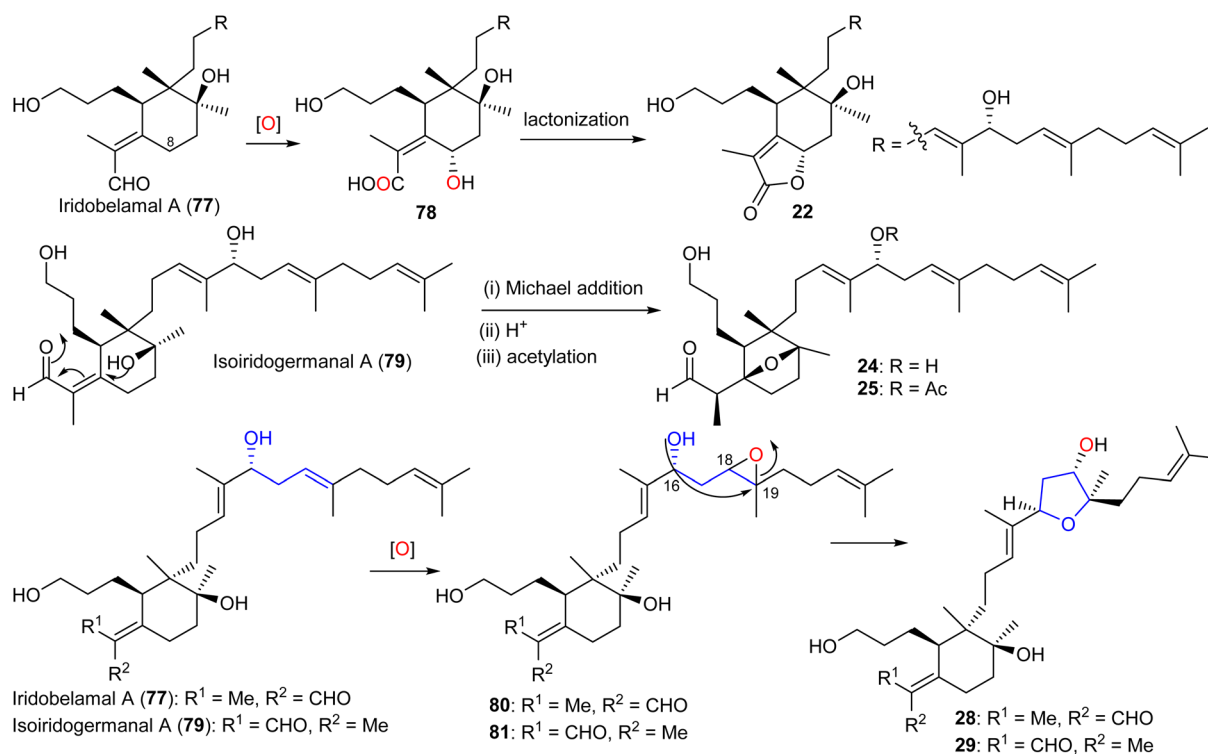
Fig. 1). The study further demonstrated that the *Arabidopsis thaliana* gene At5g42600 is responsible to encode an oxidosqualene cyclase acting as a catalyst for the Grob-type fragmentation. In addition, further hydroxylation and dehydration, and dehydrogenation in the polyene side chains provided iridals **1–19**.

### 3.2 Biosynthesis of bicyclic iridals

Plausible biosynthetic pathways for some bicyclic iridals were proposed as shown in Schemes 2 and 3.<sup>23</sup> Upon oxidation of the Me-26 groups in iridal **75a** and its geometric isomer **75b**,<sup>23,32,33</sup> nucleophilic attack of the C-14 double bond to the C-26 aldehyde carbonyl (**76a,b**) forms the 6/5 spiro bicyclic skeletons

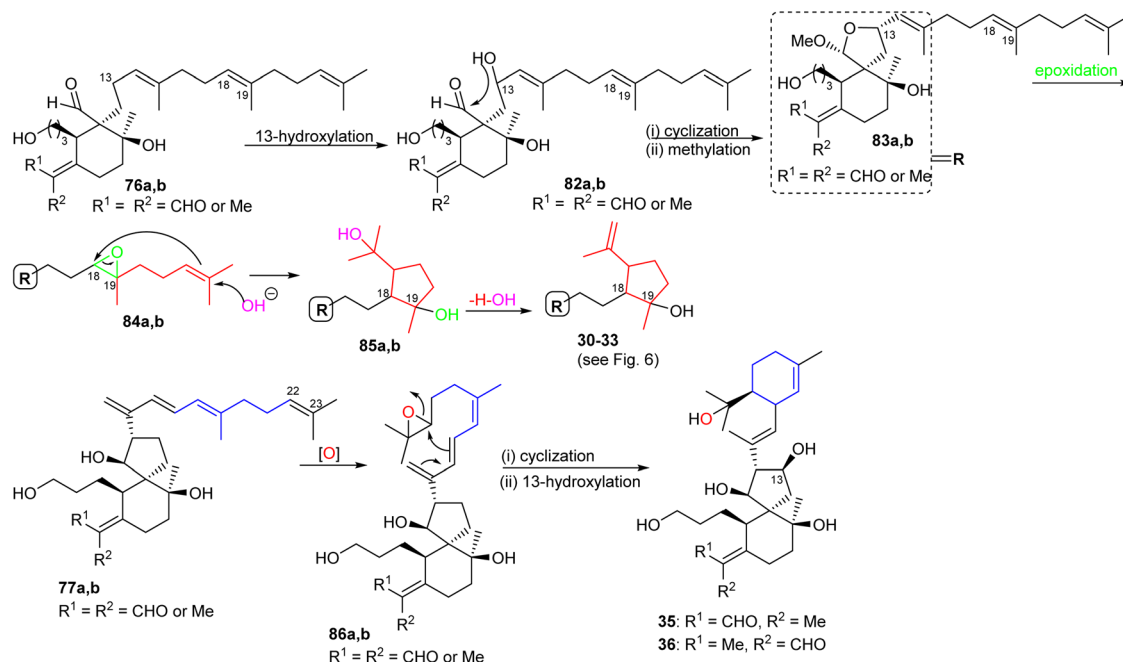
**77a,b** in an ene-type reaction. Subsequently, further functionalization would be possible at the unsaturated polyene side chain *via* hydroxylation, dehydrogenation, and acetylation and thus could provide iridals **20** and **21**.

After oxidation of the C-25 aldehyde moiety in iridobelamal A (**77**) along with C-8 hydroxylation, the subsequent lactonization between the CO<sub>2</sub>H group at C-25 and the C-8 hydroxyl group to belamcanolide A (**22**) is initiated (Scheme 3). Moreover, belamcanoxide B (**24**) and 16-*O*-acetylbelamcanoxide B (**25**) are suggested to be derived from belamcanoxide A (**79**), which would involve an oxa-Michael addition, and acetylation to lead to the target compounds **24** and **25**.<sup>20</sup> On the other hand, iridectols C (**28**) and G (**29**) could biosynthetically be derived from iridobelamal A (**77**) and its isomeric isoiridogermanal (**79**),



Scheme 3 Plausible biosynthesis of bicyclic iridals **22**, **24**, **25**, **28**, and **29**. Reproduced from ref. 11 and <sup>20</sup> with permission from the Elsevier and Royal Society of Chemistry respectively.





Scheme 4 Plausible biosynthesis of tricyclic iridals **30–33**, **35**, and **36**. Reproduced from ref. 23 with permission from the Elsevier.

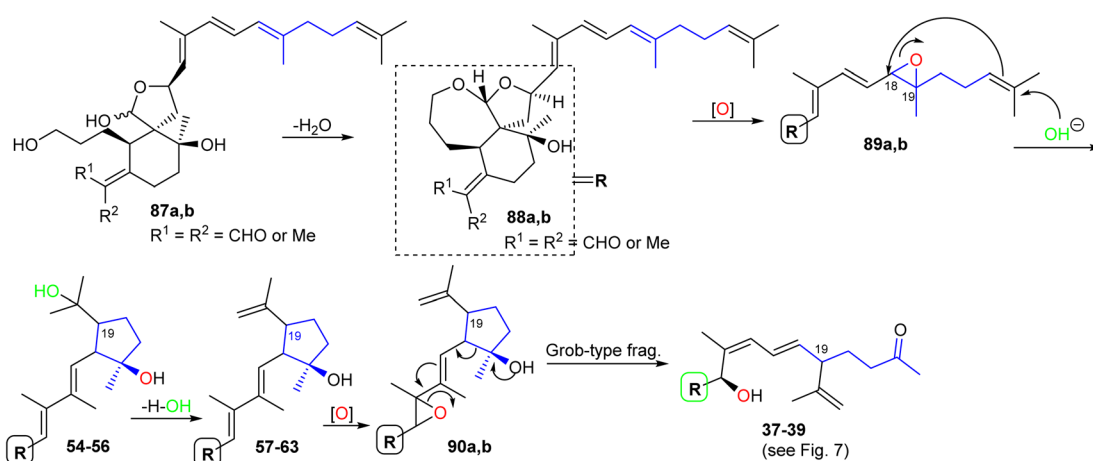
which after epoxidation at C-18/C-19 following by nucleophilic attack of the C-16 hydroxyl group to C-19 is formed.<sup>11</sup>

### 3.3 Biosynthesis of tri- and tetracyclic iridals

The biosynthesis of tri- and tetracyclic iridals **30–33** is initiated by C-13 hydroxylation in compound **76** to yield intermediate **82a,b**, followed by nucleophilic attack of the C-13 OH group to the C-26 aldehyde carbonyl to achieve the 6/5 spiro bicyclic hemiacetals **83a,b** (Scheme 4). Subsequently, epoxidation at C-18/C-19 which is consequently opened by hydroxyl attack at C-23 is followed by the cascade reaction resulting in attack of the resulting C-22 nucleophile at C-18 of the epoxide ring leading to the C-22/C-18 cyclopentane ring systems (**85a,b**). The latter compound could then undergo a dehydration of the tertiary alcohol to produce iridals **30–33**. On the other hand the C-22/C-23 double in the side chain could

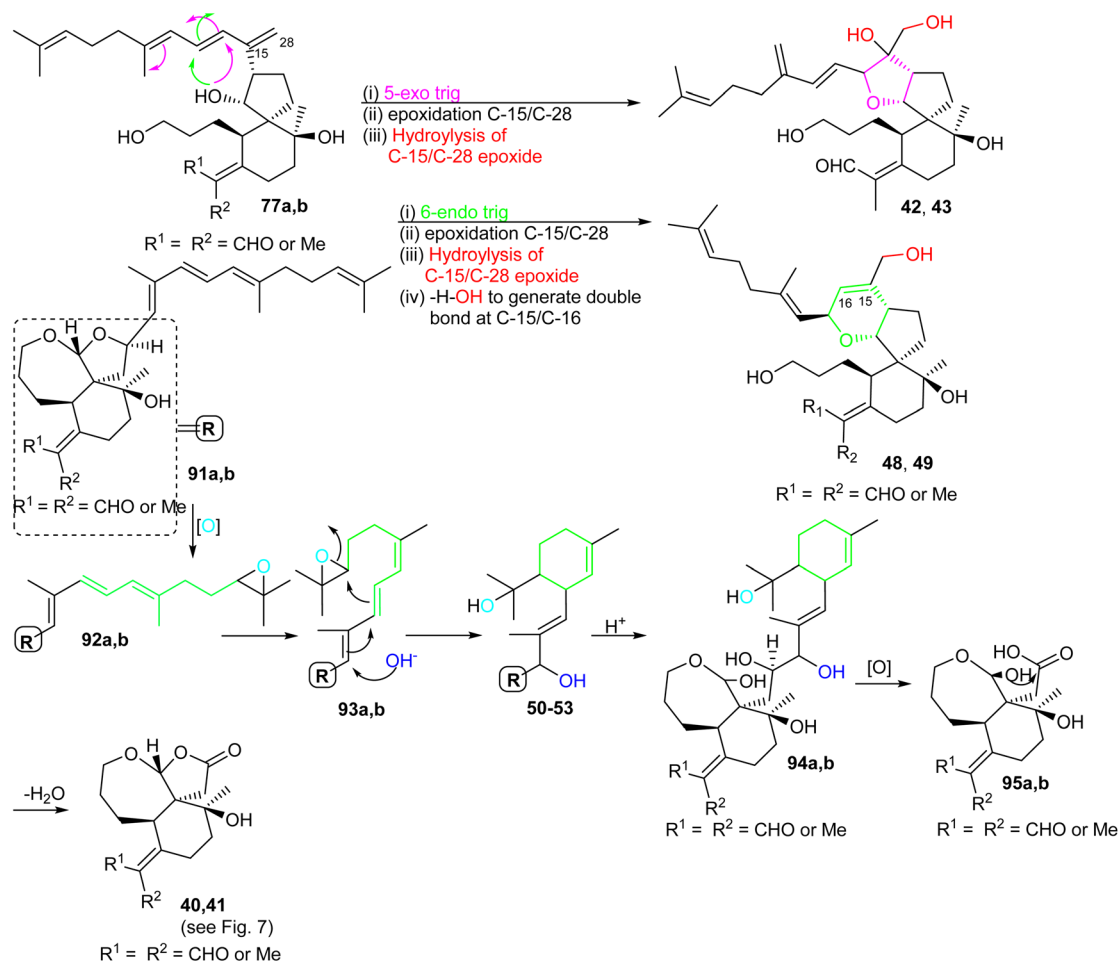
be epoxidized to form **86a,b** and the iridals **35/36** could then be formed through cyclization of the unsaturated side chain *via* nucleophilic attack of the C-16/C-17 double to C-22 followed by C-13 hydroxylation.<sup>23</sup>

The biosynthesis of iridals **37–39** and **54–63** is initiated by acetal formation between the C-3 hydroxyl group and C-26 hemiacetal in **87a,b** affording ketal **88a,b** which is followed by epoxidation at C-18/C-19 to epoxide **89a,b** (Scheme 5).<sup>25</sup> Further conversion steps *viz.*, nucleophilic addition of an OH at C-23, nucleophilic attack of the double bond to C-18, and dehydration lead to iridals **54–63**. The final formation to iridals **37–39** could be considered by an additional epoxidation at C-15/C-16 to form **90a,b** followed by attack at the epoxide ring and cleavage of the cyclopentane ring leading to the ring-opened hydroxy ketones **37–39**.<sup>25</sup>



Scheme 5 Hypothetical biosynthesis of tricyclic iridals **37–39** and **54–63**. Reproduced from ref. 25 with permission from the Elsevier.





Scheme 6 Hypothetical biosynthesis of tricyclic iridals 40–43 and 48–53. Reproduced from ref. 16 with permission from the Elsevier.

For the formation of iridals 40–43, 48–53, spirocyclic 77a,b (Scheme 6) undergoes a 5-*exo trig* cyclization followed by C-15/C-28 epoxidation and then resulting epoxide hydrolysis could provide iridals 42 and 43. Similarly, the same intermediate might also undergo 6-*endo trig* cyclization followed by C-15/C-28 epoxidation and dehydration to produce iridals 48 and 49. According to Baldwin's rule, 5-*exo trig* and 6-*endo trig* cyclizations are favored but enzymes can possibly catalyze the chemically disfavoured pathways as well.<sup>34</sup> Moreover, the biosynthetic precursor of iridals 50–53 might possibly be traced back to either *epi*-anhydrobelachinal or *iso*-anhydrobelachinal (91a,b),<sup>28,35</sup> which could undergo a series of conversions such as epoxidation at C-22/C-23, nucleophilic hydroxyl addition at C-14, and intramolecular cyclization to form 50–53 (Scheme 6). The biosynthetic route of iridals 40 and 41 could commence from iridals 50–53 *via* acid catalysis to produce the key intermediates 94a,b. Subsequently, intermediates 94a,b might undergo C-13/C-14 bond oxidative cleavage to afford 95a,b. Finally, dehydration of the later compound could form the degraded iridals, iridojaponals A (40) and B (41).<sup>16</sup>

### 3.4 Biosynthesis of miscellaneous iridals

Belamcandal (96) or its geometrical isomer could initially undergo deacetylation, double bond isomerization, and C-17

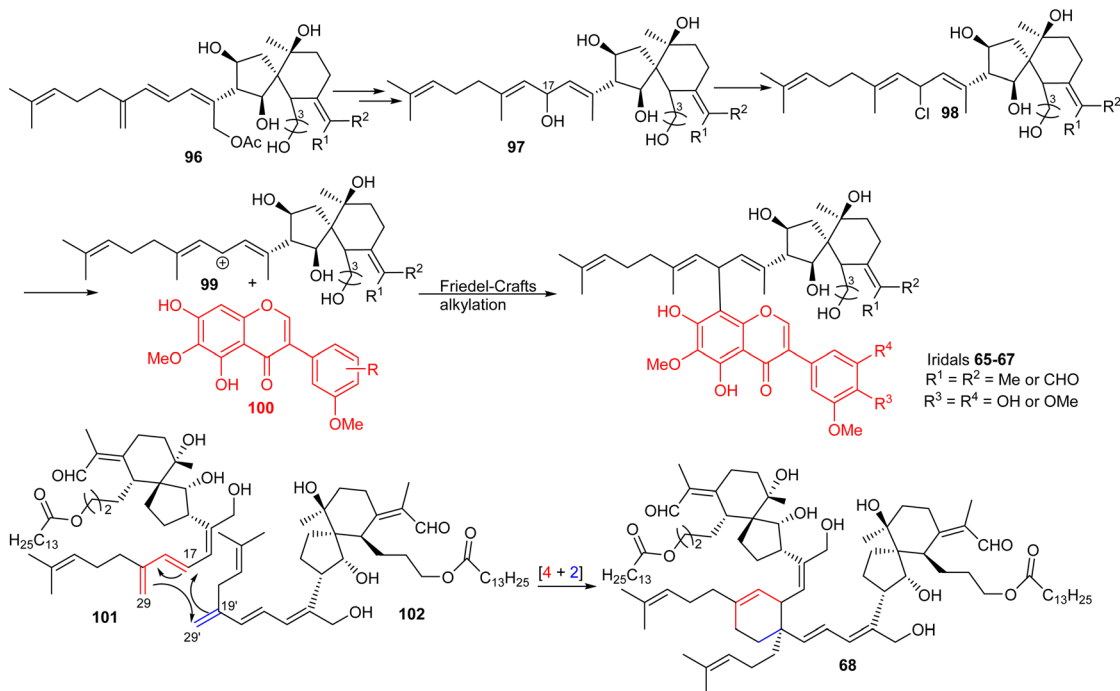
hydroxylation. Moreover chlorination of the resulting hydroxyl group could afford the chlorinated product 98, which might undergo dechlorination to provide cation 99 (Scheme 7). Subsequent, Friedel–Crafts alkylation between later cation 99 with isoflavone 100 *via* typical Friedel–Crafts alkylation mechanism would produce belamcandansins A–C (65–67).<sup>20</sup> On the other hand, dibelamcandal A (68) could be biosynthesized through the [4 + 2] $\pi$  Diels–Alder reaction at C-29/C-29' and C-17/C-19' between the two monomers 101 and 102 (Scheme 7).<sup>29</sup>

## 4 Tricyclic 6-6-5 triterpenes

### 4.1 Isomalabaricanes-type terpenes

Literature revealed that the genus *Rhabdastrella*, which can be found in tropical oceans<sup>36</sup> produced various isomalabaricane triterpenes with intriguing chemical diversity and demonstrating a wide range of biological effects.<sup>37–39</sup> Isomalabaricanes are a group of tricyclic triterpenes bearing a 6/6/5 *trans-syn-trans* tricyclic core attached to a polyene side chain (Table 1, structure “B”). The difference between isomalabaricanes and malabaricanes is in the stereochemistry of the B–C ring junction: *trans-syn-trans* (iso) and *trans-anti-trans*, respectively. The overwhelming number of structural features distinguishing these metabolites can be found in the terpenoid side chain, which





**Scheme 7** Plausible biosynthesis of miscellaneous iridals **65–68**. Reproduced (with slight modification from **97** to **65–67**) from ref. 20 and <sup>29</sup> with permission from the Royal Society of Chemistry and American Chemical Society respectively.

consists of acyclic isoprene-units up to sesquiterpenes. The side chains remain acyclic, or depending on the oxidation state, have been cyclized into gamma and delta lactones. Carbocyclic moieties within the side-chains most likely result from ene- or aldol reactions.

Among the isomalabaricanes isolated from *R. aff. distincta* (**103–108**), only rhabdastrellin A (**103**) showed moderate cytotoxic effects toward leukemia (HL-60:  $\text{IC}_{50}$ :  $4.2 \mu\text{g mL}^{-1}$ ), which may be related to the 2-pyrone modified side chain and which closely resembles previously reported Jaspolidis A and B.<sup>40</sup> Rhabdastrellins B–F (**104–108**) contain only acyclic side chains altering in their oxidized positions, although the stereochemistry of the C-24 hydroxyl group of the side chain in Rhabdastrellin B (**104**) could not be unambiguously established. For the relative stereoconfiguration of isomalabaricanes, it was demonstrated during isolation, that these triterpenoids are isomerized at C-13 *via* exposure to light and thus, it was suggested that the 13-*Z* isomers might be artefacts rather than new entities.<sup>36</sup> In another report, Kiem *et al.*<sup>41</sup> reported isomalabaricane derived *nor*-terpenoids named rhabdastrellins G–K (**109–113**) from the sponge *R. providentiae*. Compounds **109–111** possessed cytotoxic effects towards HepG2, MCF-7, LU-1, SK-Mel2, and HL-60 with  $\text{IC}_{50}$  ranging from 11 to  $85 \mu\text{M}$ . Notably, the 20(22)-*Z* isomer **110** illustrated much better cytotoxic effects ( $\text{IC}_{50}$ : from 11 to  $16 \mu\text{M}$ ) in comparison with the 20(22)-*E* isomer **109** ( $\text{IC}_{50}$ : from 56 to  $87 \mu\text{M}$ ).

The marine sponge *R. globostellata* produced the side-chain shortened isomalabaricane triterpenes globostelletins B–I (**114–121**) (Table 1).<sup>42</sup> Compounds **114–121** were tested against various cancer cell lines with only moderate activities. Again,

among the 13*E*/13-*Z* isomers, globostelletins H (**120**) and I (**121**), isomer **121** (13-*Z*) illustrated better inhibitory effects towards A2780 ( $\text{IC}_{50} = 7.6 \mu\text{M}$ ) than its *E* isomer *viz.*, compound **120** (13-*E*) (A2780:  $\text{IC}_{50} = 8.1 \mu\text{M}$ ).

The same organism also produced globostelletins J–R (**122–130**) bearing cyclopentane modified side chains. Natural products **122–126** have the five-membered cyclopentane core formed between C-15 and C-23 in the polyene side chain while compounds **127** and **128** (Table 1) feature a 25-dimethyltetrahydrofuran moiety, which was joined to another cyclopentane core such as 20-hydroxy-20-methylcyclopentane at the C-17 and C-24 positions.<sup>43</sup> Moreover, compounds **129** and **130** bearing a substituted cyclopentane core feature a hydroxyl group at C-22. Globostelletins K (**123**) and L (**124**) illustrated moderate inhibition towards focal adhesion kinase (FAK), protein kinases (ALK), Aurora-B, and VEGF-R2. On the other hand, the remaining compounds were not active towards sixteen tumor-related protein kinase enzymes.<sup>43</sup>

In another report the sponge *Stelletta* sp. collected from Hainan, China, produced the isomalabaricane triterpene stellettin N (**131**).<sup>44</sup> This single member was associated with a natural product family resulting from isolation studies done on *St. tenuis*. In this regard Li *et al.*<sup>45</sup> isolated isomalabaricane triterpenes *viz.*, stellettins N–P (**132–134**) from this marine sponge. Unfortunately, one of the compounds *viz.*, **132** was again published as “stellettin N” because metabolite **131** was already named as “stellettin N”.<sup>44</sup> Some features of compound **132** are unique such as the C-13  $\beta$ -hydroxyl group as well as the saturated C-13/C-14 bond. The vast majority of this family have fully conjugated polyene side chains. Very few isomalabaricane



Table 1 Triterpenes with the isomalabaricane skeleton

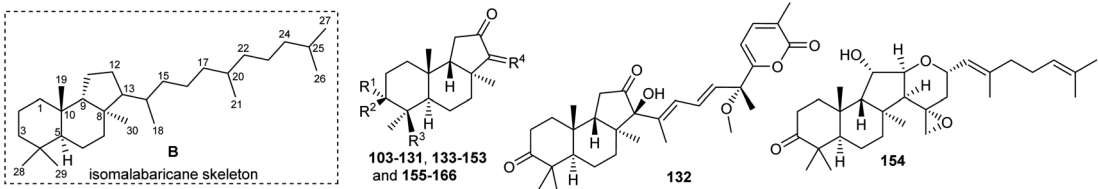
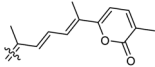
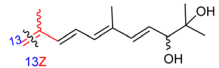
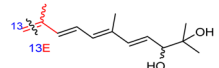
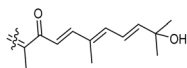
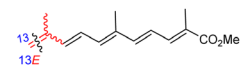
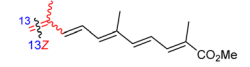
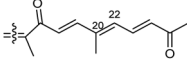
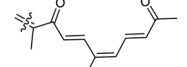
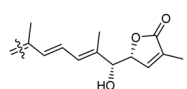
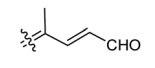
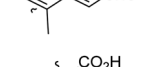
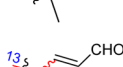
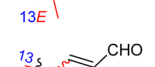
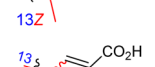
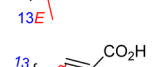

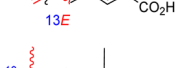

Compound	R <sup>1</sup>	R <sup>2</sup>	R <sup>3</sup>	R <sup>4</sup>	Source
 <p>The figure shows the isomalabaricane skeleton (labeled B) with carbons numbered 1 to 30. To its right are several triterpenes: 103-131, 133-153, and 155-166 (general structure with R<sup>1</sup>, R<sup>2</sup>, R<sup>3</sup>, R<sup>4</sup>); 132 (a complex structure with multiple functional groups); and 154 (a complex structure with multiple functional groups).</p>					
Rhabdastrellin A (103)	H	OH	CH <sub>2</sub> OH		<i>Rhabdastrella</i> aff. <i>distincta</i> <sup>36</sup>
Rhabdastrellin B (104)	H	OH	CH <sub>2</sub> OH		<i>Rhabdastrella</i> aff. <i>distincta</i> <sup>36</sup>
Rhabdastrellin C (105)	H	OH	CH <sub>2</sub> OH		<i>Rhabdastrella</i> aff. <i>distincta</i> <sup>36</sup>
Rhabdastrellin D (106)	H	OH	CH <sub>2</sub> OH		<i>Rhabdastrella</i> aff. <i>distincta</i> <sup>36</sup>
Rhabdastrellin E (107)	H	OH	Me		<i>Rhabdastrella</i> aff. <i>distincta</i> <sup>36</sup>
Rhabdastrellin F (108)	H	OH	Me		<i>Rhabdastrella</i> aff. <i>distincta</i> <sup>36</sup>
Rhabdastrellin G (109)	O	—	Me		<i>Rhabdastrella providentiae</i> <sup>41</sup>
Rhabdastrellin H (110)	O	—	Me		<i>Rhabdastrella providentiae</i> <sup>41</sup>
Rhabdastrellin I (111)	O	—	Me		<i>Rhabdastrella providentiae</i> <sup>41</sup>
Rhabdastrellin J (112)	H	OAc	Me		<i>Rhabdastrella providentiae</i> <sup>41</sup>
Rhabdastrellin K (113)	H	OAc	Me		<i>Rhabdastrella providentiae</i> <sup>41</sup>
Globostelletin B (114)	O	—	Me		<i>Rhabdastrella globostellata</i> <sup>42</sup>
Globostelletin C (115)	O	—	Me		<i>Rhabdastrella globostellata</i> <sup>42</sup>
Globostelletin D (116)	O	—	Me		<i>Rhabdastrella globostellata</i> <sup>42</sup>
Globostelletin E (117)	O	—	Me		<i>Rhabdastrella globostellata</i> <sup>42</sup>
Globostelletin F (118)	O	—	Me		<i>Rhabdastrella globostellata</i> <sup>42</sup>
Globostelletin G (119)	O	—	Me		<i>Rhabdastrella globostellata</i> <sup>42</sup>
Globostelletin H (120)	O	—	Me		<i>Rhabdastrella globostellata</i> <sup>42</sup>



Table 1 (Contd.)

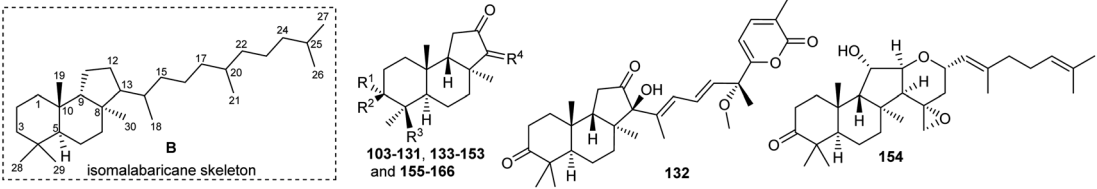
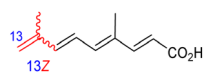
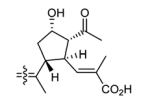
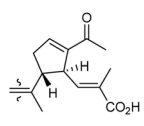
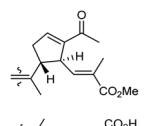
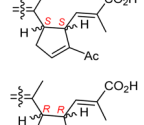
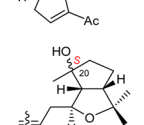
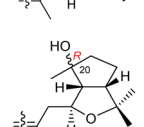
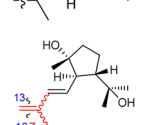
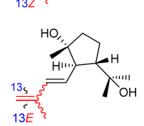
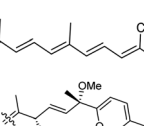
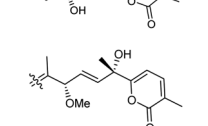
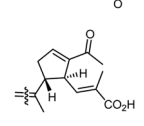


Compound	R <sup>1</sup>	R <sup>2</sup>	R <sup>3</sup>	R <sup>4</sup>	Source
 <p>isomalabaricane skeleton</p> <p>103-131, 133-153 and 155-166</p> <p>132</p> <p>154</p>					
Globostelletin I (121)	O	—	Me		<i>Rhabdastrella globostellata</i> <sup>42</sup>
Globostelletin J (122)	O	—	Me		<i>Rhabdastrella globostellata</i> <sup>43</sup>
Globostelletin K (123)	O	—	Me		<i>Rhabdastrella globostellata</i> <sup>43</sup>
Globostelletin L (124)	O	—	Me		<i>Rhabdastrella globostellata</i> <sup>43</sup>
Globostelletin M (125)	O	—	Me		<i>Rhabdastrella globostellata</i> <sup>43</sup>
Globostelletin N (126)	O	—	Me		<i>Rhabdastrella globostellata</i> <sup>43</sup>
Globostelletin O (127)	H	OH	CH <sub>2</sub> OH		<i>Rhabdastrella globostellata</i> <sup>43</sup>
Globostelletin P (128)	H	OH	CH <sub>2</sub> OH		<i>Rhabdastrella globostellata</i> <sup>43</sup>
Globostelletin Q (129)	H	OH	CH <sub>2</sub> OH		<i>Rhabdastrella globostellata</i> <sup>43</sup>
Globostelletin R (130)	H	OH	CH <sub>2</sub> OH		<i>Rhabdastrella globostellata</i> <sup>43</sup>
Stelletin N (131)	H	OAc	Me		<i>Stelletta</i> sp. <sup>44</sup>
Stelletin O (133)	O	—	Me		<i>Stelletta tenuis</i> <sup>45</sup>
Stelletin P (134)	O	—	Me		<i>Stelletta tenuis</i> <sup>45</sup>
Stelletin Q (135)	H	OAc	Me		<i>Stelletta</i> sp. <sup>47</sup>



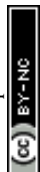
Table 1 (Contd.)

Compound	R <sup>1</sup>	R <sup>2</sup>	R <sup>3</sup>	R <sup>4</sup>	Source
Stelletin R (136)	H	OAc	Me		<i>Stelletta</i> sp <sup>47</sup>
Auroral 137	OH	H	CH <sub>2</sub> OH		<i>Rhabdastrella globostellata</i> <sup>48</sup>
Auroral 138	OH	H	CH <sub>2</sub> OH		<i>Rhabdastrella globostellata</i> <sup>48</sup>
Auroral 139	OH	H	CH <sub>2</sub> OH		<i>Rhabdastrella globostellata</i> <sup>48</sup>
Auroral 140	OH	H	CH <sub>2</sub> OH		<i>Rhabdastrella globostellata</i> <sup>48</sup>
Jaspiferin C (141)	O	—	Me		<i>Jaspis stellifera</i> <sup>49</sup>
Jaspiferin D (142)	H	OH	CH <sub>2</sub> OAc		<i>Jaspis stellifera</i> <sup>49</sup>
Jaspiferin E (143)	H	OH	CH <sub>2</sub> OAc		<i>Jaspis stellifera</i> <sup>49</sup>
Jaspiferin F (144)	H	OH	Me		<i>Jaspis stellifera</i> <sup>49</sup>
Jaspiferin G (145)	H	OH	CH <sub>2</sub> OH		<i>Jaspis stellifera</i> <sup>50</sup>
Jaspiferin H (146)	O	—	Me		<i>Jaspis stellifera</i> <sup>51</sup>
Jaspiferin I (147)	H	OH	Me		<i>Jaspis stellifera</i> <sup>51</sup>
Jaspiferin J (148)	H	OH	Me		<i>Jaspis stellifera</i> <sup>51</sup>
Rhabdaprovidine A (149)	H	OAc	Me		<i>Rhabdastrella providentiae</i> <sup>52</sup>
Rhabdaprovidine B (150)	H	OAc	Me		<i>Rhabdastrella providentiae</i> <sup>52</sup>



Table 1 (Contd.)

Compound	R <sup>1</sup>	R <sup>2</sup>	R <sup>3</sup>	R <sup>4</sup>	Source
Rhabdaprovidine C (151)	H	OAc	Me		<i>Rhabdastrella providentiae</i> <sup>52</sup>
Rhabdaprovidine D (152)	O	—	Me		<i>Rhabdastrella providentiae</i> <sup>53</sup>
Rhabdaprovidine E (153)	O	—	Me		<i>Rhabdastrella providentiae</i> <sup>53</sup>
Stelliferin J (155)	H	OAc	Me		<i>Rhabdastrella globostellata</i> <sup>46</sup>
Stelliferin K (156)	H	OAc	Me		<i>Rhabdastrella globostellata</i> <sup>46</sup>
Stelliferin L (157)	H	OAc	Me		<i>Rhabdastrella globostellata</i> <sup>46</sup>
Stelliferin M (158)	H	OAc	Me		<i>Rhabdastrella globostellata</i> <sup>46</sup>
Stelliferin N (159)	H	OAc	Me		<i>Rhabdastrella globostellata</i> <sup>46</sup>
Rhabdastin A (160)	H	OAc	Me		<i>Rhabdastrella globostellata</i> <sup>54</sup>
Rhabdastin B (161)	H	OH	Me		<i>Rhabdastrella globostellata</i> <sup>54</sup>
Rhabdastin C (162)	H	OAc	CO <sub>2</sub> Me		<i>Rhabdastrella globostellata</i> <sup>54</sup>
Rhabdastin D (163)	H	OAc	Me		<i>Rhabdastrella globostellata</i> <sup>54</sup>
Rhabdastin E (164)	H	OAc	Me		<i>Rhabdastrella globostellata</i> <sup>54</sup>
Rhabdastin F (165)	H	OAc	Me		<i>Rhabdastrella globostellata</i> <sup>54</sup>
Rhabdastin G (166)	H	OAc	Me		<i>Rhabdastrella globostellata</i> <sup>54</sup>



triterpenes have been reported which have only one or two of the normally unsaturated bonds saturated *viz.*, stelliferins J–N and globostelletins J–P.<sup>43,46</sup> Compounds **132–134** were evaluated against lung cancer (A549), gastric cancer (AGS), and glioblastoma (U-251MG) where it was found that these compounds were only active towards AGS with  $IC_{50}$ : in the range from 4.5 to 9.6  $\mu\text{M}$ .<sup>45</sup> Stelletins Q (**135**) and R (**136**) were isolated from *Stelletta* sp. and both compounds have a cyclopentane ring in the polyene side chain formed between C-15 and C-22. Moreover, isomalabaricane triterpenes **135** and **136** (Table 1) are a 13-*Z/E* geometric pair of the same 15*R*,23*S* isomers.<sup>47</sup>

Isomalabaricanes such aurorals **137–140** are produced by the sponge *R. globostellata*. Biological studies revealed that aurorals **137** and **138** possessed good cytotoxic effects towards epidermoid carcinoma (KB cells) with  $ID_{50}$ : 0.2  $\mu\text{g mL}^{-1}$ . On the other hand, compounds **139** and **140** displayed moderate effects with an  $ID_{50}$ : 8  $\mu\text{g mL}^{-1}$ .<sup>48</sup>

Jaspiferins C–F (**141–144**) were isolated from the marine sponge *Jaspis stellifera* and jaspiferin C (**141**) has a six-membered carbon core formed between C-15 and C-23 which is rather rare among isomalabaricane triterpenes.<sup>49</sup> An isomalabaricane triterpenoid, jaspiferin G (**145**), comprising a cyclopentane ring in the pendant polyene side chain was produced by the sponge *Jaspis stellifera*.<sup>50</sup> Jaspiferins H–J (**146–148**) were obtained from *J. stellifera*, among which Jaspiferin H (**146**) has a five membered lactone ring ( $\gamma$ -lactone).<sup>51</sup> From the sponge *R. providentiae* Dung *et al.*<sup>52,53</sup> reported rhabdaprovidines A–E (**149–153**) and G (**154**). The latter one, rhabdaprovidine G (**154**) has an additional pyran ring formed between C-12 and C-15. Notably, this metabolite possesses a novel chemical structure of the 6-6-5-6-tetracyclic core along with nine chiral carbon centres which is quite unique among isomalabaricane skeletons.<sup>53</sup> Bioactivity studies revealed that rhabdaprovidines A–C (**149–151**) inhibited NO production in LPS in which the  $IC_{50}$ : ranged from 17.5 to 46.8  $\mu\text{M}$  with **150** (Table 1) being the most potent  $IC_{50}$ : 17.5  $\mu\text{M}$ .<sup>52</sup>

Stelliferins J–N (**155–159**) were isolated from the sponge *R. globostellata* collected from Hainan Island, China. The configuration of the stereogenic centres in triterpenoids **155–159** were determined *via* CD and NMR measurements using Mosher's method. All these natural products possess a diol (secondary/tertiary hydroxyl group) in the polyene side chains with terpenes **155** and **156** featuring a acyclic side chain and **157–159** a cyclopentane diol unit. Metabolites **157** and **159** illustrated antimicrobial effects towards *Bacillus subtilis* with  $IC_{50}$  8  $\mu\text{g mL}^{-1}$ .<sup>46</sup>

Rhabdastins A–G (**160–166**, Table 1) were produced by the sponge *R. globostellata*. Furthermore, compounds **160–166** have a cyclopentane group generated in the conjugated polyene side chains.<sup>54</sup> Compounds **163**, **164**, and **166** demonstrated modest cytotoxicity on leukemia cells (HL-60) with  $IC_{50}$ : 21, 29, and 44  $\mu\text{M}$ , respectively. Isomalabaricanes **163** and **164** have been studied in detail revealing to cause caspase 3 cleavage in HL-60 cells at 10  $\mu\text{M}$  without effecting expression of Bcl-2 in HL-60 cells.<sup>54</sup> Among the latest natural products of this class, Lai *et al.*<sup>55</sup> isolated rhabdastins H (**167**) and (**168**) (Fig. 8) from the sponge *Rhabdastrella* sp. These isolates demonstrate anti-proliferative effects towards leukemic cells (Molt4 and K562)

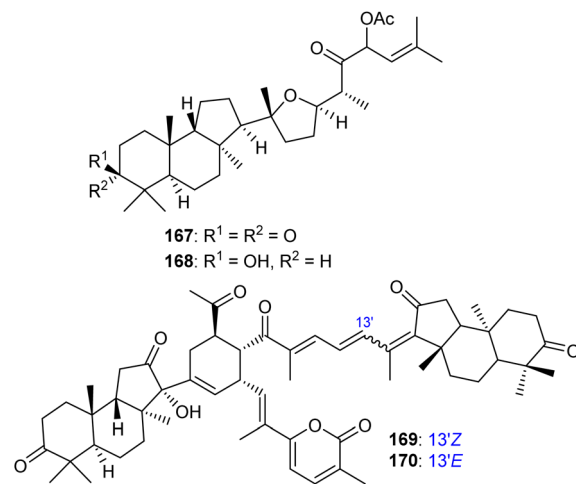


Fig. 8 Structures of isomalabaricane-type triterpenoids **167**, **168** and dimeric isomalabaricane **169**, **170**.

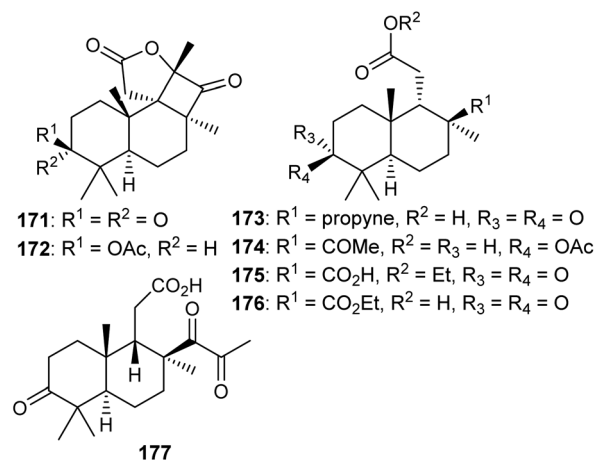


Fig. 9 Structures of isomalabaricane-derived *nor*-terpenoids **171–177**.

with  $IC_{50}$  values ranging from 9.8 to 16.5  $\mu\text{M}$ . Jaspolidides G (**169**) and H (**170**), two unusual bisomalabaricanes isomers were reported from the marine sponge *Jaspis* sp.<sup>56</sup> The intriguing structures not only involve two isomalabaricane moieties, they also possess 2-pyrone heterocycles, which makes the  $\text{C}_{60}$  natural product even more impressive.

#### 4.2 Isomalabaricane-derived *nor*-terpenoids

Two C-19-*nor* isomalabaricane triterpenes named cyclobutastellettolides A (**171**) and B (**172**) were produced by *Stelletta* sp. (Fig. 9). The bioassay-guided isolation revealed them to significantly enhance reactive oxygen species (ROS) generation in murine macrophages. Notably, these two compounds comprise four fused rings, of which one is a cyclobutanone and this is indeed a rare feature in isomalabaricane triterpenes.<sup>57</sup>

In another report, isomalabaricane-derived *nor*-terpenoids, stelletins S–V (**173–176**) were isolated from the marine sponge *Stelletta* sp. Stellettin S (**173**) represents an intriguing example



because this compound has an alkyne group and this is the first example of an isomalabaricane triterpene which features this rare functionality as a substituent.<sup>47</sup> The marine sponge *R. globostellata* produces *nor*-isomalabaricanes triterpene globos-telletin A (177) which has a rather unique structure.<sup>42</sup>

### 4.3 Malabaricane type triterpenes

Malabaricanes are a group of tricyclic triterpenes bearing a 6-6-5 *trans-anti-trans* tricyclic core attached to a polyene side chain (Fig. 10, structure “C”). Six malabaricane type triterpenes **178**, **179** with cyclobutane modified side chains, and **182–185** (Fig. 10) were reported from the oleoresin of *Ailanthus malabarica*.<sup>58</sup> During the time covered by this report, Duan *et al.*<sup>59</sup> demonstrated that triterpenes **178** and **179** with the suggested unusual cyclobutane modifications have the same NMR data (in particular <sup>13</sup>C NMR data) as the dammarane-type triterpenes ocotillone (**180**) and gardaubryone C (**181**), respectively, leading to a revision of the formerly proposed structures. Of note, their structural reassignment was established by further using DFT chemical shift analysis and the CASE algorithm. Bio-guided isolation studies on *Commiphora africana* provided the malabaricane triterpene commafric A (**186**) bearing a methyl group at C-13 instead of C-8. It illustrated significant cytotoxic effects

towards lung cancer lines (A549: IC<sub>50</sub>: 4.52 μg mL<sup>-1</sup>) along with moderate effects towards ovarian cancer (A2780), stomach cancer (SNU638), and pancreatic cancer (MIA-PaCa-2), with IC<sub>50</sub> ~ 10 μg mL<sup>-1</sup>.<sup>60</sup>

Modified side chains have been identified in ailanthusins F (**187**) and G (**188**) (Fig. 10), which are produced by the stem of *Ailanthus triphysa*, a tree commonly found in Thailand and Australia. Moreover, these metabolites were not active in cytotoxicity screening towards MOLT-3, HepG2, MDA-MB-321, HuCCA-1, T47-D, A549, HeLa, and MRC-5.<sup>61</sup> In another report, Messina *et al.*<sup>62</sup> isolated malabaricatrienone (**189**) and malabaricatrienol (**190**) from the methanol extract of the resin of *Bursera microphylla* which is called “elephant tree” and is widely present in Mexico. In addition, these metabolites were not active against various murine and human cancer cells.

## 5 Biosynthesis of isomalabaricane and malabaricane trietpenoids

Isomalabaricanes and malabaricanes feature 6-6-5 *trans-syn-trans* and *trans-anti-trans* tricyclic cores while both skeletons have different stereochemistry at the C-8 and C-9 positions (Table 1 and Fig. 10). The basic core skeleton of isomalabaricane **195** is thought to be biosynthetically generated

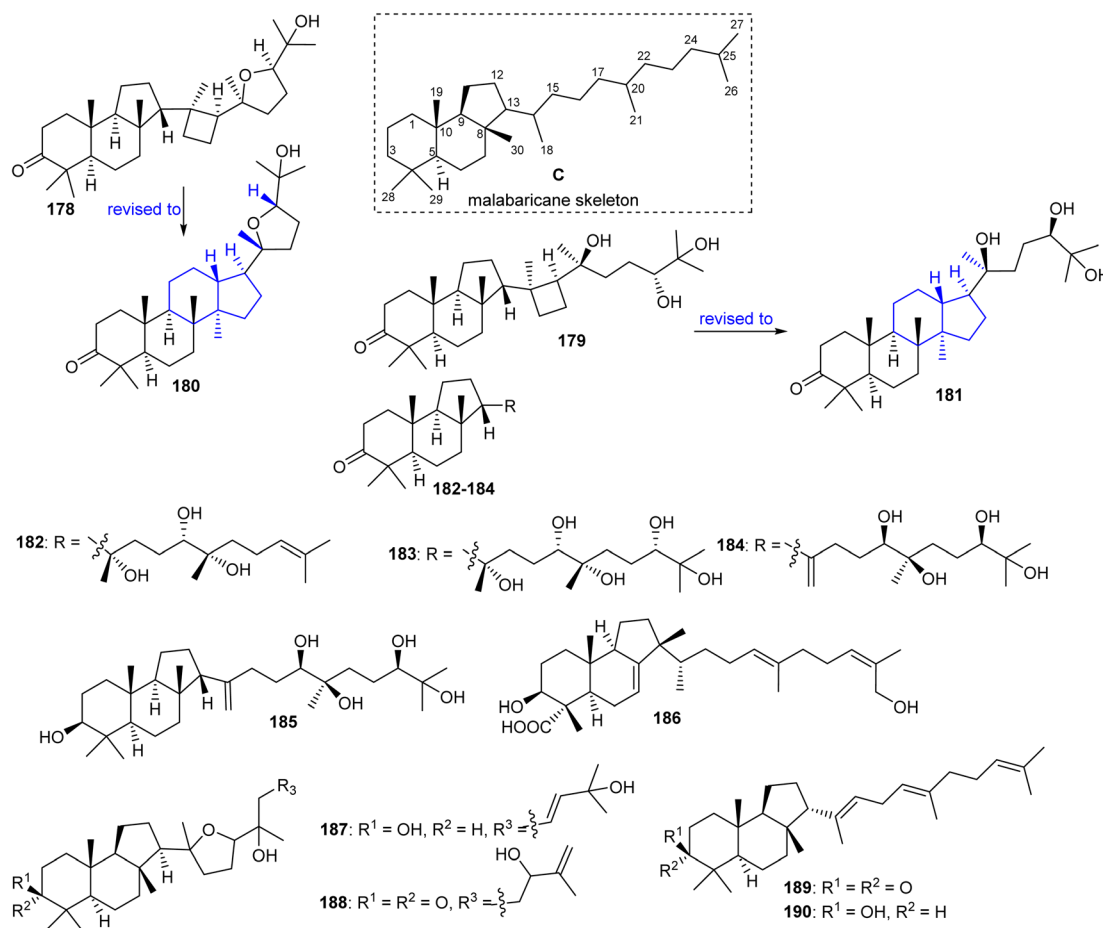


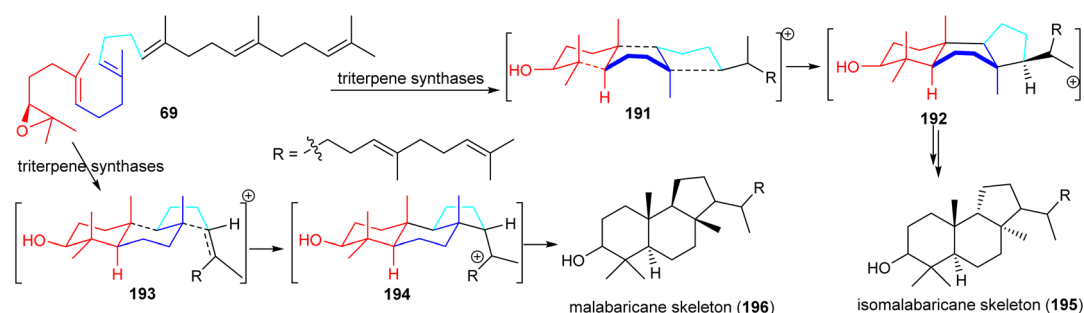
Fig. 10 Structures of malabaricane-type triterpenoids **178**, **179**, **182–190**.



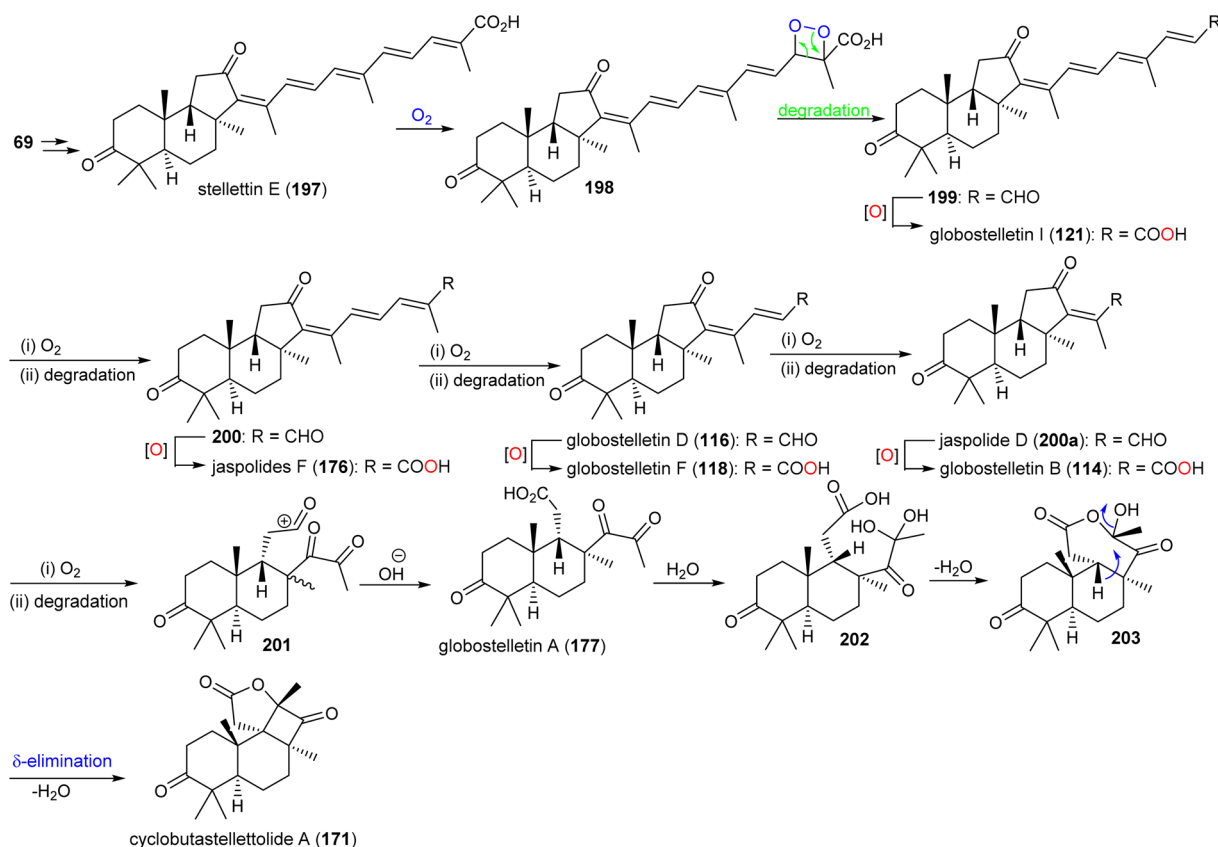
through cyclizations of 2,3-oxidosqualene (**69**) *via* chair–boat–chair (**191**) transition states (Scheme 8).<sup>57,63,64</sup> Similarly, it has been suggested that the biosynthesis of the basic core skeleton of malabaricane triterpenoids also proceeds through cyclizations of 2,3-oxidosqualene (**69**) *via* a chair–chair–chair (**193**) transition state<sup>57,63,64</sup> and triterpene synthases are responsible to generate the malabaricane basic skeleton **196** (Scheme 8).<sup>64,65</sup>

It has been reported that two *Arabidopsis thaliana* genes including At5g4810 and At4g15340 encode OSCs which furnish arabidiol and thalianol.<sup>8,66,67</sup> In addition, numerous

malabaricanes have been obtained *via* site-directed mutagenesis of *A. acidocaldarius* squalene hopene cyclase which in turn comprise point mutants of Tyr420, Phe601 and Ile261.<sup>8,68,69</sup> This suggests that the malabaricanes are produced in nature with custom tailored enzymes. Lodeiro *et al.*<sup>65</sup> demonstrated that the isomalabaricane core arises from a lanosterol cyclase mutant (Tyr510) while the native enzyme has yet to be discovered. Stelletin E (**197**) (Scheme 9) could be the plausible precursor to generate globostelletins B (**114**), D (**116**), F (**118**), and I (**121**) *via* oxidative degradation reactions.<sup>42,57,70</sup>

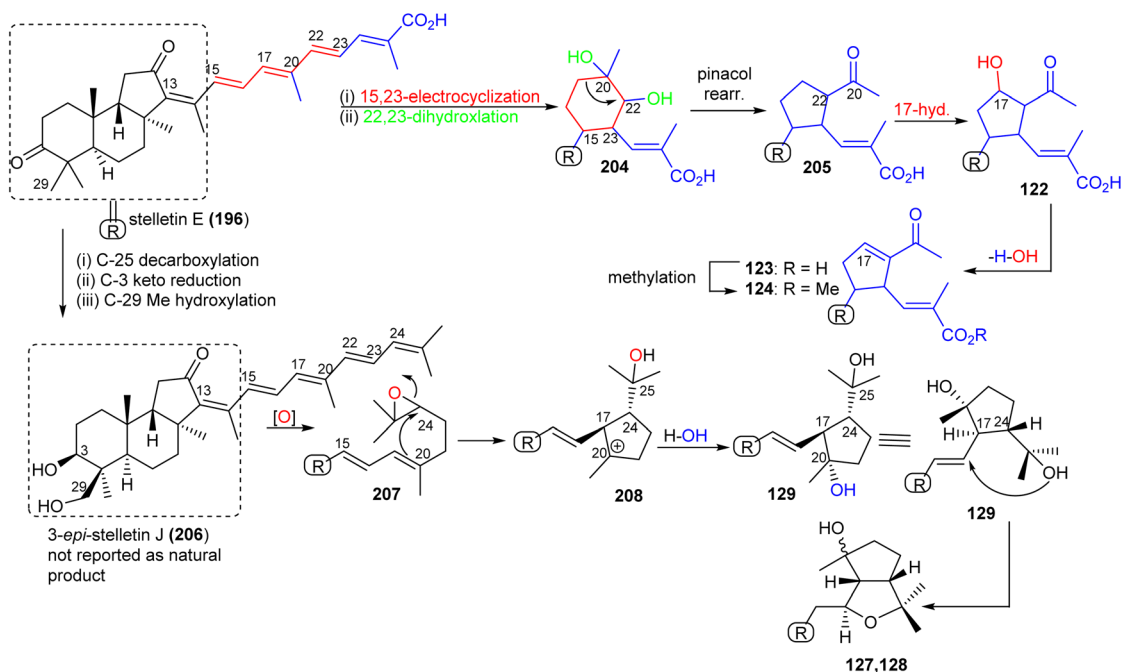


Scheme 8 Hypothetical biosynthesis of isomalabaricane (**195**) malabaricane (**196**) basic skeletons. Reproduced from ref. 64 and 65 with permission from the American Chemical Society.



Scheme 9 Hypothetical biosynthesis of isomalabaricane triterpenoids **114**, **116**, **118**, **121**, **171** and **177**. Reproduced from ref. 57 with permission from the American Chemical Society.





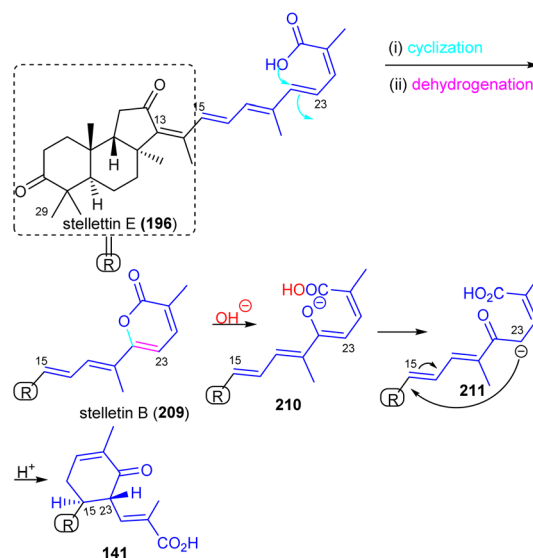
**Scheme 10** Hypothetical biosynthesis of isomalabaricane triterpenoids **122–124** and **127–129**. Reproduced from ref. 43 with permission from Elsevier.

Globostelletin A (**177**) is assumed to be generated by oxidative degradation (loss of CO<sub>2</sub>) from globostelletin B (**114**) and therefore it is also considered to be a member of the isomalabaricane class<sup>42</sup> (Scheme 9). Moreover, globostelletin A (**177**) is considered as the putative biosynthetic precursor of cyclobutastellettolide A (**171**) (Scheme 9). Globostelletin A (**177**), or its hydrate **202** may be converted into cyclobutastellettolides A (**171**) *via* an intramolecular dehydration followed by  $\delta$ -elimination. The  $\Delta G$  calculation results for possible biosynthetic intermediates indicated that the seven-membered ring formation in tricyclic **171** is preferred to happen prior to the formation of the fused  $\gamma$ -lactone, in contrast to the simultaneous generation of the cyclobutane-fused lactone.<sup>57</sup> Cyclobutastellettolide B (**172**) was presumed to be generated by the same protocol from stellettin H or I (3-OAc derivatives of stellettin E).<sup>57,71</sup>

Stellettin E (**196**), which co-existed in the same specimen (*R. globostellata*), is thought to be considered as the putative precursor for globostelletins J–L (**122–124**), which bear an unusual cyclopentane derived side chain (Scheme 10).<sup>43</sup> Formation of this unit might be initiated *via* a 15,23-electrocyclization followed by 20,22-epoxidation to afford the cyclohexane unit **204**. Moreover, the later intermediate could then undergo a semi-pinacol rearrangement, 17-hydroxylation, dehydration and methylation to generate the globostelletine triterpenes **122–124**. On the other hand, 3-*epi*-stelletin J (**206**) could be derived from stellettin E (**196**) and possibly be the precursor for the biosynthetic formation of globostelletins O–Q (**127–129**). Considering the very likely epoxidation at C-24/C-25 to form epoxide **207** followed by attack by the nucleophilic  $\Delta^{17(20)}$  double bond and hydroxylation of the resulting tertiary carbocation at C-20 (**208**), this will eventually provide

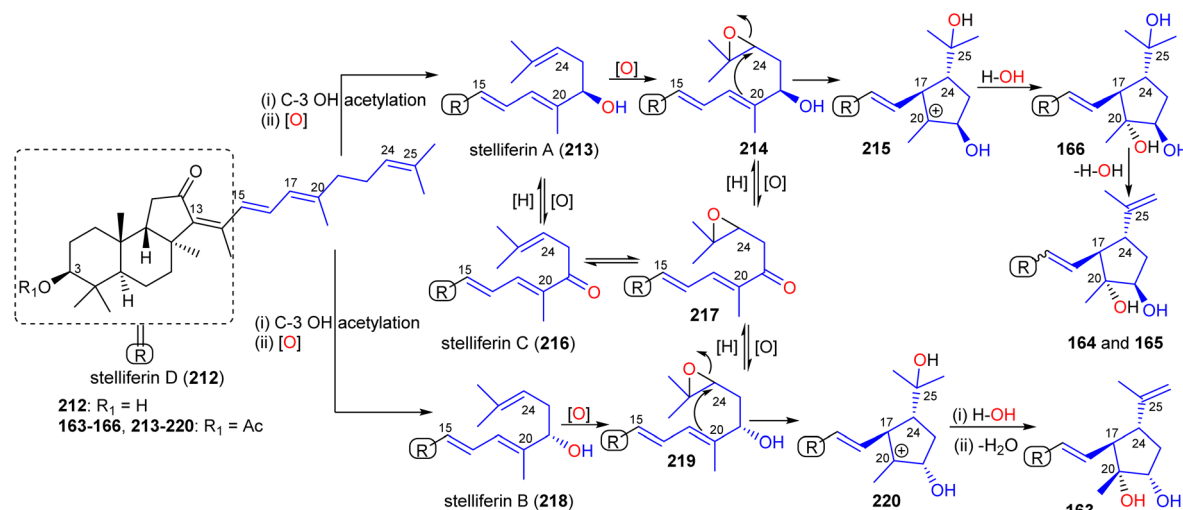
globostelletin Q (**129**). Globostelletins O (**127**) and P (**128**) are more than likely to be derived from **129** through nucleophilic attack of the C-25 hydroxyl group at the C-16 double bond to form the pyran ring.

Stelliferins can be considered to be starting materials for another modified isomalabaricane, Jaspiferin C (**141**). It contains a cyclohexenyl moiety in the side chain which is most likely derived from stellettin E (**196**). Its biosynthesis could initially be formed by lactonization between the C-25 carboxylic



**Scheme 11** Plausible biosynthesis of isomalabaricane triterpenoid **141**. Reproduced from ref. 49 with permission from the Taylor & Francis.





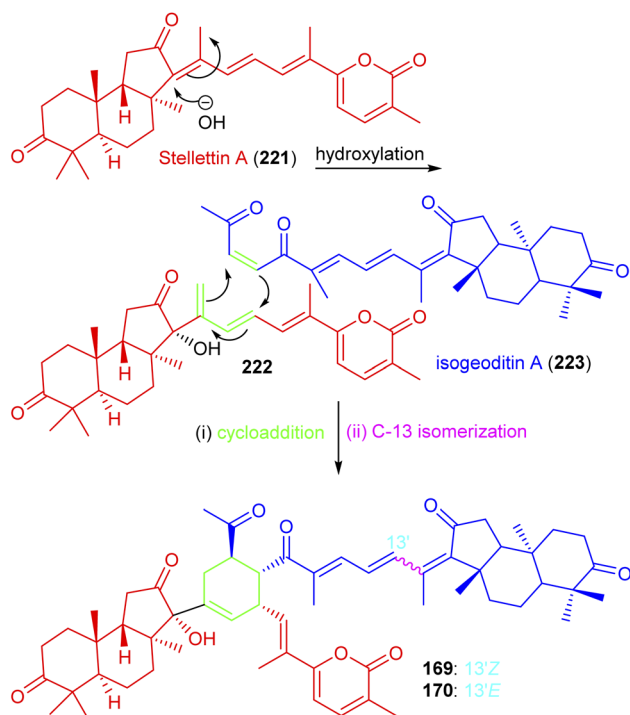
**Scheme 12** Hypothetical biosynthesis of isomalabaricane triterpenoid **163–166**. Reproduced from ref. 54 with permission from the American Chemical Society.

acid group attacking the C-24 double bond followed by dehydrogenation to afford 2-pyrone-modified stelletin B (**209**) (Scheme 11). The resulting lactone ring in the stelletin B (**209**) could reasonably be ring-opened *via* an hydroxyl attack to generate intermediate **210**. The later intermediate features an enolate tautomer. Finally, the cyclohexenyl moiety may be generated between C-15 and C-23 to form the resulting cyclohexenone core unit in the polyene side chain of jaspiferin C (**141**).<sup>49</sup>

Rhabdastins A–C (**160–162**) are thought to be biogenetically generated *via* oxidative cleavage of stelliferin derivatives as described for globostelletin B (**114**) (Scheme 9). A proposed biogenetic route for rhabdastins D–G (**163–166**) *via* oxidation and cyclization of stelliferins is depicted in Scheme 12.<sup>54</sup> Stelliferin D (**212**) formation could proceed by initial C-3 acetylation and C-21 hydroxylation followed by epoxidation of the double bond at C-24 in stelliferin A (**213**)<sup>72</sup> to form epoxide **214** at C-24/C-25. Thereafter, attack by the  $\Delta^{17(20)}$  double bond in later compound may cleave the epoxide and provide a tertiary carbocation at C-20 (**215**).

This could then be followed by nucleophilic attack by water from the  $\alpha$ -face to produce rhabdastin G (**166**) which in turn could be followed by the C-25 OH group being lost *via* a dehydration to give rhabdastin E (**164**). On the other hand, rhabdastin F (**165**) may be a photoisomer of **164**, because this later compound was slowly transformed into its C-13 isomer **165** under room light conditions. In addition, rhabdastin D (**163**) may presumably be formed through a similar route from stelliferin B (**218**)<sup>72</sup> including epoxidation, epoxide ring-opening,  $\alpha$ -face nucleophilic attack by water as described for compounds **164–166**. Additionally, alternative biogenetic routes for compounds **163–166** *via* formation of stelliferin C (**216**) from stelliferin A (**213**)<sup>72</sup> are also depicted in Scheme 12.

Jaspolides G (**169**) and H (**170**) are the first examples of isomalabaricane based dimers and these are geometrical isomers with respect to the C-13 double bond.<sup>56</sup> The authors postulated that the structure of jaspolide G (**169**) could be biosynthetically formed between stelletin A (**221**)<sup>73</sup> and isogeoditin A (**223**)<sup>74</sup> which are representative isomalabaricane type triterpenes and a *nor*-triterpenes, respectively<sup>56</sup> (Scheme 13). Initially, hydroxylation might occur at C-13 of stelletin A (**221**) which would afford the intermediate **222** with a concomitant migration of the double bond at C-14/C-18. A double bond between C-23/C-24 of geoditin A (**223**) and the conjugated double bonds at C-15/C-16 and C-14/C-18 of the intermediate **222** might then undergo a [4



**Scheme 13** Hypothetical biosynthesis of isomalabaricane triterpenoids **169** and **170**. Reproduced from ref. 56 with permission from the Elsevier.



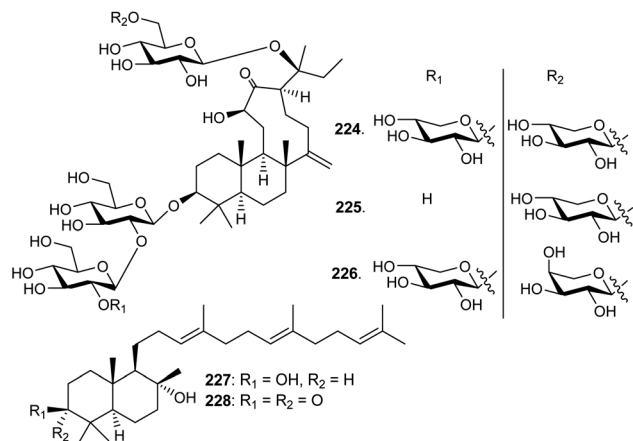


Fig. 11 Structures of triterpenes 224–228.

+ 2]<sub>π</sub> cycloaddition to afford the corresponding dimer containing the newly formed cyclohexene ring. The C-13 isomerization *viz.*, *Z*-form (169) to *E*-form (170) is frequently present in isomalabaricanes due to their thermal sensitivity.

## 6 Tetranordammarane and polypodane triterpenoids

Three unusual triterpene saponins named nototronesides A–C (224–226) (Fig. 11), that feature a rare 6/6/9 tricyclic tetranordammarane core, are produced by *Panax notoginseng*, commonly referred Chinese ginseng. They were screened for their neuroprotective effects where it was found that metabolite 225 enhanced the cell viability remarkably by 79%.<sup>75</sup> *Commiphora mukul* gum resin, also known as guggul, has been employed to treat obesity, inflammation, and lipid disorders in Ayurvedic medicine. Myrrhanol C (227) and its corresponding keto analog myrrhanone C (228), were reported from this guggul

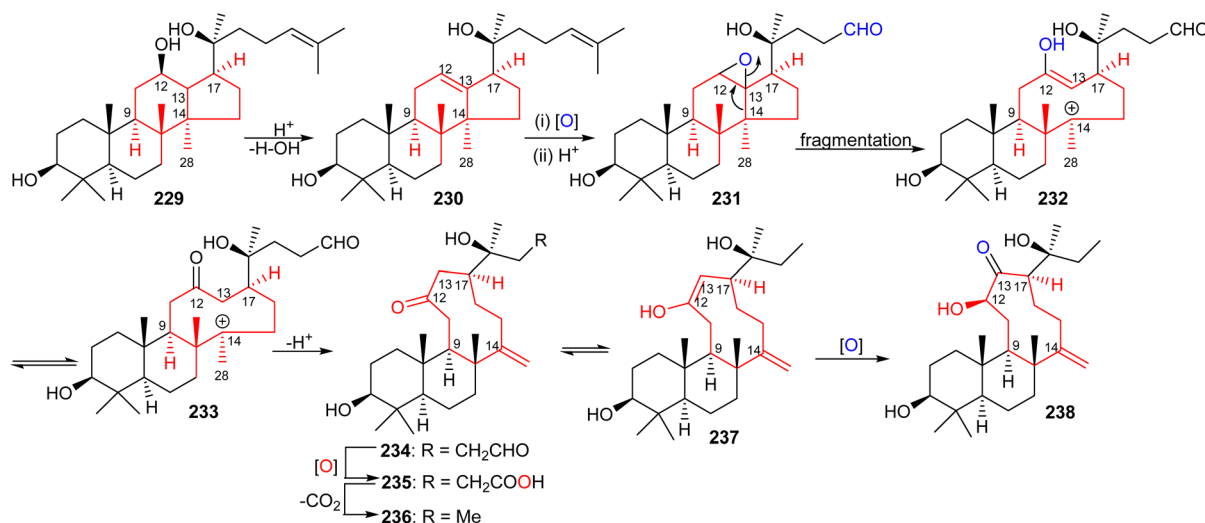
gum resin.<sup>76,77</sup> Furthermore, myrrhanol C (227) was reported from *Pistacia lentiscus* resin and found to possess potent effects towards prostate cancer cells.<sup>78</sup>

## 7 Biosynthesis of tetranordammaranes

The aglycon of nototroneside A (224) (nototrone A, 238) represents the first example of an unusual tricyclic dammarane-type triterpene.<sup>75</sup> A proposed biosynthetic pathway of nototrone A (238) is depicted in Scheme 14.<sup>75</sup> In this scheme the authors proposed that tricyclic (238) is biosynthetically derived from protopanaxadiol (229), which is a reported aglycon of numerous saponins from *Panax* plants.<sup>75,79,80</sup> Initially, dehydration of the C-12 hydroxyl group of protopanaxadiol (229) would generate a double bond at the Δ<sup>12,13</sup> position, which could subsequently undergo epoxidation *via* an enzyme-catalyzed epoxidation to afford the corresponding oxidized analog 231. This latter derivative could then undergo a fragmentation of the highly strained epoxide intermediate by cleavage of the C-13/C-14 bond to produce a nine-membered enol 232.<sup>81</sup> The intermediate enol 232 is thought to then undergo keto–enol a plausible tautomerisation which would lead to the generation the keto anion 233 and upon a deprotonation lead to the formation of tricyclic triterpene 234. Enzymatic oxidation of 234 to acid 235, its decarboxylation and C-13 oxidation would ultimately lead to nototrone A (238).

## 8 Schiglautone and volvalerane type triterpenes

Chemical investigation of the evergreen shrubs *Schisandra glaucescens* (Schisandraceae) provided the schiglautane-type triterpene named schiglautone A (239) (Fig. 12), which feature an unusual 6/7/9-fused tricyclic core. The structure of this



Scheme 14 Hypothetical biosynthesis of nototroneside A (224) sapogenin nototrone A (238). Reproduced from ref. 75 with permission from the American Chemical Society.



unusual scaffold was confirmed *via* spectroscopic as well as X-ray analysis. Compound **239** with an unusual 7,9-membered bicyclic moiety seems to have no precedent among reported secondary metabolites or synthetic compounds and is clearly different from numerous skeletons reported from the Schisandraceae family. Moreover, it illustrated weak cytotoxic effects towards HeLa, Hep G2, and SGC-7901.<sup>82</sup> Volvalerenol A (**240**), which features a 7/12/7 tricyclic ring system, was obtained from the EtOH extracts of the roots of *Valeriana hardwickii*.<sup>83</sup>

## 9 Biosynthesis of schiglautone and volvalerane type triterpenes

As could be expected, the biosynthesis of these very unusual triterpenes was of tremendous interest. The starting point for schiglautone A (**239**) is thought to be derived from anwuweizic acid (**241**) (Scheme 15),<sup>82</sup> which was also reported from the same plant species in large quantities. The authors postulated that triterpene **239** might conceivably be generated from **241** *via* enzymatic conversion reactions which include oxidation, acidification hydroxylation, and most importantly ring expansion. The key biosynthetic conversions include two ring expansions *i.e.* degradation of one isoprene unit in the purple color in intermediate **243** to form a nine-membered ring and ring expansion *via* the shifting of one carbon unit of the isoprene unit in green color (**245**) to form a seven member ring (**246**).<sup>82</sup> On the other hand, the 7/12/7 tricyclic comprising triterpene volvalerenol A (**240**) could be biogenetically derived from two units of FPP (farnesyl pyrophosphate, **250**). Initially FPP **250** could undergo head-to-tail condensation followed by a series of

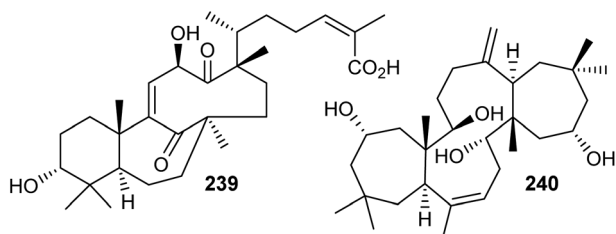
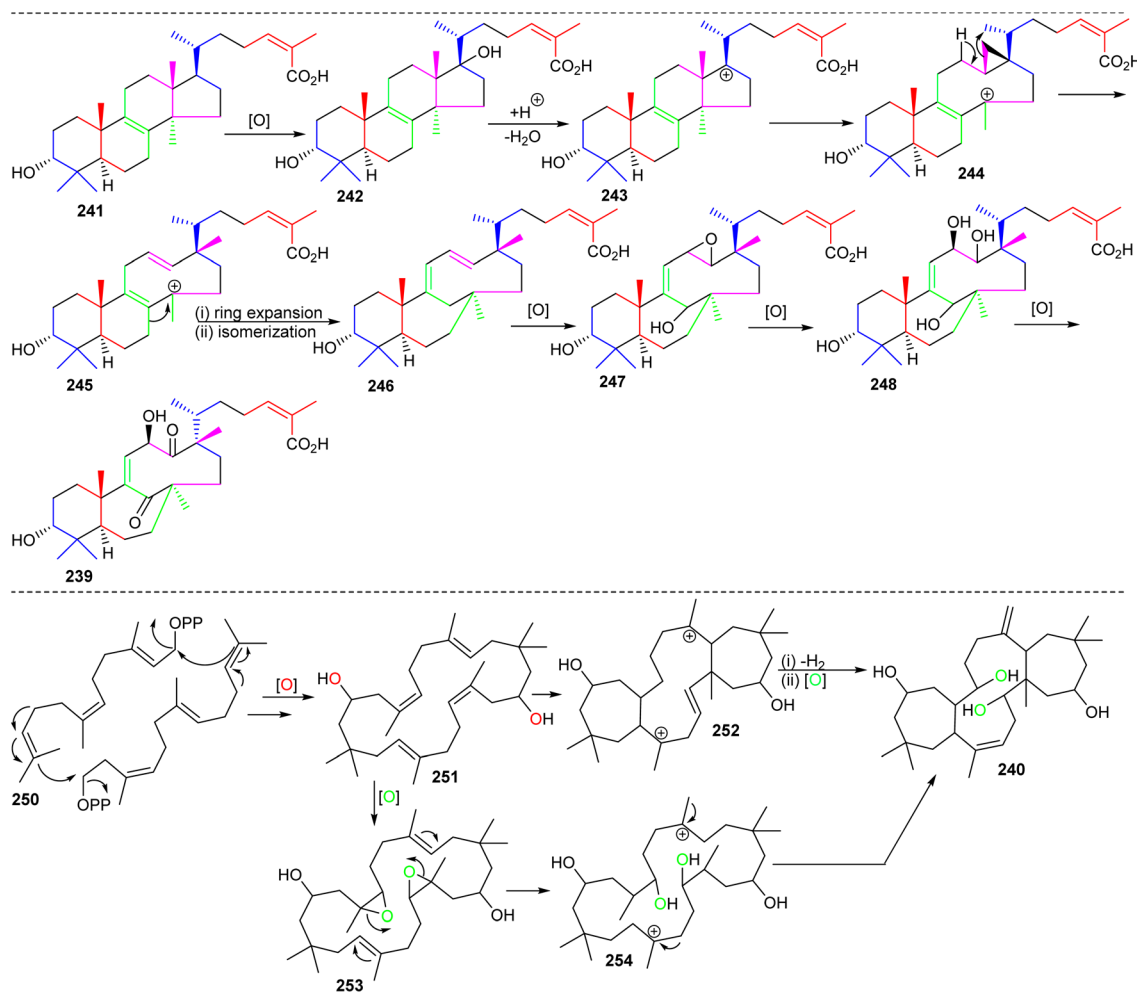


Fig. 12 Structures of triterpenes **239** and **240**.



Scheme 15 Hypothetical biosynthesis for schiglautone A (**239**) and volvalerenol A (**240**). Reproduced from ref. 82 and <sup>83</sup> with permission from the American Chemical Society.



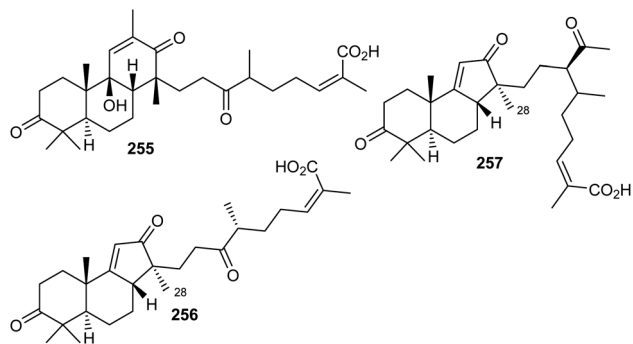


Fig. 13 Structures of triterpenes 255–257.

enzymatic reactions including epoxidation, dehydrogenation, electrophilic addition, and oxidation reactions (Scheme 15).<sup>83</sup>

## 10 Unusual tricyclic seco/nor-lanostane

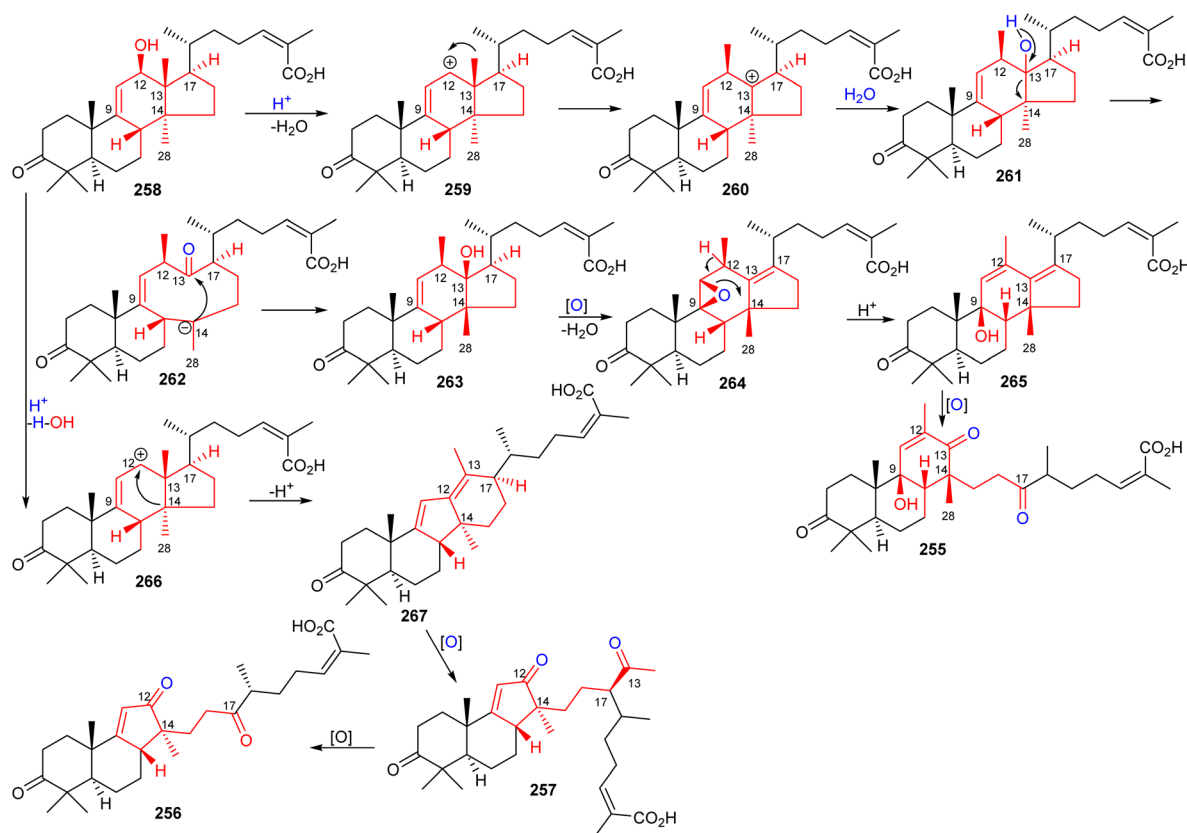
Chemical investigation of traditionally used *Kadsura coccinea*, which was collected from China, yielded one unusual tricyclic triterpenoid, kadcotrine A (255) (Fig. 13) bearing an 18(13 → 12)-abeo-13,17-seco-14β-lanostane skeleton.<sup>84</sup> Notably, metabolite 255 bears a 6/6/6-fused skeleton having a β-oriented C-14

methyl group which is not consistent with the methyl group at the C-28 position present in lanostane-type triterpenoids. In addition, this compound also features a C<sub>11</sub> side chain attached to C-14. This side chain comprises a keto, methyl, and carboxylic group. Furthermore, its absolute configuration was established *via* both the calculated and experimental ECD spectra.<sup>84</sup>

The norlanostane triterpenoid named kadcotrine B (256), having a 14(13 → 12)-abeo-13,18-dinorlanostane core was also produced by *K. coccinea*. Additionally, this plant produced kadcotrine C (257) which features a 14(13 → 12)-abeo-12,13-secolanostane core system. Both triterpenes 256 and 257 have a 6/6/5 ring scaffold system which is configurationally similar to the isomalabaricane skeleton but is different from that of isomalabaricane, because of a C<sub>13</sub> or C<sub>11</sub> side chain along with a Me group at the 28 position. Furthermore, only compound 256 illustrated weak anti-HIV-1 effects with EC<sub>50</sub>: 30.2 μM. In addition, compounds 255 and 256 were not active towards SMMC-7721, A-549, MCF-7, and SW480.<sup>84</sup>

## 11 Biosynthesis of seco/nor-lanostane

The structures of kadcotrones A-C (255–257) possess the same ring A-B *trans*-relationship to that of 12β-hydroxycoccinic acid (258), a lanostane triterpene which was also isolated from *K. coccinea* together with triterpenes 255–257 (Scheme 16).<sup>84</sup> Based



Scheme 16 Hypothetical biosynthesis of kadcotrones A-C (255–257). Reproduced from ref. 84 with permission from the American Chemical Society.



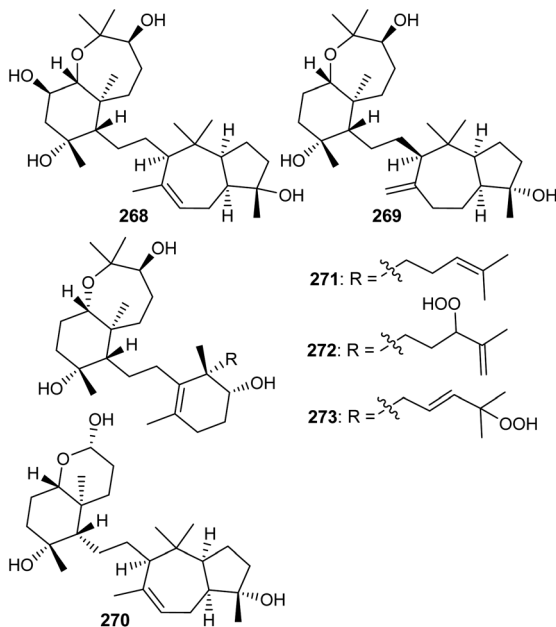


Fig. 14 Structures of sipholanones and siphonellines 268–273.

on their structural similarities, the triterpene 258 could be considered to be the biosynthetic precursor and thus might undergo a series of enzymatic conversions including dehydration, 1,2-migration of a methyl group, and oxidation/oxidative degradations.<sup>84</sup> Furthermore, the key step in the biosynthesis of kadcotriones A–C (255–257) is a fragmentation of the C–D ring in intermediate 261, and oxidative cleavage of the C-13/C-17 double bond in 265 (to generate compound 255), and, similarly, tricyclic 267 in order to biosynthesize triterpenes 256 and 257.

## 12 Sipholanones and siphonellines

The sipholane skeleton may be described as a *cis*-fused cyclopentane-cycloheptane ethylene linked hexane-oxepane.<sup>85</sup> Investigations of the sponge *Siphonochalina siphonella* yielded the two benzoxepine-azulene linked sipholane type triterpenes, sipholenols N (268) and O (269) (Fig. 14).<sup>86</sup> On the other hand sipholane type triterpenoids also include the octahydrochromene-azulene system linked<sup>87</sup> *via* a two carbon bridge. Jain *et al.* reported sipholane 270 from *Siphonochalina siphonella*, which possessed no cytotoxic effects toward epidermoid cancer cells such as KB-C2 and KB-3-1.<sup>87</sup>

Siphonellines comprising of decahydro tetramethylbenzoxepine ring systems attached to cyclohexenol analogs *via* an ethylene bridge are also known. *Callyspongia* sp. produced siphonelline triterpenes named siphonellinol D (271), E (272), and siphonellinol C-23-hydroperoxide (273) (Fig. 14) and these triterpenes were inactive toward the two epidermoid cancer cells (KB-C2 and KB-3-1).<sup>87</sup>

## 13 Sodwanones and neviotines

Sodwanones have structural similarities to the sipholanones as well as possess a hexane-oxepane subunit attached to a variety

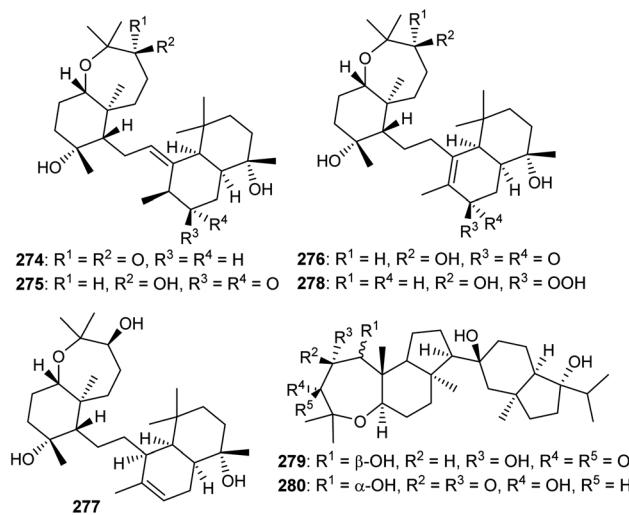


Fig. 15 Structures of sodwanones and neviotines 274–280.

of decalins. Chemical examination of the red sea sponge *S. siphonella* yielded five sodwanones 274–278 (Fig. 15) and these triterpenes proved to be inactive toward the two epidermoid cancer cell lines KB-C2 and KB-3-1.<sup>87</sup> Neviotine type triterpenoids are comprised of a pentacyclic core system including a bicyclic (octahydro-1*H*-indene) ethylene linked with a tricyclic (dodecahydro-2*H*-indeno[5,4-*b*]oxepine).

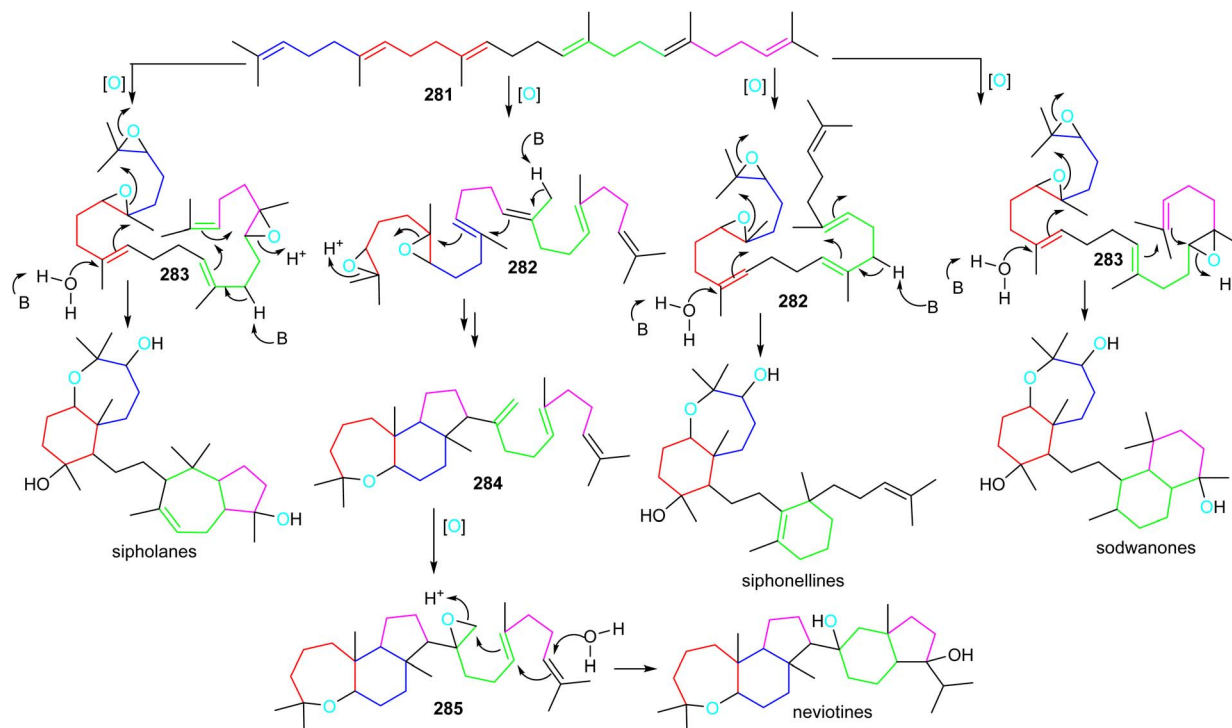
*Siphonochalina siphonella* produced the two neviotine triterpenes named neviotines C (279)<sup>88</sup> and D (280).<sup>86</sup> Moreover, compound 280 illustrated significant inhibition of RANKL induced osteoclastogenesis with IC<sub>50</sub>: 12.8 μM.<sup>86</sup> On the other hand, neviotines C (279) illustrated moderate cytotoxic effects towards MCF-7, PC-3 and A549.<sup>88</sup>

## 14 Biosynthesis of sipholanones, siphonellines, sodwanones, and neviotines

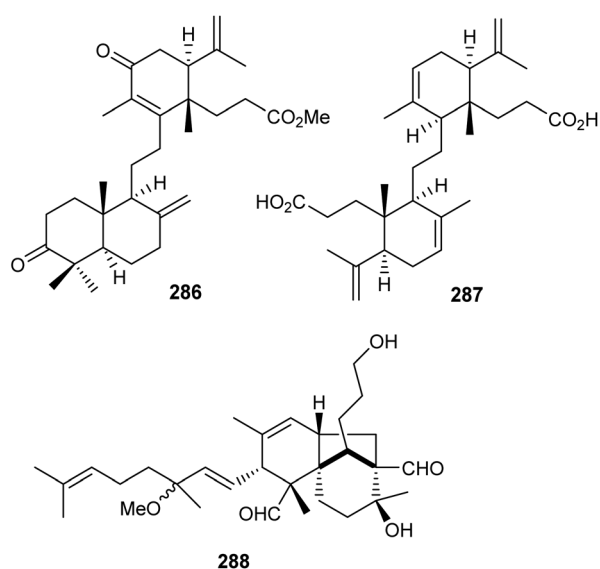
Sipholanones, siphonellines, sodwanones, and neviotines could feasibly be biosynthesized *via* two separate cascade cyclizations starting from the multiple-oxidized di- (282) or triepoxy-squalenes (283). In all triterpene skeletons, cyclization of the doubly epoxidized half could be initiated by acid catalyzed enzymatic opening of the epoxide moiety in 282 and 283 (Scheme 17).<sup>89</sup> On the other hand, for the siphonellinols the western part appears to follow a cascade-cyclization protocol *via* an electrophilic protonation of a double bond (Scheme 17), while the western part in sodwanones could be biosynthesized after protonation of the western half carrying a mono-epoxidized terminal moiety.

A more different and complex biosynthetic route could involve the biogenesis of neviotine type triterpenes (Scheme 17).<sup>89,90</sup> The starting di-epoxide in 282 could be the same as for the biosynthesis of sipholanones, and sodwanones, with an interrupted cyclization cascade, delivering the tricyclic core





**Scheme 17** Hypothetical biosynthesis of sipholane, siphonelline, sodwanone and neviotine skeletons. Reproduced from ref. 89 and <sup>90</sup> with permission from the American Chemical Society and Springer Nature respectively.



**Fig. 16** Structures of onocerane and belamchinane-type triterpenoids 286–288.

structure 284. Subsequently, the eastern half cyclization could be initiated *via* late-stage epoxidation of the C-15 methylene group to form epoxide 285, thus setting up the second cascade cyclization to generate the neviotane skeleton.

## 15 Onocerane and belamchinane-type triterpenoids

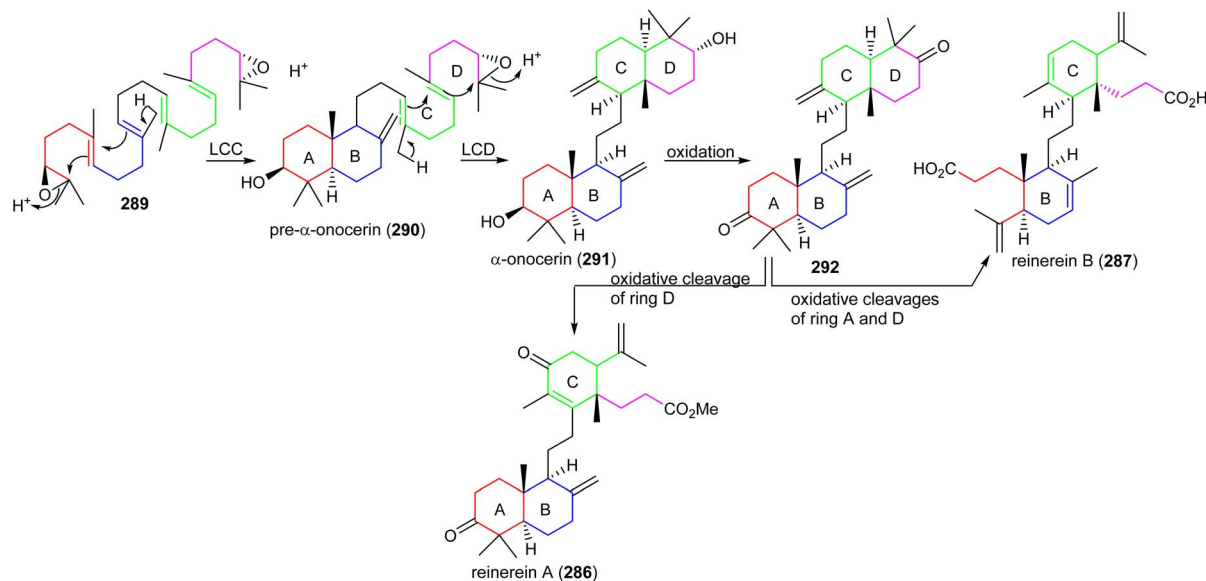
Two onocerane triterpenoids named reinereins A (286) and B (287) (Fig. 16), were isolated *via* a bioassay guided chromatographic protocol from the bark of *Reinwardtiadendron cinereum*, found in Malaysia and Indonesia. Triterpene 286 illustrated moderate cytotoxic effects towards HL-60, A549, MCF7, and HepG2 cancer cells with  $IC_{50}$  ranging from 11.5 to 27.8  $\mu M$ . On the other hand, compound 287 was only active towards HL-60 and A549 with  $IC_{50}$ : 27.8 and 29.7  $\mu M$ , respectively.<sup>91</sup>

In another report, the belamchinane-type triterpenoid named belamchinenin A (288), exhibiting an unusual 6/5/6-fused tricyclic skeleton has been reported from *Belamcanda chinensis*, whose root extract is widely used in China and found successful in curing various diseases including cancer. Notably, metabolite 288 bears a half-caged tricyclic core along with a flexible geranyl group. As could be expected by the activity guided fractionation studies, compound 288 demonstrated cytotoxic effects towards NCI-H1650, HepG2, BGC 823, HCT-116, and MCF-7 cancer cells in which the  $IC_{50}$ : ranged from 2.29 to 4.47  $\mu M$ .<sup>92</sup>

## 16 Biosynthesis of onocerane and belamchinane-type triterpenoids

Members of the natural product family of onoceranes have been isolated previously, *e.g.*  $\alpha$ -onocerin (291) was discovered in 1855



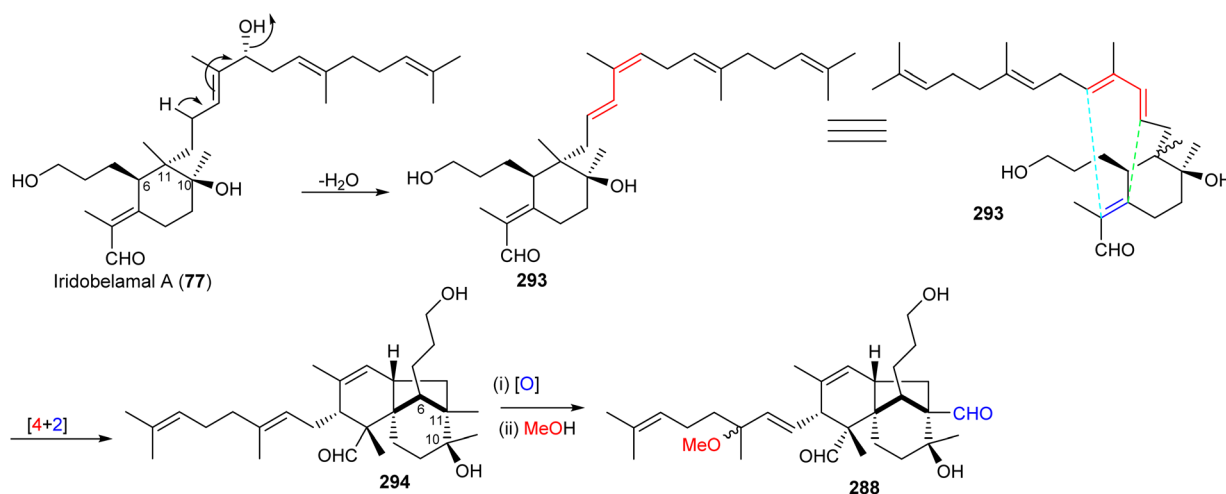


**Scheme 18** Hypothetical biosynthesis of onoceranes **286** and **287**. Reproduced from ref. 96 and 97 with permission from the John Wiley and Sons and American Chemical Society respectively.

and its complete structure was established in 1955.<sup>93</sup> Later, its biosynthetic route was postulated to involve two cyclizations starting from 2,3,22,23-dioxidosqualene (**289**).<sup>94,95</sup> Despite the fact that these findings on  $\alpha$ -onocerin (**291**) were established over six decades ago, the nature of the enzymes or genes that catalyze the two right and left cyclizations remained elusive. In 2016, Kushiro and his team<sup>96,97</sup> investigated the biosynthesis of  $\alpha$ -onocerin (**291**) (Scheme 18) and identified the two elusive genes from the fern *Lycopodium clavatum*, LCC and LCD of the oxidosqualene cyclase (OSC) family. The findings demonstrated that dioxidosqualene cyclase LCC catalyzed the first cyclization to get a decalin-intermediate (ring A,B) pre- $\alpha$ -onocerin (**290**) and subsequently onocerin synthase LCD catalyzed the second cyclization to afford  $\alpha$ -onocerin (**291**). Moreover, reinereins A (**286**) and B (**287**) could be biosynthetically derived from  $\alpha$ -

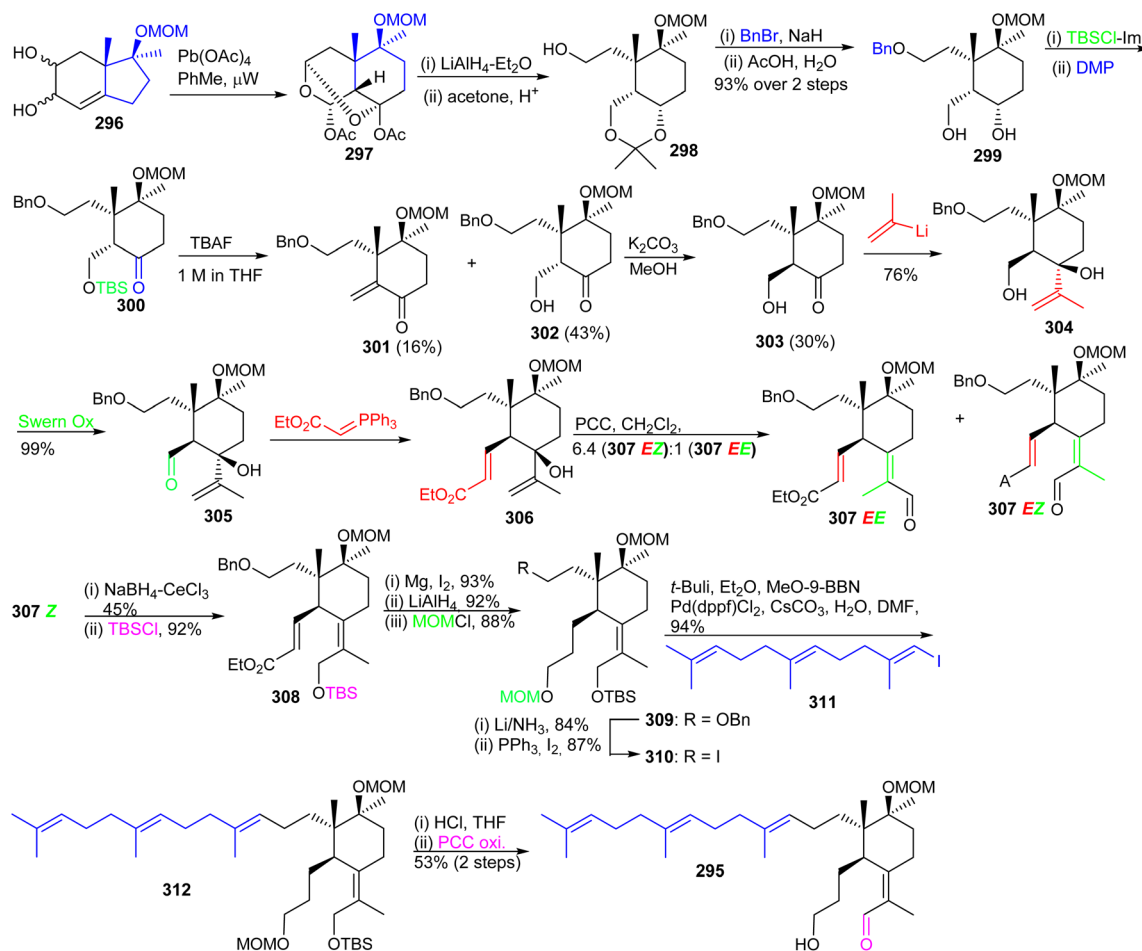
onocerin (**291**) through biosynthetic conversions including oxidative ring A and D cleavage, oxidation and double bond isomerization.

Most of the iridal-type triterpenoids have the same absolute configurations at C-6, C-10, and C-11 (e.g. iridobelamal A (**77**), Scheme 19).<sup>92,98</sup> Furthermore, belamchinenin A (**288**), which feature a novel 6/5/6-tricyclic core system, has stereochemistry at C-6, C-10, and C-11 being the same as for iridal-type triterpenoids, indicating that triterpene **288** could likely be derived from iridal-type triterpenoids. The iridal-type triterpenoid iridobelamal A (**77**) could be considered to be the biogenetic precursor, which after dehydration to **293** might be converted into tricyclic **294** through intramolecular [4 + 2] cyclisation followed by oxidative and dehydrogenative steps to afford the scaffold of belamchinenin A (**288**).<sup>92</sup>



**Scheme 19** Biosynthesis of belamchinenin A (**288**). Reproduced from ref. 92 with permission from the Royal Society of Chemistry.





Scheme 20 Diastereoselective synthesis of 21-deoxy-iridogermaal (295).

## 17 Chemical synthesis of unusual cyclized triterpenoids

### 17.1 Isomalabaricane-type triterpenoids

**17.1.1 Synthesis of 21-desoxy-iridogermaal.** A well-designed synthetic approach for the accomplishment of monocyclic triterpene 21-desoxy-iridogermaal (295)<sup>99</sup> was established by Arseniyadis and co-workers.<sup>100</sup> The synthesis of this natural product started with the preparation of the tetra-substituted cyclohexane 298 with two adjacent quaternary carbon centers (Scheme 20). This cyclohexane was synthesized through the intermediate 297 from the key octahydro-1H-indene analog 296 in three steps.<sup>101</sup> Next, benzyl protection of the C-13 hydroxyl group in 298, followed by a selective acetal cleavage produced diol 299, which was further converted into 300 via selective protection of the primary alcohol group as its TBS derivative. The remaining secondary hydroxyl group was subsequently oxidized with the Dess–Martin protocol to afford ketone 300 which then underwent fluoride-mediated desilylation to produce a mixture of enone 301, together with C6(S) 302 which was equilibrated to the C6(R) 303 epimer.

Precursor 303 on reaction with (2-propenyl)lithium furnished the corresponding carbinol 304 by Swern oxidation of

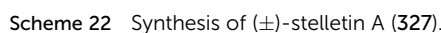
the primary hydroxyl group at C-5 provided aldehyde 305. The latter aldehyde was subjected to a Wittig olefination to afford the  $\alpha,\beta$ -unsaturated ester 306 which upon a Dauben–Michno oxidative rearrangement<sup>102</sup> gave a mixture of the aldehydes 307 *EZ* and 307 *EE*. Reduction of aldehyde 307 *EZ* under Luche reduction conditions and a subsequent silylation of the resulting primary hydroxyl group afforded 308. Next, selective Mg/MeOH mediated reduction of the double bond of the acrylate moiety of 308<sup>103</sup> followed by LiAlH<sub>4</sub> mediated reduction of the ester group and subsequent MOM protection of the resulting alcohol at C-3 provided the advanced intermediate 309.

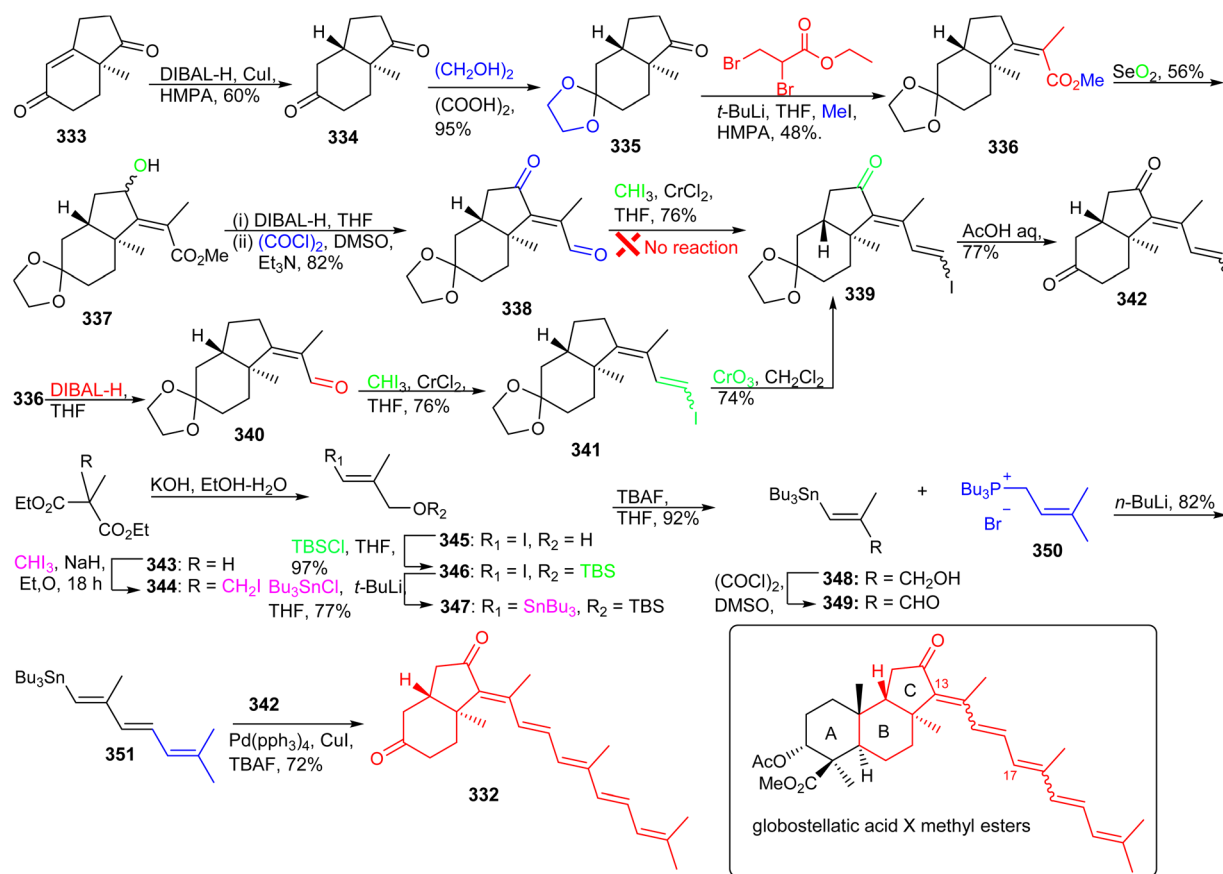
Debenzylation of 309 with Li/NH<sub>3</sub> afforded the resulting C-13 alcohol which was subsequently transformed to iodide 310. Moreover, *E*-vinyl iodide 311 which was produced from geranyl acetone according to a published two step procedure<sup>104</sup> and using the Marshall protocol<sup>105</sup> for a Suzuki–Miyaura reaction.<sup>106</sup> The latter compound was coupled to the key iodide 310 to produce the sp<sup>2</sup>–sp<sup>3</sup> coupled 312 which contains the complete iridal triterpene skeleton. Synchronized acidic deprotection of all protecting groups and then PCC-mediated selective allylic oxidation provided the desired (+)-iridal 295 in 53% isolated yield. Throughout the synthesis, the chiral quaternary center at C-4a was evident in governing the diastereoselective synthesis.





The  $\alpha$ -fluoro hydrazone **318** was prepared *via* an efficient annulation and functionalization protocol by reacting **317** with a cationic gold(I) catalyst in the presence of Selectfluor to give the C-ring  $\alpha$ -fluoro enone as a single diastereomer. Notably, *in situ* *p*-toluenesulfonyl hydrazone formation facilitates construction of the  $\alpha$ -fluoro hydrazone **318**. The key *trans-syn-trans* intermediate **319** was obtained from **318** first by treating the latter with triethylamine in methanol to promote a conjugate addition of the methanol solvent and produce an





Scheme 23 Synthesis of 13E,17E-globostellatic acid X methyl ester mimic 332.

azoalkene followed by stereospecific addition of hydrogen *via* a retro-ene rearrangement of the allylic diazene. Next, **319** was transformed into the enone **320** by employing reductive zirconation and copper-catalyzed cross-coupling with acetyl chloride as C-2 unit. The triketone skeleton **321** was synthesized by the relay hydroboration of the double bond of the ketone **320** followed by an *in situ* silyl group deprotection and IBX oxidation. The key tricyclic intermediate **322** was synthesized as a single isomer from ketone **321** by bromination using a Vilsmeier reagent. The next core skeleton to be synthesized was the polyene side chain **326**. In order to prepare polyene side chain **326**, initially, stannane dienal **324** was synthesized from 3-picolone (**323**) according to a published procedure.<sup>111</sup>

Compound **324** was coupled with phosphonate **325** (Scheme 21) under typical Horner–Wadsworth–Emmons olefination conditions to furnish the polyene coupling partner **326**. Coupling between the tricyclic vinyl bromide **322** and **326** was achieved to produce the methyl ester of rhabdastrellic acid A which upon saponification produces the (±)-rhabdastrellic acid A (**313**). The geometric isomer stelletin E (**196**) was prepared upon irradiation of (±)-rhabdastrellic acid A (**313**).

In order to prepare stelletin A (**327**),<sup>112</sup> initially, gibepyrone C (**330**) was prepared for the pyrone side-chain in both target molecules (Scheme 22). Dimerization of tiglic acid (**328**)<sup>113</sup> provided lactone **329** which was subsequently converted into gibepyrone C (**330**) through a Johnson–Lemieux oxidation to

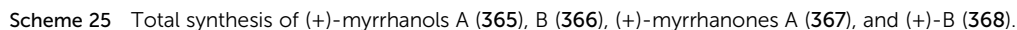
afford a ketone. This is followed by ethoxy vinyl zinc addition and hydrolysis to afford the target aldehyde **330**. This in turn was subjected to a Boron–Wittig reaction<sup>114</sup> to furnish the pyrone coupling partner **331**. Finally, Suzuki coupling of diketone **321** and the pyrone derivative **331** gave stelletin A (**327**). Unfortunately, stelletin A (**209**) *via* the photoisomerization protocol due to significant decomposition under UV light.<sup>112</sup>

**17.2.2 Synthesis of BC-ring model of globostellatic acid X methyl esters.** Kobayashi *et al.*<sup>115</sup> prepared a biological mimic of 13E,17E-globostellatic acid X methyl ester **332** (Scheme 23) in a 10-step synthetic approach starting from the commercially available Hajos–Wiechert ketone (**333**). The four parent globostellatic acid X methyl esters have been reported from the sponge *Rhabdastrella globostellata*.<sup>116</sup> Accordingly, ketone **333** was stereoselectively reduced to *trans*-hydrindanedione **334**, employing DIBAL-H followed by conversion into the ethylene ketal **335** to protect the less-hindered ketone. Notably, a single *E*-configured isomer **336**, was produced by the enolate olefination after treatment with ethyl 2, 3-dibromopropionate and iodomethane. Moreover, SeO<sub>2</sub>-mediated allylic oxidation of **336** furnished the racemic allylic alcohol **337** which was followed by ester reduction with DIBALH and oxidation of the resulting two hydroxyl groups which afforded the keto-aldehyde **338**. Unfortunately, the precursor **338** could not be transformed into **339** *via* an attempted Takai olefination.





vinyl iodide **341** *via* a Takai olefination. Notably, the keto group in ring C of the latter compound was generated by using CrO<sub>3</sub>/3,5-dimethylpyrazole and this was followed by ketal



deprotection to afford the coupling fragment **342**. The aldehyde **349** which was required for installation of the polyene side chain, was prepared in six steps from methylmalonate (**343**) (Scheme 23). Wittig reaction between aldehyde **349** and tributylphosphonium salt **350** established the side chain precursor **351**. Lastly, the desired BC-ring **332** was achieved *via* Stille cross-coupling between fragments **342** and **351**.<sup>116</sup>

### 17.3 Polypdanes

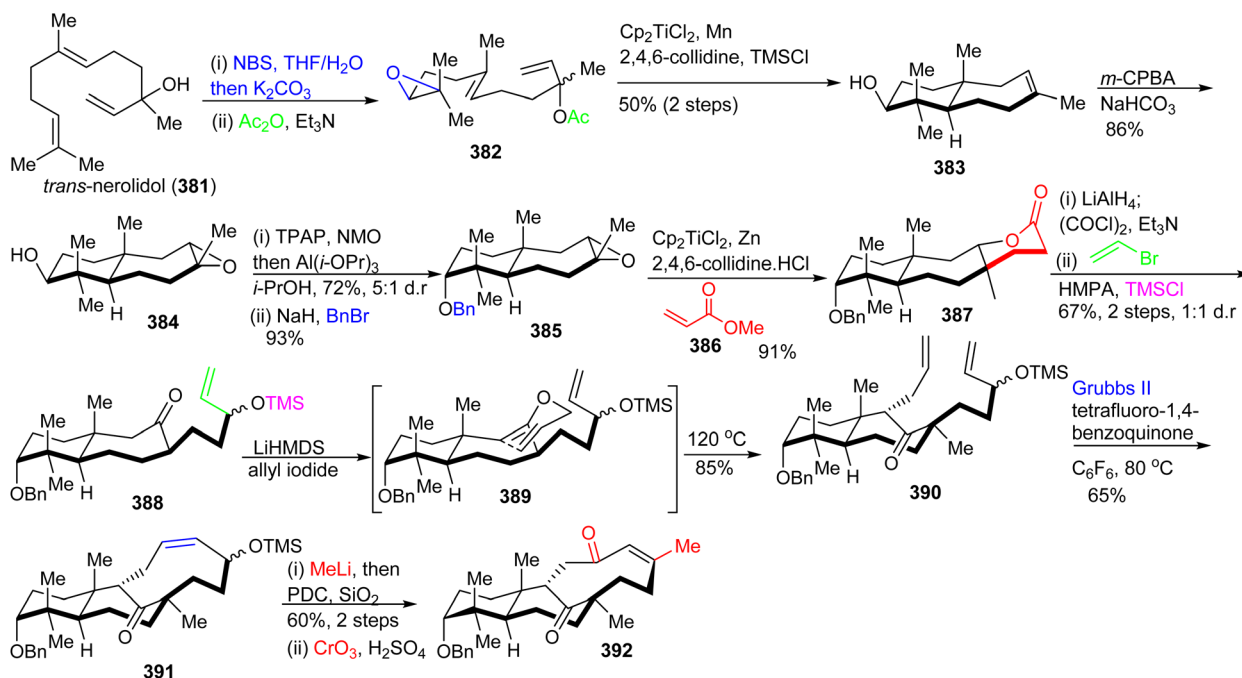
**17.3.1 Total synthesis of (+)-myrrhanol C.** Domingo *et al.*<sup>117</sup> prepared (+)-myrrhanol C (**227**) for which the detailed synthesis is depicted in Scheme 24. In the course of this synthesis, the bicyclic diol fragment **352** was prepared using ex-chiral pool precursors including (–)-sclareol, (–)-sclareolide, or farnesol.<sup>118–120</sup> The bicyclic diol fragment **352** was converted to the trihydroxy intermediate **353** *via* a biotransformation based C–H oxidation. The primary alcohol group in **353** was chemoselectively protected with the pivaloyl protecting group to provide diol **354** followed by the secondary hydroxyl group being protected as its TBS ether (**355**) and thirdly the tertiary hydroxyl group was protected as its MEM ether to the fully alcohol protected **356**.

The advanced intermediate **359** was synthesized by *via* primary alcohol **357**, formed by reduction of the pivaloyl ester of **356** and Swern oxidation to the corresponding aldehyde **358**. This latter compound was subjected to a Wittig olefination employing methyltriphenylphosphonium bromide to afford the bicyclic fragment **359**. Vinyl halide **363** was prepared by coupling geranyl bromide **360** and **361** followed by Zirconium-catalyzed carboalumination of the acetylene group and iodination. Suzuki–Miyaura coupling of precursor **359** and iodide **363**

provided bicyclic **364** and lastly, acid hydrolysis furnished myrrhanol C (**227**).

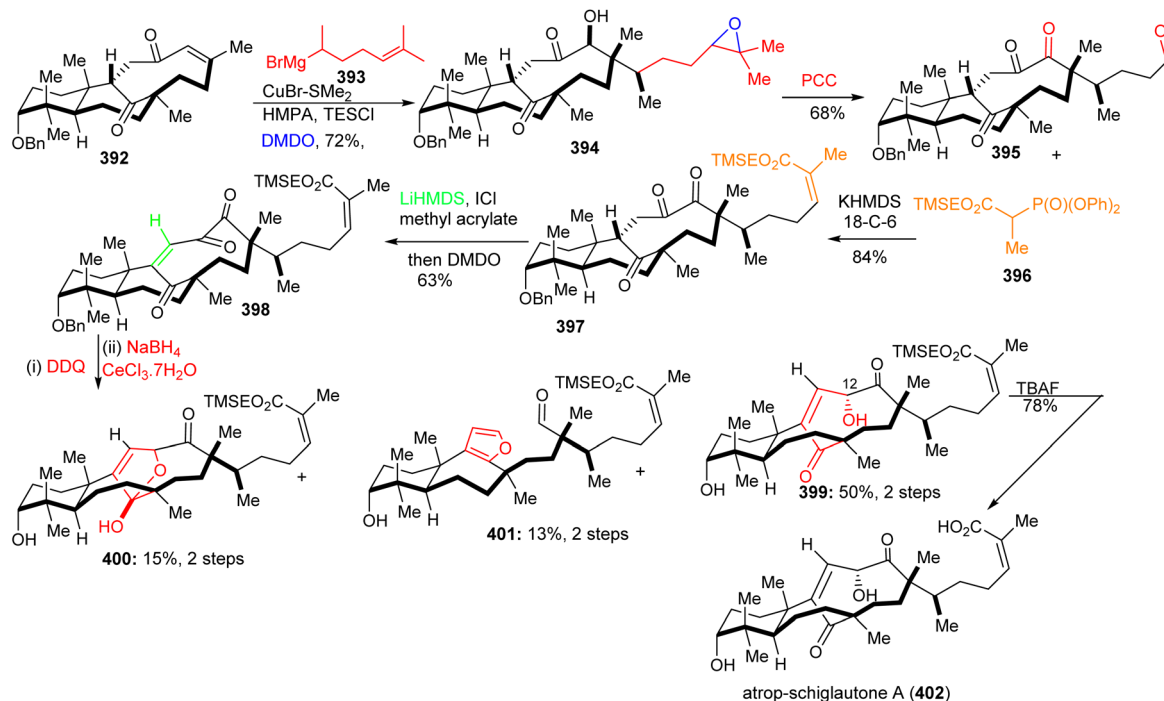
**17.3.2 Total synthesis of (+)-myrrhanols A, B and (+)-myrrhanones A, B.** The triterpenes (+)-myrrhanols A (**365**), B (**366**), (+)-myrrhanones A (**367**), and (+)-B (**368**) were prepared by Barro and co-workers (Scheme 25).<sup>121</sup> The synthesis of intermediate **359** started from farnesyl acetate **369** which was converted into the bicyclic precursor **371** *via* a two step sequence including the Sharpless epoxidation protocol and an Ti(III)-mediated cyclization.<sup>122</sup> Furthermore, the secondary hydroxyl group at C-3 was protected as its TBS ether to furnish **372** and then deprotection of the acetoxy group provided alcohol **373**. Next, the tertiary hydroxyl group in **374** was produced as the only diastereoisomer through epoxidation of the exocyclic double bond with *m*CPBA followed by LiAlH<sub>4</sub> mediated reductive opening of the epoxide ring. Diol **374** was then converted into precursor **357** *via* a three step protocol including protection of the primary alcohol group as its acetyl, the tertiary hydroxyl group as its MEM ether and deacetylation.

Precursor **357** was transformed to the bicyclic synthon **359** by Swern oxidation of the primary alcohol followed by a Wittig olefination of with resulting aldehyde. Preparation of the coupling partner, vinyl iodide **379**, was accomplished using geranyl acetate and employing the same synthetic protocol described for iodide **363**. The key intermediates, bicyclic synthon **359** and vinyl iodide **379** were coupled using the Suzuki–Miyaura protocol to produce **380** which was finally converted to the target compound, (+)-myrrhanol A (**365**) upon deprotection of the three protecting groups. Following on to this, (+)-myrrhanol A (**365**) was converted to (+)-myrrhanone A (**367**) employing a Dess–Martin oxidation of the C-3 hydroxyl group. The (+)-myrrhanone A (**367**) could be converted to



Scheme 26 Synthesis of tricyclic core **392**.





Scheme 27 Synthesis of atrop-schiglautone A (402).

(+)-myrrhanone B (368) upon further Dess–Martin oxidation to produce firstly the corresponding aldehyde and after further oxidation, the corresponding carboxylic acid. Formation of the final target (+)-myrrhanol B (366) was achieved by chemo- and stereoselective reduction of (+)-myrrhanone B (368) with  $\text{NaBH}_4$ .<sup>121</sup>

## 17.4 Schiglautanes

### 17.4.1 Total synthesis of an atropisomer of schiglautone A.

The structural features of this natural product are quite unique and it possesses a cyclohexyl-fused bicyclo[6.4.1]tridecane skeleton, including six stereogenic centers, three of them being quaternary. This natural product appears as an atropisomer and the diastereoselective synthesis was achieved by Ding and coworkers. Preparation of the tricyclic enone 392 (Scheme 26),<sup>123</sup> which carries the entire cyclic carbon skeleton, commenced with the regioselective epoxidation of *trans*-nerolidol (381) followed by acetylation to furnish epoxypolyprene 382. Furthermore, titanium(III)-catalyzed radical cyclization<sup>124</sup> of 382 afforded the desired *trans*-fused bicyclic precursor 383. *m*CPBA mediated epoxidation of ring double bond of 383 followed by inversion of the C-3 hydroxyl group through oxidation (Ley–Griffith oxidation) and reduction (Meerwein–Ponndorf–Verley reduction) protocols, and benzylic protection of the resulting hydroxyl group generated epoxide 385.

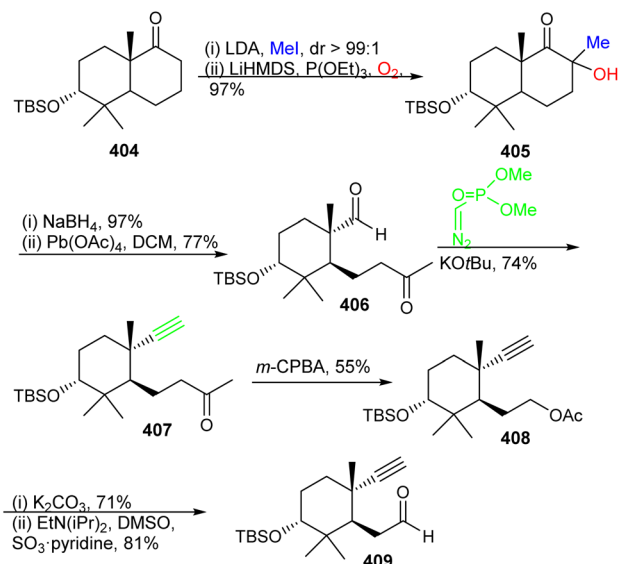
The lactone 387 was constructed from 385 by employing the Gansäuer protocol,<sup>125</sup> which upon reduction, Swern oxidation, subsequent chemoselective Grignard addition and silylation, provided bicyclic ketone 388. The O-allylated 389 was generated after treatment of 388 with LiHMDS/allyl bromide and this was followed by a Claisen rearrangement to construct diene 390.

This rearrangement afforded the C-1 bridging unit. The tricyclic carbon skeleton 391 was prepared from diene 390 *via* a Grubbs II catalyst based ring closing metathesis, yielding a *cis*-configured double bond. The correctly folded and substituted 392 was generated from ketone 391 through a Jones oxidation along with an addition of methyl lithium and a formal allylic ([3,3]-rearrangement) oxidation *via* the Dauben–Michno protocol.

Michael addition of the CuBr-modified Grignard reagent 393 to 392 (Scheme 27) followed by a subsequent Rubottom oxidation with DMDO resulted in formation of the hydroxylated and epoxidized 394. Treatment of the epoxide of 394 with the strong oxidant PCC afforded the 'diol'-cleaved aldehyde 395. Horner–Wadsworth–Emmons reaction of the latter aldehyde with 396 provided the *Z*-configured 397 selectively upon addition of crown ethers. This triketone was first treated with methyl acrylate to give the correct side-chain moiety and then with DMDO to afford the ene-dione 398 in a one-pot procedure. After cleavage of the C-3 benzyl group, reduction of the C-12 ketone was achieved *via* Luche conditions and delivered the major diastereomer 399 along with hemiketal 400 and aldehyde 401. Lastly, desilylation of 399 with TBAF afforded diastereoselectively 402. Surprisingly, NMR data of 402 did not accurately resemble that of natural schiglautone A (239)<sup>82</sup> and based on NMR and X-ray data the structure of the synthesized compound 402 was established as a diastereomeric atropisomer of 239.

**17.4.2 Synthesis of an advanced intermediate of schiglautone A.** Chapelain *et al.*<sup>126</sup> prepared the advanced intermediate 403 *via* a clever convergent enantioselective route and this synthesis is presented in Scheme 28. Thus  $\alpha$ -methylation of ketone 404 followed by hydroxylation furnished keto-alcohol

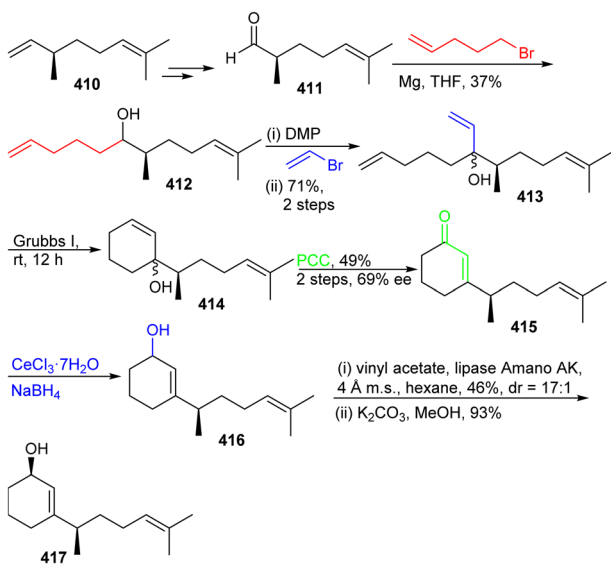




Scheme 28 Synthesis of fragment 409.

**405.** The keto group in the latter molecule was reduced with  $\text{NaBH}_4$ , and the resulting diol underwent  $\text{Pb}(\text{OAc})_4$  mediated oxidative cleavage to furnish keto-aldehyde **406**. The aldehyde **406** was transformed into alkyne **407** through the Seyferth–Gilbert protocol<sup>127</sup> and this latter compound was next subjected to a Baeyer–Villiger oxidation which delivered acetate **408**. The precursor **408** was elaborated to aldehyde **409** through a two step protocol including cleavage of the acetate group and oxidation of the resulting primary hydroxyl group into an aldehyde.

The preparation of ketone **419** commenced from (–)-citronellene (**410**), which was initially transformed to aldehyde **411** in two steps<sup>128</sup> (Scheme 29). The latter molecule was subjected to a Grignard addition (derived from 5-bromo-1-pentene) to



Scheme 29 Synthesis of fragment 417.

afford alcohol **412** and this step was followed by oxidation to the ketone and then followed by a second Grignard addition to furnish triene **413**. Grubbs I catalyst based ring-closing metathesis between the terminal primary alkene groups delivered allylic alcohol **414** and oxidative transposition provided enone **415**. Luche reduction of enone **415** provided allylic racemic alcohol **416**. This mixture was subjected to enzymatic resolution to afford allylic alcohol **417**.

The precursor **417** was subjected to chemoselective cyclopropanation to furnish alcohol **418** (Scheme 30) and PCC mediated oxidation to the ketone along with Birch reduction mediated cyclopropane ring opening provided ketone **419**. Aldol addition between aldehyde **409** and ketone **419** provided enone **420** which was elaborated into ketone **421** through conjugate reduction with  $\text{LAH}/\text{CuI}$ . The thermodynamically stable silyl enol ether of **421** was constructed and subjected to Furukawa's cyclopropanation reagent<sup>129</sup> to provide the desired product **422** together with side products **423–425**. Lastly, the desired precursor **422** was transformed into ketone **403** through cyclopropane ring opening with  $\text{NaOH}/\text{EtOH}$ .

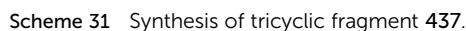
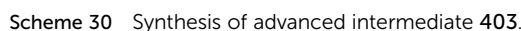
## 17.5 Unusual tricyclic seco/nor-lanostane

### 17.5.1 Studies towards the total synthesis of kadcotrine B.

The synthesis of kadcotrine B (**256**) started from construction of the bicyclic precursor **434** depicted in Scheme 31.<sup>130</sup> Michael addition of diketone **426** and ethyl vinyl ketone **427** afforded triketone **428** which was subsequently elaborated organo-catalytically into *trans*-decalone **429** via the Hagiwara protocol.<sup>131</sup> Regioselective ketal protection of ketone **429** as its ketal **430** was followed by reductive methylation incorporating Birch reduction to furnish the  $\alpha,\alpha$ -dimethyl *trans*-decalone **431**.  $\text{LiAlH}_4$  mediated C-3 ketone reduction furnished the *sec*-alcohol **432**. The resulting hydroxyl group was protected as its benzyl ether to afford **433**. The ketal group was cleaved in **433** via acid hydrolysis to ketone **434**. In order to construct 6/6/5-tricyclic ketone **437**, the bicyclic ketone **434** was then subjected to a four step procedure developed by Smith and coworkers<sup>132</sup> which provided diketone **435** and was subsequently elaborated into tricyclic ketone **436** through  $\text{NaH}$  mediated internal aldol condensation. Notably, insertion of the methyl group in the 5-membered ring in **436** was achieved at the  $\alpha$ -position to the keto group via treatment with  $\text{LiHMDS}$  and  $\text{MeI}$  to afford the tricyclic core **437**.

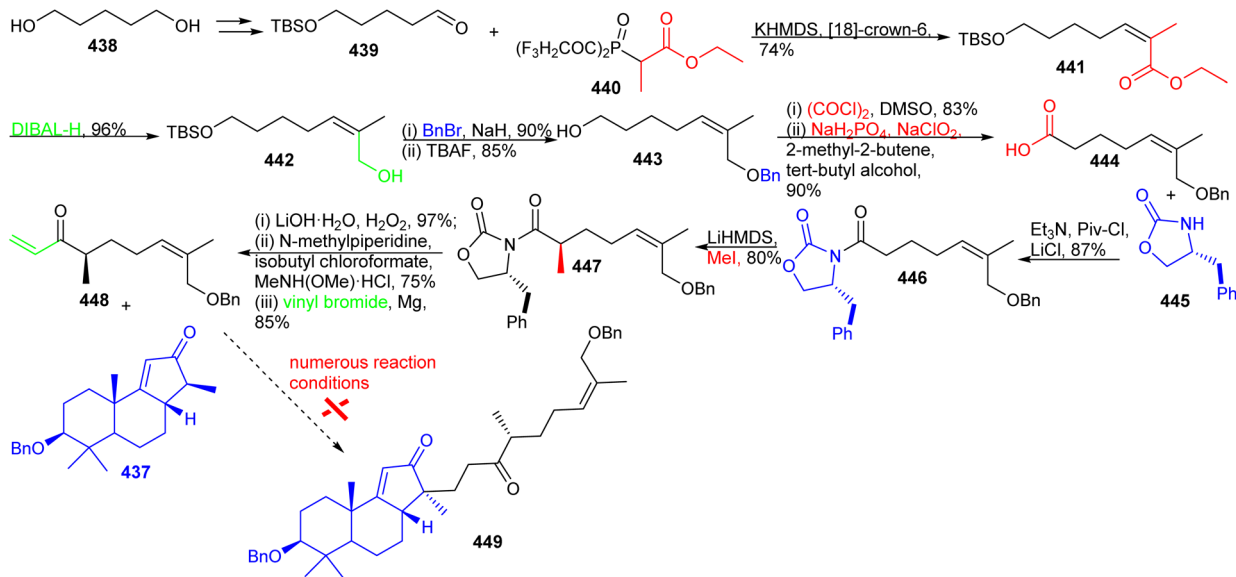
The synthesis of aliphatic fragment **448**, as depicted in Scheme 32, commenced with 1,5-pentanediol (**438**) via the protected aldehyde **439** by following the Tsuji protocol.<sup>133</sup> This latter compound was elaborated into the *Z*-methacrylate derivative **441** with the Still–Gennari phosphonate **440** under the Horner–Wadsworth–Emmons reaction protocol. The ester group in **441** was reduced to the primary alcohol via  $\text{DIBAL-H}$  to afford alcohol **442** which was followed by protection of the resulting hydroxyl group as its benzyl ether and then cleavage of the TBS group afforded **443**. Furthermore, the primary alcohol group in the latter molecule was transformed into the corresponding carboxylic acid through two oxidation procedures *viz.*, Swern and Pinnick oxidations to afford **444**.<sup>134</sup>



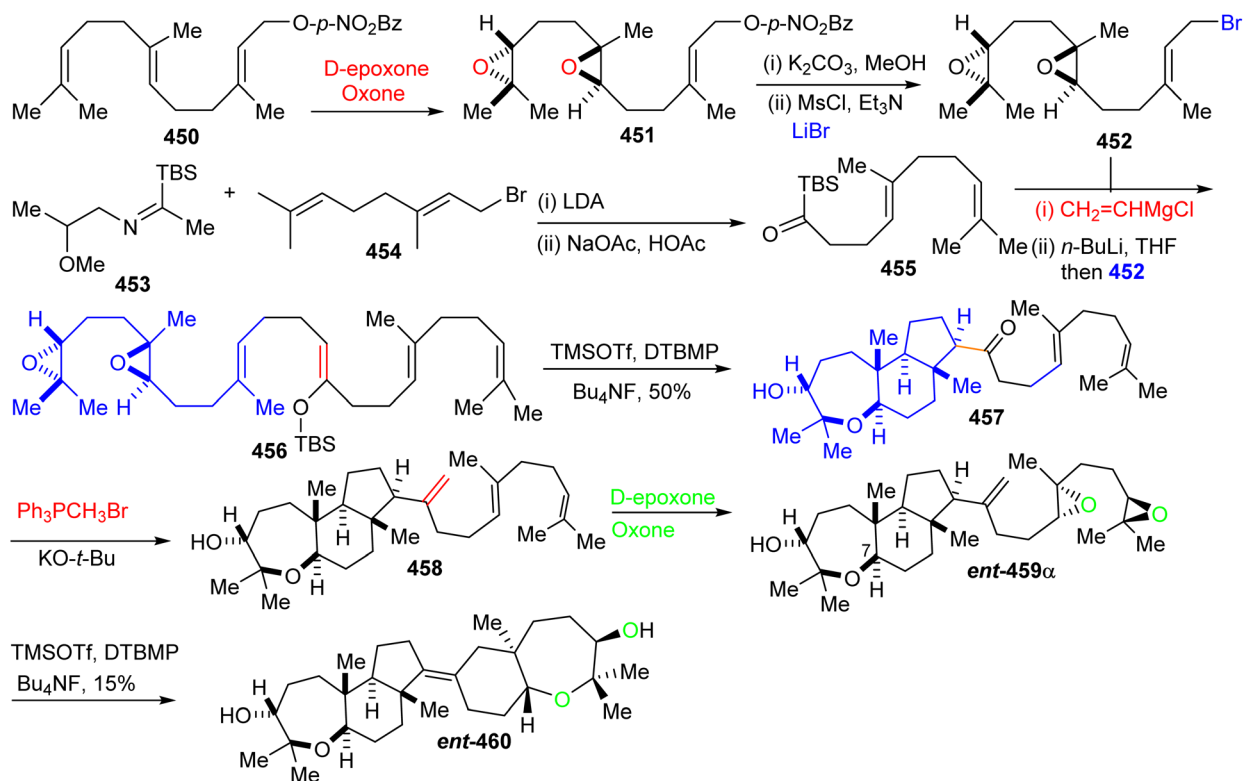


oxidation of primary and secondary alcohols in a single step were investigated but proved inadequate to deliver the desired **449**. The various reaction conditions that were investigated (NaOEt, *t*-BuOK, LDA, KHMDS, NaHMDS, LiHMDS) for the crucial Michael addition between **437** and **448** resulted in the decomposition of starting materials.

**17.6.1 Total synthesis *ent*-abudinol B.** McDonald and co-workers<sup>136</sup> reported on the synthesis of an enantiomer of the marine natural product abudinol B described as *ent*-abudinol



Scheme 32 Synthesis of fragment 448.

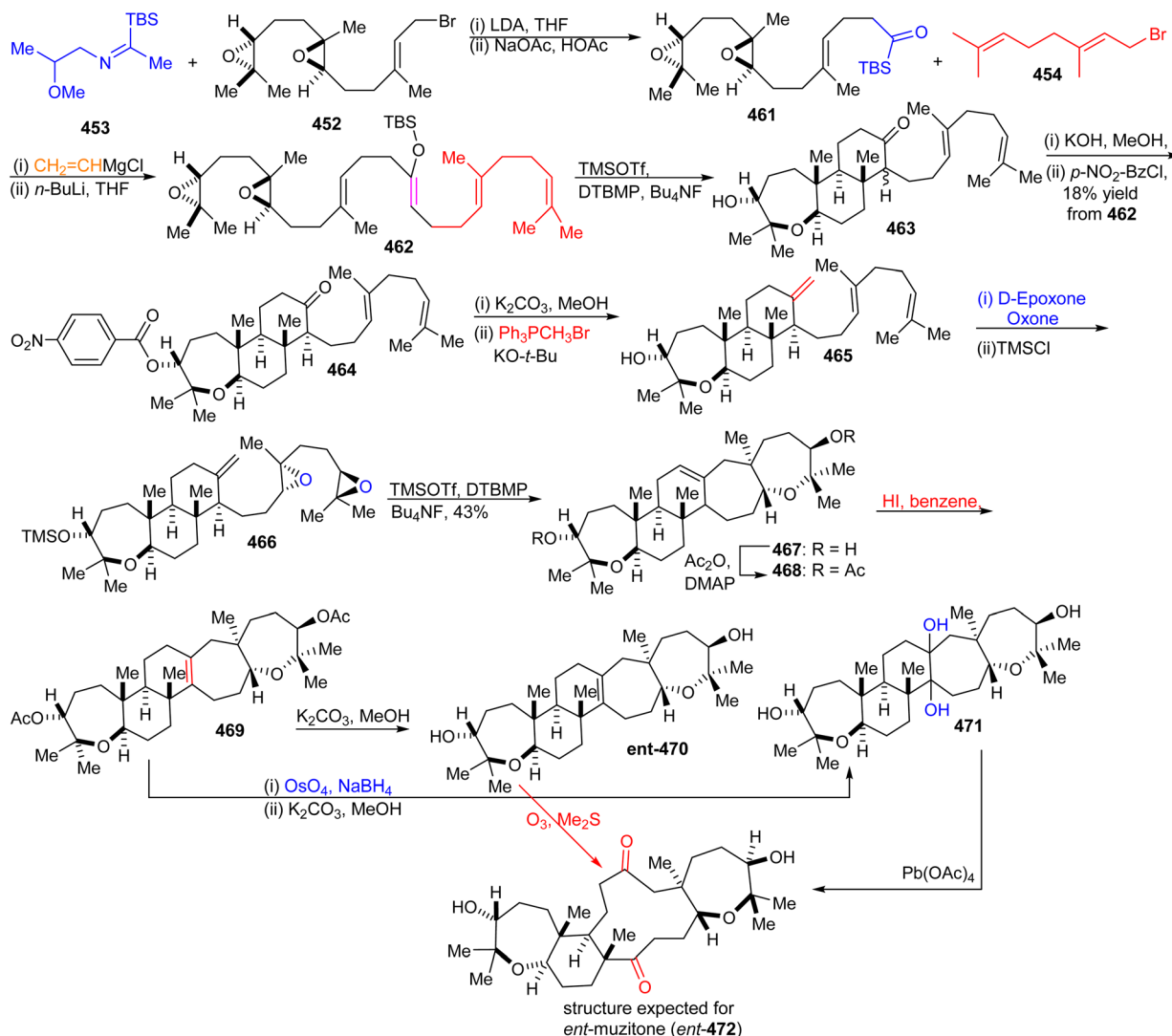
Scheme 33 Total syntheses *ent*-abudinol B (*ent*-460).

(*ent*-460) (Scheme 33). In the course of their synthesis, the precursor, farnesyl *p*-nitrobenzoate **450**, was transformed into diepoxide **451** via regio- and enantioselective epoxidation followed by elaboration into allylic bromide **452** via a standard series of reactions including ester saponification, mesylation, and bromide substitution. The other key component *i.e.* alpha-silyl ketone **455** was prepared by alkylation of geranyl bromide

(**454**) with the metalloenamine derived from **453** followed by imine hydrolysis.

Furthermore, ketone **455** was elaborated into diepoxy-enolsilane **456** through two steps including addition of vinylmagnesium chloride to the acylsilane **455** and Brook rearrangement. The TMSOTf mediated regio- and stereoselective tandem tricyclization of **456** provided the *trans-anti-trans*-fused



Scheme 34 Total synthesis of muzitone (*ent*-472) and *ent*-muzitone (*ent*-470).

tricyclic core **457** which upon treatment with the classical Wittig reagent, transformed it into the disubstituted alkene **458**. Diepoxide *ent*-459 $\alpha$  was subsequently prepared from alkene **458** through regio- and stereoselective double epoxidation. Lastly, TMSOTf catalyzed cyclization of diepoxide *ent*-459 $\alpha$  produce *ent*-abudinol B (*ent*-460) in low yield (15%).<sup>136</sup>

## 17.7 Muzitones

**17.7.1 Total synthesis of muzitone and *ent*-muzitone.** McDonald and co-workers<sup>136</sup> presented (Scheme 34) an elegant research investigation to reassess the structure of muzitone that had previously been incorrectly assigned.<sup>137,138</sup> The synthesis commenced with the preparation of diepoxide **461**, which was constructed by reaction between allylic bromide **452** and imine **453**. The diepoxide **461** was further elaborated into the precursor **462** by treatment with vinylmagnesium bromide and geranyl bromide (**454**) through a Brook rearrangement. Moreover, TMSOTf mediated cyclization of **462** produced the tricyclic

ketone **463** having a free tertiary hydroxyl group which upon treatment with *p*-nitrobenzoyl chloride, afforded the corresponding *p*-nitrobenzoate ester **464**. After removal of the *p*-nitrobenzoate group, installation of the 30th carbon was achieved through a classic Wittig reaction to produce the triene **465**. Following on to this, the triene **465** was converted into diepoxide **466** by employing the Shi epoxidation protocol and this was followed by TMSOTf mediated cyclization to afford the pentacyclic core **467**.

Protection of the two free hydroxyl groups as their acetates in the latter compound and migration of the double bond from the C-13/C-14 into the C-14/C-25 position was accomplished after treatment with HI to afford isomer **469**. The compound *ent*-470, which is considered as “pre muzitone” was achieved by deacetylation of **469** employing K<sub>2</sub>CO<sub>3</sub> in methanol. Finally, *ent*-muzitone (*ent*-472) was constructed *via* the oxidative cleavage of the tetrasubstituted alkene in *ent*-470 with O<sub>3</sub>/Me<sub>2</sub>S or indirectly by from **469** by producing diol **471** initially through osmylation followed by reduction and then deacetylation along with



Pb(OAc)<sub>4</sub> mediated oxidative cleavage which produces the same desired *ent*-muzitone (**ent-472**). In addition, X-ray analysis of bis-*p*-nitrobenzoate analog **ent-472** established the **ent-472** is truly *ent*-muzitone. Unfortunately, Boone *et al.*<sup>136</sup> observed some discrepancies in their NMR data for **ent-472** and the original natural muzitone.<sup>137</sup> Based on this synthetic investigation, the structure of muzitone assigned by Kashman group is consequently incorrect.

## 18 Conclusions

This review provides the second comprehensive overview on some intriguing unusual cyclized triterpenes. Marine organisms, in particular sponges, produce unusual cyclized triterpenoids with remarkable chemical diversity. Advanced scientific studies into these unusually cyclized triterpenes establishes a sound strategy in the importance of these molecules. These triterpenoids have shown a broad spectrum of biological effects including anti-epileptic, cytotoxic, hepatoprotective, neuro-protective, anti-inflammatory, and antidiabetic effects.

The majority of these unusual triterpenes include malabaricane, isomalabaricane, and iridal-type triterpenoids. Overall, isomalabaricanes were reported from four genera of sponges including *Rhabdastrella*, *Jaspis*, *Geodia*, and *Stelletta*. However, taxonomic identification of these sponges remains questionable.<sup>139,140</sup> On the other hand, malabaricane triterpenoids were present in higher plants, fungi, ferns, and bottom sediments.<sup>140</sup> Moreover, iridals were found in the Iridaceae family, mainly in the genus *Iris*. However only a few were reported from the genera *Tigridia* and *Belamcanda*. Furthermore, the unusual and quite fascinating structures have challenged the esteemed synthetic chemists to construct these demanding molecules with the correct absolute configuration and which has required them establishing new synthetic methodologies.

There is no doubt that nature has established fascinating pathways to construct natural products which has unfortunately resulted in less effort by scientists being focused on investigating biosynthetic pathways of unusual cyclized triterpenoids and also understanding the structures along with mechanisms of SC and OSC enzymes which generate these molecules. On the positive side, Xiong *et al.*<sup>30</sup> investigated how oxidosqualene is converted into the monocyclic iridal skeleton. In addition, two *Arabidopsis thaliana* genes encode OSCs which furnish the malabaricane skeleton<sup>8,66–69</sup> Lodeiro *et al.*<sup>65</sup> demonstrated that the isomalabaricane core arises from a lanosterol cyclase mutant (Tyr510) while the native enzyme has yet to be discovered. Moreover, Kushiro and his team<sup>96,97</sup> investigated the biosynthesis of the  $\alpha$ -onocerin skeleton and successfully identified the two genes from the fern *Lycopodium clavatum*, LCC and LCD of the oxidosqualene cyclase (OSC) family.

Thus, more intensive investigations on cyclizing enzymes which generate these triterpenes, will be an intriguing and challenging research field for future natural product research. In addition, there are still numerous fundamental questions about enzyme mechanisms which still need to be fully investigated. Notably, the relationship between active-site structure and cyclization mechanism of the numerous SC and OSC

enzymes presents a formidable task. Further studies are required for the enzyme proteins structure-based engineering along with manipulating substrates. Finally, future research needs to focus on the genomics and synthetic biology for identifying and diversifying these unusual triterpenoid molecules because we believe that this will facilitate remarkable progress in finding new lead compounds for potential biomedical applications.

## 19 Author contributions

H. H. and B. W.: conceptualized, supervised, and edited the review process. J. X. and A. A. wrote the manuscript and drew the figures/schemes. I. R. G. wrote and edited the manuscript.

## 20 Conflicts of interest

There are no conflicts to declare.

## 21 Acknowledgments

H Hussain is thankful to the Alexander von Humboldt Foundation for its generous support in providing the opportunity to do work in Germany which facilitated the writing of this review.

## 22 Notes and references

- 1 K. Muffler, D. Leipold, M. C. Scheller, C. Haas, J. Steingroewer, T. Bley, H. E. Neuhaus, M. A. Mirata, J. Schrader and R. Ulber, *Process Biochem.*, 2011, **46**, 1.
- 2 R. Xu, G. C. Fazio and S. P. T. Matsuda, *Phytochemistry*, 2004, **65**, 261.
- 3 H. Tao, L. Lauterbach, G. Bian, R. Chen, A. Hou, T. Mori, S. Cheng, B. Hu, L. Lu, X. Mu, M. Li, N. Adachi, M. Kawasaki, T. Moriya, T. Senda, X. Wang, Z. Deng, I. Abe, J. S. Dickschat and T. Liu, *Nature*, 2022, **606**, 414.
- 4 H. N. Sultani, I. Morgan, H. Hussain, A. H. Roos, H. H. Haeri, G. N. Kaluderović, D. Hinderberger and B. Westermann, *Int. J. Mol. Sci.*, 2021, **22**, 7125.
- 5 B. A. Shah, G. N. Qazi and S. C. Taneja, *Nat. Prod. Rep.*, 2009, **26**, 72.
- 6 H. Hussain, I. Ali, D. Wang, F. L. Hakkim, B. Westermann, L. Rashan, I. Ahmed and I. R. Green, *Expert Opin. Drug Discovery*, 2021, **16**, 851–867.
- 7 H. Tenga, B. Yuan, S. Gothai, P. Arulselvan, X. Song and L. Chen, *Trends Food Sci. Technol.*, 2018, **72**, 34.
- 8 V. Domingo, J. F. Arteaga, J. F. Q. del Moral and A. F. Barrero, *Nat. Prod. Rep.*, 2009, **26**, 115.
- 9 J. Li, G. Ni, L. Li, Y. Liu, Z. Mai, R. Wang and D. Yu, *Bioorg. Chem.*, 2019, **83**, 20.
- 10 G. Ni, J. Y. Li and D. Q. Yu, *Phytochem. Lett.*, 2019, **31**, 43.
- 11 C. L. Zhang, Y. Wang, Y. F. Liu, D. Liang, Z. Y. Hao, H. Luo, Q. J. Zhang, G. R. Shi, R. Y. Chen, Z. Y. Cao and D. Q. Yu, *Tetrahedron*, 2015, **71**, 5579.
- 12 Y. Hasegawa, X. Gong and C. Kurod, *Nat. Prod. Commun.*, 2011, **6**, 789.



- 13 Q. Xiong, W. K. Wilson and S. P. Matsuda, *Angew. Chem., Int. Ed.*, 2006, **45**, 1285.
- 14 L. Taillet, J. Bonfils, F. Marner and Y. Sauvaire, *Phytochemistry*, 1999, **52**, 1597.
- 15 G. Ni, J. Y. Li and Y. De-Quan, *J. Asian Nat. Prod. Res.*, 2019, **21**, 881–886.
- 16 G. R. Shi, X. Wang, Y. F. Liu, C. L. Zhang, G. Ni, R. Y. Chen and D. Q. Yu, *Tetrahedron Lett.*, 2016, **57**, 5761.
- 17 X. Chen, X. Zhang, Y. Ma, Z. Deng, C. Geng and J. Chen, *Fitoterapia*, 2018, **129**, 126.
- 18 K. Takahashi, Y. Hoshino, S. Suzuki, Y. Hano and T. Nomura, *Phytochemistry*, 2000, **53**, 925.
- 19 F. J. Marner and B. Hanisch, *Helv. Chim. Acta*, 2001, **84**, 933.
- 20 G. Ni, G. R. Shi, J. Y. Li and D. Q. Yu, *RSC Adv.*, 2017, **7**, 20160.
- 21 C. Zhang, J. Chen, F. Zhao, R. Chen, D. Yu and Z. Cao, *Fitoterapia*, 2017, **122**, 20–25.
- 22 J. Li, G. Ni, Y. Liu, Z. Mai, R. Wang and D. Yu, *J. Nat. Prod.*, 2019, **82**, 1759.
- 23 G. Ni, J. Y. Li, Z. P. Mai and D. Q. Yu, *Tetrahedron Lett.*, 2018, **59**, 151.
- 24 K. Takahashi, S. Suzuki, Y. Hano and T. Nomura, *Biol. Pharm. Bull.*, 2002, **25**, 432.
- 25 C. L. Zhang, Y. Wang, F. Zhao, Y. F. Liu, G. R. Shi, R. Y. Chen, D. Q. Yu and Z. Y. Cao, *Fitoterapia*, 2019, **137**, 104193.
- 26 C. L. Zhang, Y. Wang, Y. F. Liu, G. Ni, D. Liang, H. Luo, X. Y. Song, W. Q. Zhang, R. Y. Chen, N. H. Chen and D. Q. Yu, *J. Nat. Prod.*, 2014, **77**, 411.
- 27 C. L. Zhang, Z. Y. Hao, Y. F. Liu, Y. Wang, G. R. Shi, Z. B. Jiang, R. Y. Chen, Z. Y. Cao and D. Q. Yu, *J. Nat. Prod.*, 2017, **80**, 156.
- 28 C. L. Zhang, Y. F. Liu, Y. Wang, D. Liang, Z. B. Jiang, L. Li, Z. Y. Hao, H. Luo, G. R. Shi, R. Y. Chen, Z. Y. Cao and Y. De-Quan, *Org. Lett.*, 2015, **17**, 5686.
- 29 Z. J. Song, X. M. Xu, W. L. Deng, S. L. Peng, L. S. Ding and H. H. Xu, *Org. Lett.*, 2011, **13**, 462–465.
- 30 Q. Xiong, W. K. Wilson and S. P. T. Matsuda, *Angew. Chem.*, 2006, **118**, 1307.
- 31 C. I. Lin, R. M. McCarty and H. W. Liu, *Angew. Chem., Int. Ed.*, 2017, **56**, 3446.
- 32 F. J. Marner, D. Gladtke and L. Jaenicke, *Helv. Chim. Acta*, 1988, **71**, 1331.
- 33 F. J. Marner, K. N. Yasmin and L. Jaenicke, *Helv. Chim. Acta*, 1990, **73**, 433.
- 34 J. A. Piccirilli, *Chem. Biol.*, 1999, **6**, R59.
- 35 L. Zhang, K. Wei, J. Xu, D. Yang, C. Zhang, Z. Wang and M. Li, *J. Ethnopharmacol.*, 2016, **186**, 1–13.
- 36 F. Lv, M. Xu, Z. Deng, N. J. de Voogd, R. W. M. van Soest, P. Proksch and W. Lin, *J. Nat. Prod.*, 2008, **71**, 1738.
- 37 J. W. Blunt, B. R. Copp, W.-P. Hu, M. H. G. Munro, P. T. Northcote and M. R. Prinsep, *Nat. Prod. Rep.*, 2007, **24**, 31.
- 38 J.-F. Guo, J.-M. Zhou, Y. Zhang, R. Deng, J.-N. Liu, G.-K. Feng, Z.-C. Liu, D.-J. Xiao, S.-Z. Deng and X.-D. Zhu, *Cell Biol. Int.*, 2008, **32**, 48.
- 39 J. A. Clement, M. Li, S. M. Hecht and D. G. I. Kingston, *J. Nat. Prod.*, 2006, **69**, 373.
- 40 S. Tang, Y. Pei, H. Fu, Z. Deng, J. Li, P. Proksch and W. Lin, *Chem. Pharm. Bull.*, 2006, **54**, 4.
- 41 P. V. Kiem, D. T. Dung, P. H. Yen, N. X. Nhiem, T. H. Quang, B. H. Tai and C. V. Minh, *Phytochem. Lett.*, 2018, **26**, 199.
- 42 J. Li, B. Xua, J. Cui, Z. Deng, N. J. de Voogd, P. Proksch and W. Lin, *Bioorg. Med. Chem.*, 2010, **18**, 4639.
- 43 J. Li, H. Zhu, J. Ren, Z. Deng, N. J. de Voogd, P. Proksch and W. Lin, *Tetrahedron*, 2012, **68**, 559.
- 44 D. Q. Xue, S. C. Mao, X. Q. Yu and Y. W. Guo, *Biochem. Syst. Ecol.*, 2013, **49**, 101.
- 45 Y. Li, H. Tang, X. Tian, H. Lin, M. Wang and M. Yao, *Fitoterapia*, 2015, **106**, 226.
- 46 N. Tanaka, R. Momose, A. Shibasaki, T. Gono, J. Fromont and J. Kobayashi, *Tetrahedron*, 2011, **67**, 6689.
- 47 S. A. Kolesnikova, E. G. Lyakhova, A. B. Kozhushnaya, A. I. Kalinovsky, D. V. Berdyshev, R. S. Popov and V. A. Stonik, *Molecules*, 2021, **26**, 678.
- 48 M. L. Bourguet-Kondracki, A. Longeon, C. Debitus and M. Guyot, *Tetrahedron Lett.*, 2000, **41**, 3087.
- 49 D. J. Jin, S. A. Tang, G. S. Xing, W. J. Zhao, C. Zhao, H. Q. Duan and W. Han, *J. Asian Nat. Prod. Res.*, 2014, **16**, 427.
- 50 W. G. Xu, J. Wang, G. S. Xing, J. J. Xu, W. Qiao, C. Zhao and S. A. Tang, *Z. Naturforsch., C: J. Biosci.*, 2016, **71**, 111.
- 51 W. G. Xu, J. Wang, W. Qiao, C. Zhao and S. A. Tang, *Chem. Nat. Compd.*, 2018, **54**, 84.
- 52 D. T. Dung, P. H. Yen, N. X. Nhiem, T. H. Quang, B. H. Taia, C. V. Minh, D. C. Kim, H. Oh, Y. C. Kim and P. V. Kiem, *Nat. Prod. Commun.*, 2018, **13**, 661.
- 53 D. T. Dung, D. T. T. Hang, N. Nhiem, T. H. Quang, B. H. Tai, P. H. Yen, N. T. Hoai, D. C. Thung, C. V. Minh and P. V. Kiem, *Nat. Prod. Commun.*, 2018, **13**, 1251.
- 54 M. Hirashima, K. Tsuda, T. Hamada, H. Okamura, T. Furukawa, S. I. Akiyama, Y. Tajitsu, R. Ikeda, M. Komatsu, M. Doe, Y. Morimoto, M. Shiro, R. W. M. van Soest, K. Takemura and T. Iwagawa, *J. Nat. Prod.*, 2010, **73**, 1512.
- 55 K. H. Lai, Z. H. Huang, M. El-Shazly, B. R. Peng, W. C. Wei and J. H. Su, *Mar. Drugs*, 2021, **19**, 206.
- 56 S. Tang, Z. Deng, P. Proksch and W. Lin, *Tetrahedron Lett.*, 2007, **48**, 5443.
- 57 S. A. Kolesnikova, E. G. Lyakhova, A. I. Kalinovsky, D. V. Berdyshev, E. A. Pislyagin, R. S. Popov, B. B. Grebnev, T. N. Makarieva, C. V. Minh and V. A. Stonik, *J. Nat. Prod.*, 2019, **82**, 3196.
- 58 P. S. Achanta, R. K. Gattu, A. R. V. Belvotagi, R. R. Akkinapally, R. K. Bobbala and A. R. V. N. Achanta, *Fitoterapia*, 2015, **100**, 166.
- 59 Z. K. Duan, T. M. Lv, G. S. Song, Y. X. Wang, B. Lin and X. X. Huang, *Nat. Prod. Res.*, 2020, **36**, 229.
- 60 W. Dinku, J. Isaksson, F. G. Rylandsholm, P. Bouř, E. Brichtová, S. U. Choi, S. H. Lee, Y. S. Jung, Z. S. No, J. S. M. Svendsen, A. J. Aasen and A. Dekebo, *Appl. Biol. Chem.*, 2020, **63**, 16.



- 61 S. Thongnest, J. Boonsombat, H. Prawat, C. Mahidol and S. Ruchirawat, *Phytochemistry*, 2017, **134**, 98.
- 62 F. Messina, M. Curini, C. Di Sano, C. Zadra, G. Gigliarelli, L. A. Rascón-Valenzuela, R. E. R. Zepeda and M. C. Marcotullio, *J. Nat. Prod.*, 2015, **78**, 1184.
- 63 Q. Xiong, F. Rocco, W. K. Wilson, R. Xu, M. Ceruti and S. P. T. Matsuda, *J. Org. Chem.*, 2005, **70**, 5362.
- 64 C. J. Huck, Y. D. Boyko and D. Sarlah, *Acc. Chem. Res.*, 2021, **54**, 1597.
- 65 S. Lodeiro, W. K. Wilson, H. Shan and S. P. T. Matsuda, *Org. Lett.*, 2006, **8**, 439.
- 66 T. Xiang, M. Shibuya, Y. Katsube, T. Tsutsumi, M. Otsuka, H. Zhang, K. Masuda and Y. Ebizuka, *Org. Lett.*, 2006, **8**, 2835.
- 67 G. C. Fazio, R. Xu and S. P. T. Matsuda, *J. Am. Chem. Soc.*, 2004, **126**, 5678.
- 68 T. Hoshino and T. Sato, *Chem. Commun.*, 2002, 291.
- 69 I. Abe, *Nat. Prod. Rep.*, 2007, **24**, 1311.
- 70 G. Klaus and G. Axel, *Tetrahedron*, 1984, **40**, 3235.
- 71 D. Tasdemir, G. C. Mangalindan, G. P. Concepcion, S. M. Verbitski, S. Rabindran, M. Miranda, M. Greenstein, J. N. A. Hooper, M. K. Harper and C. M. Ireland, *J. Nat. Prod.*, 2002, **65**, 210.
- 72 M. Tsuda, M. Ishibashi, K. Ageta, T. Sasaki and J. Kobayashi, *Tetrahedron*, 1991, **47**, 2181.
- 73 J. Su, Y. Meng, L. Zeng, X. Fu and F. J. Schmitz, *J. Nat. Prod.*, 1994, **57**, 1450.
- 74 F. Lv, Z. Deng, J. Li, H. Fu, R. W. M. van Soest, P. Proksch and W. Lin, *J. Nat. Prod.*, 2004, **67**, 2033–2036.
- 75 X. Y. Liu, C. J. Li, F. Y. Chen, J. Ma, S. Wang, Y. H. Yuan, L. Li and D. M. Zhang, *Org. Lett.*, 2018, **20**, 4549.
- 76 J. A. Francis, S. N. Raja and M. G. Nair, *Chem. Biodiversity*, 2004, **1**, 1842.
- 77 L. O. Hanus, T. Rezanka, V. M. Dembitsky and A. Moussaieff, *Biomed. Pap.*, 2005, **149**, 3.
- 78 S. A. F. Morad, C. Schmidt, Be. Buechele, B. Schneider, M. Wenzler, T. Syrovets and T. Simmet, *J. Nat. Prod.*, 2011, **74**, 1731.
- 79 H. Z. Li, Y. J. Zhang and C. R. Yang, *Nat. Prod. Res.*, 2006, **18**, 549.
- 80 M. Yoshikawa, T. Morikawa, Y. Kashima, K. Ninomiya and H. Matsuda, *J. Nat. Prod.*, 2003, **66**, 922.
- 81 K. Prantz and J. Mulzer, *Chem. Rev.*, 2010, **110**, 3741.
- 82 F. Y. Meng, J. X. Sun, X. Li, H. Y. Yu, S. M. Li and H. L. Ruan, *Org. Lett.*, 2011, **13**, 1502.
- 83 P. C. Wang, X. H. Ran, H. R. Luo, Q. Y. Ma, Y. Q. Liu, H. F. Dai, J. Zhou and Y. X. Zhao, *Org. Lett.*, 2013, **15**, 2898.
- 84 C. Q. Liang, Y. M. Shi, X. Y. Li, R. H. Luo, Y. Li, Y. T. Zheng, H. B. Zhang, W. L. Xiao and H. D. Sun, *J. Nat. Prod.*, 2013, **76**, 2350.
- 85 U. Shmueli, S. Carmely, A. Groweiss and Y. Kashman, *Tetrahedron Lett.*, 1981, **22**, 709.
- 86 A. A. Beih, A. H. El-Desoky, M. A. Al-Hammady, A. I. Elshamy, M. E. F. Hegazy, H. Kato and S. Tsukamoto, *Fitoterapia*, 2018, **128**, 43.
- 87 S. Jain, I. Abraham, P. Carvalho, Y. H. Kuang, L. A. Shaala, D. T. A. Youssef, M. A. Avery, Z. S. Chen and K. A. El Sayed, *J. Nat. Prod.*, 2009, **72**, 1291.
- 88 R. F. Angawi, E. Saqer, A. Abdel-Lateff, F. A. Badria and S. E. N. Ayyad, *Pharmacogn. Mag.*, 2014, **10**, S334–S341.
- 89 Y. Kashman, T. Yosief and S. Carmeli, *J. Nat. Prod.*, 2001, **64**, 175.
- 90 Y. Kashman and A. Rudi, *Phytochem. Rev.*, 2004, **3**, 309.
- 91 A. E. Nugroho, D. Inoue, C. P. Wong, Y. H. Iwasawa, T. Kaneda, O. Shiota, A. H. A. Hadi and H. Morita, *J. Nat. Rem.*, 2018, **72**, 588.
- 92 G. Ni, J. Y. Li and D. Q. Yu, *Org. Biomol. Chem.*, 2018, **16**, 3754.
- 93 D. H. R. Barton and K. H. Overton, *J. Chem. Soc.*, 1955, 2639.
- 94 M. G. Rowan, P. D. G. Dean and T. W. Goodwin, *FEBS Lett.*, 1971, **12**, 229.
- 95 M. G. Rowan and P. D. G. Dean, *Phytochemistry*, 1972, **11**, 3111.
- 96 T. Araki, Y. Saga, M. Marugami, J. Otaka, H. Araya, K. Saito, M. Yamazaki, H. Suzuki and T. Kushi, *ChemBioChem*, 2016, **17**, 288.
- 97 Y. Saga, T. Araki, H. Araya, K. Saito, M. Yamazaki, H. Suzuki and T. Kushi, *Org. Lett.*, 2017, **19**, 496.
- 98 W. Krick, F. J. Marner and M. L. Jaenicke, *Helv. Chim. Acta*, 1984, **67**, 318.
- 99 W. Krick, F. J. Marner and L. Z. Jaenicke, *Naturforsch.*, 1983, **C38**, 179.
- 100 A. Corbu, M. Aquino, T. V. Pratap, P. Retailleau and S. Arseniyadis, *Org. Lett.*, 2008, **10**, 1787.
- 101 A. Corbu, G. Gauron, J. M. Castro, M. Dakir and S. Arseniyadis, *Org. Lett.*, 2007, **9**, 4745.
- 102 W. G. Dauben and D. M. Michno, *J. Org. Chem.*, 1977, **42**, 643.
- 103 J. A. Profitt, D. S. Watt and E. J. Corey, *J. Org. Chem.*, 1975, **40**, 127.
- 104 E. Negishi, A. O. King and W. L. Klima, *J. Org. Chem.*, 1980, **45**, 2526.
- 105 J. Marshall and G. M. Schaaf, *J. Org. Chem.*, 2003, **68**, 7428.
- 106 N. Miyaura and A. Suzuki, *Chem. Rev.*, 1995, **95**, 2457.
- 107 Y. D. Boyko, C. J. Huck and D. Sarlah, *J. Am. Chem. Soc.*, 2019, **141**, 14131.
- 108 O. H. Oldenziel, D. Van Leusen and A. M. Van Leusen, *J. Org. Chem.*, 1977, **42**, 3114.
- 109 C. P. Ting, G. Xu, X. Zeng and T. J. Maimone, *J. Am. Chem. Soc.*, 2016, **138**, 14868.
- 110 A. Fernandez-Mateos, H. P. Teijon, R. R. Clemente, R. R. Gonzalez and F. S. Gonzalez, *Synlett*, 2007, **17**, 2718.
- 111 T. D. Michels, J. U. Rhee and C. D. Vanderwal, *Org. Lett.*, 2008, **10**, 4787.
- 112 Y. D. Boyko, C. J. Huck, S. Ning, A. S. Shved, C. Yang, T. Chu, J. Tonogai, P. J. Hergenrother and D. Sarlah, *J. Am. Chem. Soc.*, 2021, **143**, 2138.
- 113 A. F. Barrero, J. E. Oltra, M. M. Herrador, E. Cabrera, J. F. Sanchez, J. F. Quilez, F. J. Rojas and J. F. Reyes, *Tetrahedron*, 1993, **49**, 141.
- 114 J. R. Coombs, L. Zhang and J. P. Morken, *Org. Lett.*, 2015, **17**, 1708.



- 115 N. Kotoku, N. Tamada, A. Hayashi and M. Kobayashi, *Bioorg. Med. Chem. Lett.*, 2008, **18**, 3532.
- 116 S. Aoki, M. Sanagawa, Y. Watanabe, A. Setiawan, M. Arai and M. Kobayashi, *Bioorg. Med. Chem.*, 2007, **15**, 4818.
- 117 V. Domingo, L. Lorenzo, J. F. Quilez del Moral and A. F. Barrero, *Org. Biomol. Chem.*, 2013, **11**, 559.
- 118 A. F. Barrero, E. A. Manzaneda, J. Altarejos, S. Salido, J. M. Ramos, M. S. Simmonds and W. M. Blaney, *Tetrahedron*, 1995, **51**, 7435.
- 119 J. H. George, J. E. Baldwin and R. M. Adlington, *Org. Lett.*, 2010, **12**, 2394.
- 120 H. Tanimoto and T. Oritani, *Tetrahedron: Asymmetry*, 1996, **7**, 1695.
- 121 V. Domingo, L. Silva, H. R. Dieguez, J. F. Arteaga, J. F. Quilez del Moral and A. F. Barrero, *J. Org. Chem.*, 2009, **74**, 6151.
- 122 A. F. Barrero, M. M. Herrador, J. F. Quilez delMoral, P. Arteaga, J. F. Arteaga, M. Piedra and E. M. Sanchez, *Org. Lett.*, 2005, **7**, 2301.
- 123 B. Ma, Y. Zhao, C. He and H. Ding, *Angew. Chem.*, 2018, **130**, 15793.
- 124 A. F. Barrero, J. M. Cuerva, M. M. Herrador and M. V. Valdivia, *J. Org. Chem.*, 2001, **66**, 4074.
- 125 A. Gansäuer, M. Pierobon and H. Bluhm, *Angew. Chem., Int. Ed.*, 1998, **37**, 101.
- 126 C. L. Chapelain, *Org. Biomol. Chem.*, 2017, **15**, 6242.
- 127 J. C. Gilbert and U. Weerasooriya, *J. Org. Chem.*, 1982, **47**, 1837.
- 128 B. V. Burger, W. G. B. Petersen, W. G. Weber and Z. M. Munro, *J. Chem. Ecol.*, 2002, **28**, 2527.
- 129 A. Gris, N. Cabedo, I. Navarro, I. de Alfonso, C. Agullo and A. Abad-Somovilla, *J. Org. Chem.*, 2012, **77**, 5664.
- 130 J. S. Reddy, M. Gangababu, P. Manimala, A. Rammohan and J. S. Yadav, *Synthesis*, 2020, **52**, 735.
- 131 H. Hagiwara and H. Uda, *J. Org. Chem.*, 1988, **53**, 2308.
- 132 A. B. Smith and R. Mewshaw, *J. Org. Chem.*, 1984, **49**, 3685.
- 133 J. Tsuji, I. Shimizu and K. Yamamoto, *Tetrahedron Lett.*, 1976, **34**, 2975.
- 134 B. S. Bal, W. E. Childers Jr and H. W. Pinnick, *Tetrahedron*, 1981, **37**, 2091.
- 135 D. A. Evans, M. D. Ennis and D. J. Mathre, *J. Am. Chem. Soc.*, 1982, **104**, 1737.
- 136 M. A. Boone, R. Tong, F. E. McDonald, S. Lense, R. Cao and K. I. Hardcastle, *J. Am. Chem. Soc.*, 2010, **132**, 5300.
- 137 A. Rudi, T. Yosief, M. Schleyer and Y. Kashman, *Tetrahedron*, 1999, **55**, 5555.
- 138 A. N. L. Batista, B. R. P. Angrisani, M. E. D. Lima, S. M. P. da Silva, V. H. Schettini, H. A. Chagas, F. M. dos Santos Jr, J. M. Batista Jr and A. L. Valverde, *J. Braz. Chem. Soc.*, 2021, **32**, 1499.
- 139 P. Cárdenas, J. Gamage, C. M. Hettiarachchi and S. Gunasekera, *Mar. Drugs*, 2022, **20**, 190.
- 140 V. A. Stonik and S. A. Kolesnikova, *Mar. Drugs*, 2021, **19**, 327.

